

AD-A104 560

UNITED TECHNOLOGIES RESEARCH CENTER EAST HARTFORD CT

F/G 20/4

FLOW DISTRIBUTION CONTROL CHARACTERISTICS IN MARINE GAS TURBINE--ETC(U)

AUG 81 S C KUO, H SHU

N00014-80-C-0476

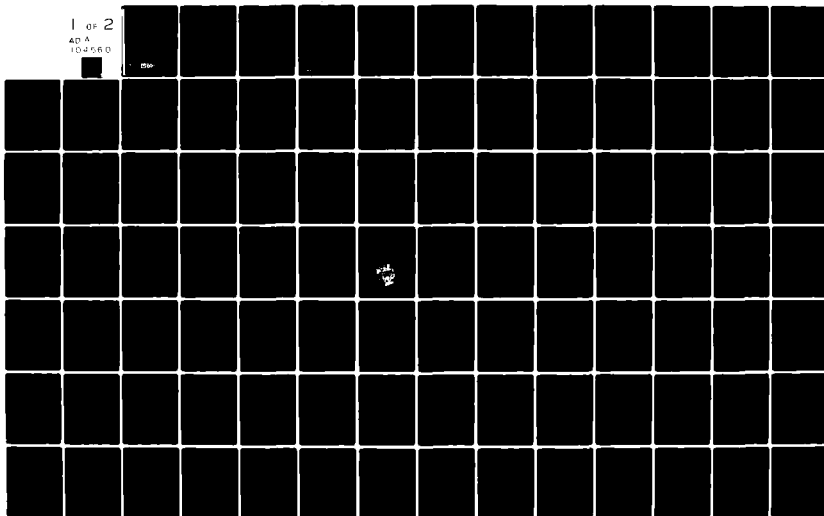
UNCLASSIFIED

UTRC/R81-955200-4

NL

1 of 2

AD A
104560



R81-955200-4

LEVEL

12

FLOW DISTRIBUTION CONTROL CHARACTERISTICS IN MARINE GAS TURBINE WASTE-HEAT RECOVERY SYSTEMS

Phase I — Flow Distribution Characteristics and Control in Diffusers

Annual Technical Report August 1981

Ho-Tien Shu
Simion C. Kuo, Principal Investigator

DTIC
SEP 4 1981
A

Prepared for
The Office of Naval Research, Arlington, Virginia
Under Contract No. N00014-80-C-0476, Modification P00002



**UNITED
TECHNOLOGIES
RESEARCH
CENTER**

East Hartford, Connecticut 06108

This document has been approved
for public release and its
distribution is unlimited.

AD A104560

DTIC FILE COPY

186

UNCLASSIFIED

SECURITY CLASSIFICATION OF THIS PAGE (When Data Entered)

REPORT DOCUMENTATION PAGE		READ INSTRUCTIONS BEFORE COMPLETING FORM
1. REPORT NUMBER UTRC/R81-955200-4	2. GOVT ACCESSION NO. AD-A104	3. RECIPIENT'S CATALOG NUMBER 560
4. TITLE (and Subtitle) Flow Distribution Control Characteristics in Marine Gas Turbine Waste-Heat Recovery Systems. (Phase I - Flow Distribution Characteristics and Control)	5. TYPE OF REPORT & PERIOD COVERED Annual Technical Report July 1980 to July 1981	
7. AUTHOR(s) Simion C./Kuo Ho-Tien/Shu	6. PERFORMING ORG. REPORT NUMBER UTRC R81-955200-4	
9. PERFORMING ORGANIZATION NAME AND ADDRESS United Technologies Research Center Silver Lane, East Hartford, CT 06108	8. CONTRACT OR GRANT NUMBER(s) N00014-80-C-0476 Modification P00002	
11. CONTROLLING OFFICE NAME AND ADDRESS Office of Naval Research 800 North Quincy Street Arlington, VA 22217	10. PROGRAM ELEMENT, PROJECT, TASK AREA & WORK UNIT NUMBERS Program Element: 61153N Project: RRO 24-03 Task Area: RRO 24-03-02 Work Unit: NR 097-411	
14. MONITORING AGENCY NAME & ADDRESS (if different from Controlling Office) <i>1011</i>	12. REPORT DATE August 1981	
	13. NUMBER OF PAGES	
	15. SECURITY CLASS. (of this report) Unclassified	
16. DISTRIBUTION STATEMENT (of this Report) Approved for public release; Distribution unlimited <i>1011-744-1</i>		
17. DISTRIBUTION STATEMENT (of the abstract entered in Block 20, if different from Report) Same as block 16 <i>1011-744-1</i>		
18. SUPPLEMENTARY NOTES		
19. KEY WORDS (Continue on reverse side if necessary and identify by block number) Flow Distribution Control Waste Heat Recovery Diffuser Performance Two-Dimensional Turbulent Flow Flow Maldistribution Gas Turbine Exhaust Velocity Data Marine Gas Turbine Exhausts		
20. ABSTRACT (Continue on reverse side if necessary and identify by block number) - Flow-distribution problems have become increasingly important in the design of modern fluid flow and heat transfer systems. The study of flow-distribution characteristics and control of marine gas turbine exhaust flow is the subject of this report. Major technical problems associated with nonuniform-flow distribution were reviewed and various flow-distribution control methods were evaluated. A two-dimensional, turbulent-flow model		

DD FORM 1 JAN 73 1473

EDITION OF 1 NOV 65 IS OBSOLETE
S/N 0102-014-6601

UNCLASSIFIED

SECURITY CLASSIFICATION OF THIS PAGE (When Data Entered)

UNCLASSIFIED

SECURITY CLASSIFICATION OF THIS PAGE(When Data Entered)

was developed for investigating flow-distribution characteristics and diffuser performance. The study was based on actual flow distribution data from marine gas turbine exhaust flows. Results of this study indicate that a more uniformly distributed flow can be obtained by using flow-guide vanes combined with flow injection, and an improvement of approximately 20 to 36 percentage points in diffuser efficiency can be expected depending on the diffuser geometry considered.

UNCLASSIFIED

SECURITY CLASSIFICATION OF THIS PAGE(When Data Entered)

UNITED TECHNOLOGIES RESEARCH CENTER

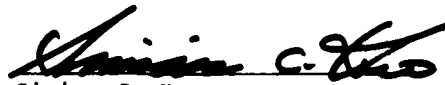
East Hartford, Connecticut 06108

R81-955200-4

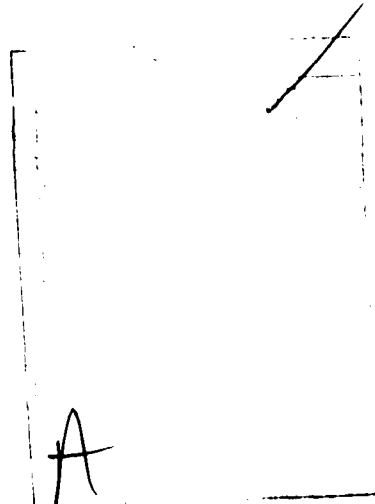
Annual Technical Report for a Study of
Flow Distribution Control Characteristics in Marine
Gas Turbine Waste-Heat Recovery Systems

Phase I - Flow Distribution Characteristics
and Control in Diffusers

ONR N00014-80-C-0476
Mod. No. P00002


Simion C. Kuo
Manager, Thermal Engineering

Date: August 1981



FOREWORD

The work described in this Annual Technical Report was performed at the United Technologies Research Center (UTRC) under Contract N00014-80-C-0476, Modification P00002, entitled "Study of Flow Distribution Control characteristics in Marine Gas Turbine Waste-Heat Steam Generator Systems", for the Office of Naval Research (ONR). This report summarizes results obtained for the Phase I - (First year) study on flow Distribution characteristics and Control in diffusers which is an integral part of a two-year study program on fluid dynamics and heat transfer problems involving the marine gas turbine waste-heat recovery systems. Dr. Simion C. Kuo is the Principal Investigator for this contract, and Dr. Ho-Tien Shu is the major contributor for this phase of the study. Many colleagues in the Computational Fluid Dynamics Group provided valuable consultation support for this study.

The research contract was signed by ONR on July 23, 1980, and the ONR Program Manager is Mr. M. Keith Ellingworth of ONR, Arlington, virginia. Valuable guidance and comments received from Mr. Ellingsworth are greatly appreciated.

Flow Distribution Control Characteristics in Marine Gas
Turbine Waste-Heat Recovery Systems
Phase I - Flow Distribution Characteristics and Control in Diffusers

TABLE OF CONTENTS

	<u>Page</u>
SUMMARY	1
RESULTS AND CONCLUSIONS	2
INTRODUCTION.	3
INTRODUCTION REFERENCES	5
SECTION I CHARACTERIZATION OF NONUNIFORM FLOW PROBLEMS	6
I.1 Flow Distribution Problems in Fluid Flow Systems.	6
I.2 Flow Distribution Problems in Marine Gas Turbine Systems	7
I.3 Evaluation of Flow-Distribution Control Methods	8
REFERENCES.	11
TABLES.	13
FIGURES	16
SECTION II ACQUISITION OF GAS TURBINE EXHAUST VELOCITY DATA.	20
II.1 Acquisition of Turbine Exhaust Flow-Distribution Data.	20
II.2 Evaluation of Flow-Distribution Data.	21
II.3 Selection of Baseline Diffuser Configuration.	22
II.4 Identification of Flow Conditions and Properties.	23
REFERENCES.	24
TABLES.	25
FIGURES	27

TABLE OF CONTENTS (Cont'd)

	<u>Page</u>
SECTION III FORMULATION OF TWO-DIMENSIONAL TURBULENT FLOW MODEL FOR DIFFUSERS	41
III.1 Streamline Orthogonal Curvilinear Coordinate System.	41
III.2 Governing Equations for Two-Dimensional Diffusers.	43
III.3 Turbulent Flow Model	48
III.4 Method of Solution	49
III.5 Flow Distribution Computer Program	57
REFERENCES	61
FIGURES.	63
SECTION IV PARAMETRIC ANALYSIS OF DIFFUSER PERFORMANCE.	67
IV.1 Preliminary Analysis of Diffuser Performance	67
IV.2 Discussion of Results.	69
IV.3 Improvement of the Analytical Model.	70
IV.4 Impact of Flow Nonuniformity on Design of Diffusers and Waste-Heat Boilers	71
REFERENCES	73
FIGURES.	74
SECTION V DIFFUSER PERFORMANCE WITH FLOW-DISTRIBUTION CONTROL	91
V.1 Selection of Flow-Distribution Control Methods	91
V.2 Diffuser Performance with Flow-Distribution Control.	93
V.3 Impact of Flow-Distribution Control on Design of Waste-Heat Recovery System	95
FIGURES.	96

Flow Distribution Control Characteristics in Marine Gas
Turbine Waste-Heat Recovery Systems
Phase I - Flow Distribution Characteristics and Control in Diffusers

SUMMARY

The object of this study was to investigate flow distribution characteristics and control in the marine gas turbine diffusers most suitable for waste heat recovery systems. The major technical problems associated with nonuniform flow distributions in heat-exchanger or flow-equipment systems were reviewed. Various means to alleviate or minimize these undesirable problems were evaluated. Four sets of candidate flow-distribution data were selected from the measured exhaust velocities of LM2500 and FT4 gas turbines for input to the present study. A two-dimensional turbulent flow model for diffusers was developed and computerized, and five diffuser geometries suitable for marine gas turbine waste-heat recovery applications were investigated based on the actual flow distribution data. The exit flow distribution characteristics (velocity, mass-flux, pressure recovery, and temperature) and diffuser performance with and without flow-distribution controls were analyzed using the computer programs developed. It was found that nonuniform flow distribution in the gas turbine exhaust can reduce diffuser efficiency to half that attainable with uniform flow, and that the diffuser exhaust velocities will be more uniform by using guide vanes and/or flow injection than merely using nonsymmetric diffusers. The diffuser efficiency can be improved 20 to 36 percentage points by using these control means.

This study program was conducted by the Thermal Engineering Group at UTRC under Contract N00014-80-C-0476, Modification P00002, from the Office of Naval Research, Mechanics Division, Arlington, Virginia.

RESULTS AND CONCLUSIONS

1. Flow distribution in marine gas turbine exhausts was found to be highly irregular and nonuniform. This nonuniform flow will remain nonuniform through a two-dimensional diffuser unless an effective means of flow distribution control is implemented. The method of using non-symmetric diffusion angles alone will not improve either the flow distribution or the diffuser efficiency.
2. The most detrimental consequence of flow maldistribution in marine gas turbine exhaust is the increase in pressure loss, or decrease in output power. Specifically, the diffuser efficiency will be lower and the thermal performance of the downstream heat exchanger, if any, will be degraded. Additionally, the flow maldistribution would also create thermal/mechanical stress concentrations, local over-heat, and flow-induced vibration all of which could significantly shorten the life expectancy of the heat exchanger.
3. For an unstalled or slightly stalled diffuser, the diffuser efficiencies based on actual flow distribution data of a marine gas turbine exhaust were only about half of the 75 percent efficiency obtainable by a diffuser with uniform-flow.
4. Analyses of existing diffuser designs for gas turbine waste-heat recovery system would indicate that many of these diffusers might have been over-sized because most of the kinetic energy at inlet can be converted into pressure in the first half of the diffuser length. Possible reduction in diffusers length can be made through careful flow-modeling and control.
5. The nonuniform flow distribution of a typical marine gas turbine exhaust can be made more uniform for waste-heat recovery applications by using a specially designed diffuser which incorporates appropriate guide vanes and, if necessary, additional flow injection methods. With properly designed flow-distribution control, an improvement of approximately 20 to 36 percentage points in diffuser efficiency can be expected.
6. The potential improvement in diffuser efficiency indicated above corresponds to increased static pressure recovery of 0.8 to 1.4 inches of water, which would allow a higher pressure loss for the heat exchanger design and reduce the heat exchanger size and weight.
7. The boundary layer separation problem caused some difficulties in analyzing the diffuser performance based on nonuniform velocity distribution data. These difficulties disappeared when flow injection was considered for velocity distribution control. The flow injection which uses the cooling air from the casing of the gas turbine apparently suppressed or at least delayed the flow separation in diffusers.

INTRODUCTION

The successful implementation of open-cycle gas turbines (OCGT) as a ship propulsion engine in the US and abroad has stimulated interest in various means for further improvements in propulsion efficiency. The OCGT propulsion system indeed has many unique advantages, such as being lightweight, having a small volume, and responding quickly to power variations. However, because of some basic design requirements, constraints, and/or inherent performance characteristics, the specific fuel consumption (sfc) of the current OCGT propulsion systems have been equal to or greater than 0.42 lb/shp-hr (Refs. 1 and 2) which may still be too high for some advanced naval ship applications. One of the inherent performance characteristics is that the sfc of an OCGT when operated at partload increases almost inversely proportionally to the power rating. This undesirably high part-load sfc is of major concern to the Navy, because most naval ships are operated under part-load conditions (such as cruise) for most of the time (Ref. 3). Therefore, many alternative propulsion concepts have been proposed and investigated in the past (Refs. 1 to 6) to improve the part-load performance. These include: a) an OCGT propulsion system with cruise engines, b) a regenerative OCGT concept, c) a regenerative closed-cycle gas turbine, and d) a combined gas and steam turbine. Each alternative propulsion concept has its own advantages and disadvantages. Final selection of the most attractive candidate propulsion systems would depend on the results of trade-off studies between system performance, cost characteristics and the capability to meet specific integration and operational requirements. However for all of these alternative concepts, the flow distribution of the gas turbine exhaust and the effect of these flow characteristics on the waste-heat exchanger performance is a consideration which must be properly assessed before evaluating the potential of the alternatives.

The combined-cycle gas and steam turbine system (COGAS) has been widely and successfully used in petrochemical, industrial, and utility fields. Studies (Refs. 5 and 6) have also indicated that the COGAS is promising for marine propulsion applications. However, the limitations on engine volume and weight in marine applications are more stringent than for the land-based applications. In the land-based COGAS systems, a huge diffuser (as big as the entire waste-heat boiler) has been used to diffuse or to regulate the highly turbulent, nonuniformly-distributed gas turbine exhaust before the gas enters the waste-heat recovery equipment. The design of this diffuser and waste-heat recovery equipment has typically been based on the manufacturer's experience and judgement. Few analytical studies have been performed to examine these flow-distribution characteristics and hence to more effectively design the diffusers.

A thorough knowledge of flow distribution problems and the necessity of being able to quantitatively analyze problems involving flow distribution has become increasingly important in modern fluid flow and heat transfer systems. Mechanical and chemical engineers are particularly concerned with the impact of flow-distribution nonuniformity on thermal performance, component design and the reliability of a flow system. In general, the incentives for flow-distribution control studies include: (1) providing a better understanding of the flow dynamics; (2) establishing guidelines for selecting the design concept and flow system geometry; (3) predicting the actual (not just idealized) system performance; and (4) defining the research and development for the flow system identified. It is believed that the results of this study will provide not only some basic understanding of flow-distribution problems found in many existing COGAS components, but also specific guidelines in designing more reliable and efficient marine gas turbine waste-recovery systems in the future (Ref. 7).

The study was structured into two phases. Phase I emphasizes the understanding of the basic flow-distribution phenomena and its impact on two-dimensional diffuser design and performance, and Phase II will focus on investigation of heat transfer enhancement and pressure loss characteristics of waste-heat boilers with several flow-distribution controls. This report documents the work done for the Phase-I study and consists of five sections. In Section I, major problems attributable to nonuniform flow distribution were reviewed and various flow distribution control methods were evaluated. Section II presents the actual flow distribution data acquired for various marine gas turbines. Formulation of the two-dimensional turbulent flow model for diffusers was described in Section III. Performance characteristics of 2-D diffusers, with and without flow distribution controls, were presented in Sections IV and V respectively.

REFERENCES

1. Critelli, F. X. and W. I. Rowen: Five Year's Experience in Applying Heavy-Duty Gas Turbines to Marine Propulsion. The Soc. of Naval Architects and Marine Engineers, Annual Meeting, New York, November 1975.
2. Rains, D. A.: DD-963 Power Plant, Marine Technology. January 1975.
3. Kuo, S. C., T. L. O. Horton and H. T. Shu: Lightweight Propulsion Systems for Advanced Naval Ship Applications, Part I - System Studies, UTRC R77-952566-5, May 1977.
4. Woodruff, R. B.: Heavy-Duty Gas Turbine - A Viable Marine Propulsion Option. Marine Technology, July 1973.
5. Berman, P. A.: Combined Cycle Gas Turbine Systems for Marine Propulsion. PB179033, Westinghouse Electric Corp., Pittsburgh, PA, 1963.
6. Giblon, Robert P. and I. H. Rolih: COGAS, Marine Power Plant for Energy Savings, Marine Technology, July 1979, pp. 225-259.
7. The Navy Racer System Design RFP N00024-79-R-5301(Q), Attachment I, Item (17). July 20, 1979.

SECTION I

CHARACTERIZATION OF NONUNIFORM FLOW PROBLEMS

In this section, the major technical problems which can be attributed to nonuniform flow through heat exchangers or fluid flow systems were reviewed. The most serious consequence of flow maldistribution would seem to be the increase in pressure loss or pumping power. An equally serious consequence is the creation of a "hot spot" in the heat exchanger if a high-temperature fluid is involved. Other nonuniform flow problems reviewed are: deterioration in heat transfer performance, thermal/mechanical stress concentration, tube fouling and inlet-end erosion, and flow-induced vibration and noise, among others. Various means to alleviate these undesirable nonuniform flow problems were evaluated, and candidate flow distribution control methods and flow geometries for two-dimensional diffusers were identified.

I.1 Flow Distribution Problems in Fluid Flow Systems

Flow distribution nonuniformity appears in almost every real flow system for a variety of reasons. Table I.1 summarizes those principal mechanisms which can exist either in one or multiple modes and cause maldistribution of the fluid flow. These mechanisms are either related to flow properties (such as viscosity or body force effects), or flow geometry (such as a sharp-edged orifice, square-shouldered expansion or contraction, nozzle, diffuser, bend, etc.), or a flow-control device (such as a baffle, blockage, flow injection or extraction, local heating or cooling, etc.). Photographs of various flow distribution patterns are seen in the literature of fluid mechanics and heat transfer.

The most important and obvious consequence of flow maldistribution is on the pressure loss. Excessive pressure loss means that the system will require more pumping power or otherwise its mass flow rate will be lower than the design value. The effects of viscosity on flow distribution nonuniformity for various flow geometries have been discussed rather extensively in Schlichting's boundary layer theory (Ref. 1.1). For instance, the flow distribution in a pipe can be best described by the well-known Hagen-Poiseuille equation and the Prandtl universal-velocity-distribution law for laminar and turbulent flow, respectively. The effects of viscosity on pressure loss coefficients for this type of flow have also been well documented in the Moody diagram as a function of Reynolds number. This diagram has been widely used by engineers for predicting the pressure loss characteristics of many flow systems.

If the flow distribution across a heat transfer matrix is nonuniform, this maldistribution would not only reduce the heat transfer performance but would also create thermal/mechanical stress concentrations and local over-heat, dryout or freezing problems (Refs. 1.2 to 1.8). The acute difficulties created by hot spots in nuclear reactors and in coal-, oil-, and gas-fired boilers are particularly striking examples of the consequences of flow maldistribution. Thus, it can be seen that flow distribution problems vary widely, and are peculiar to the particular case. Reference 1.9 has presented several typical cases in great detail and the importance of the flow maldistribution problem, and some possible approaches to evaluate these effects have also been proposed.

In addition to those typical cases given in Ref. 1.9, the tube fouling and inlet-end erosion problems of marine heat exchangers and power plant condenser waterboxes represent another type of flow-distribution problem. The combined effect of flow rotation and excessive turbulence induced by pumps, and poor inlet piping configurations or waterbox design can also result in serious operating problems (Ref. 1.10). In his study, Richard has measured the velocity distribution with and without turning vanes in a scale model of a nuclear power plant condenser waterbox (Ref. 1.10). It was found that when the turning vanes were properly designed and located in the waterbox, the flow distribution over the entire waterbox was better and the flow turbulence was reduced, thereby reducing the inlet-end tube erosion and extending the condenser life.

It is known that the best flow pattern for a diffuser is one with a uniform velocity distribution at the inlet. A uniform flow distribution in the diffuser would provide the lowest rate of momentum outflow and thus yield maximum diffuser efficiency. In their study, Wolf and Johnston (Ref. 1.12) used screens made with unevenly distributed wires to generate a nonuniform flow velocity profile at the diffuser inlet and found that diffusers with nonuniform inlet velocity profiles exhibit a severe decrease in diffuser performance as compared to the one with a uniform inlet-velocity profile. There are other undesirable consequences related to flow distribution nonuniformity such as flow-induced vibration, flow-induced noise and inefficient combustion processes.

I.2 Flow Distribution Problems in Marine Gas Turbine Systems

Rectangular and circular exhaust elbows are used in marine and industrial gas turbine engines. The exhaust elbow is a vital component used in connecting the free turbine and the gas exhaust system which diverts the engine exhaust gas to a safe area either for sound attenuation or for waste-heat recovery before discharging it to atmosphere. The rectangular exhaust elbow is more

desirable for marine applications because it requires less space than the circular exhaust elbow. However, this saving of space is achieved at the expense of increased pressure loss because of the more abrupt turning of the flow and increased wall friction in comparison with a circular elbow.

The combined effects of abrupt turning, wall friction, and the flow-jet swirling from the free turbine often generate a highly turbulent and nonuniform flow-distribution inside and at the exit of the exhaust elbow (collector box). For gas turbines alone, this nonuniform flow has been a critical problem in efforts to improve the gas turbine performance, particularly at high engine power settings (Ref. 1.14). Experience shows that flow maldistribution is always accompanied by undesirable high pressure loss, and that a one-percent increase in pressure loss is approximately equivalent to a one-percent loss in engine power.

For a combined gas and steam turbine (COGAS) system, the severe flow distribution nonuniformity at the exit of the collector box not only affects the diffuser design and performance but also can significantly impair the waste-heat boiler performance and life expectancy (Refs. 1.14 to 1.16). Despite these problems associated with the nonuniform flow distribution, the COGAS system has been widely used with success in petrochemical, industrial, and utility fields. The typical design approach has been to use a huge diffuser (as big as the size of the waste-heat boiler, which is typically 15 to 20 ft long) to diffuse or to regulate the highly turbulent, nonuniformly distributed gas turbine exhaust before it enters the waste-heat recovery system.

Studies (Refs. 1.17 to 1.20) have also indicated that the COGAS system is very promising for marine propulsion applications. However, the limitations on engine volume and weight for marine applications are more stringent than those for land-based application that a special-design diffuser within a very restricted space would be needed to handle the nonuniform flow-distribution of the gas discharged from the turbine exhaust elbow.

1.3 Evaluation of Flow-Distribution Control Methods

Numerous flow-distribution control methods have been used by various designers in the past to achieve specific goals for a given flow system. Some of the commonly used methods are summarized in Table I.3. These methods can be generally classified into two categories: one employs internal guiding or disturbing mechanisms (such as flow guide vanes, louvers, baffles, screens, wedges, buffer plates, or agitators), and the other uses external means of control, such as changing the flow boundary through variation of flow area, flow injection, flow suction, local heating, local cooling and shaking. It is obvious that each method offers different degrees of control effectiveness, performance suitability, and cost characteristics. However, the internal control methods, in general, are more efficient than the external methods. The selection of any particular flow distribution control method should, therefore, depend on the characteristics of the flow system being investigated. Some typical cases are discussed in the following paragraphs.

The velocity distribution immediately downstream of a bend is always irregular due to the flow separation and secondary flow inside of the bend. (Fig. I.1a). A typical case is seen in the design of wind tunnels. To improve the flow distribution, one can employ turning vanes (Fig. I.1b) or contoured duct walls (Fig. I.1c) obtained from potential flow theory. Both methods have not only improved the velocity distribution downstream of the bend, but also reduced the pressure loss. If the bend with internal vanes is being used as a diffuser, a better diffuser performance can be obtained with carefully designed cascades of airfoils instead of circular arcs.

As indicated in Ref. 1.9, the velocity distribution through a heat-transfer matrix may be affected by the manner in which fluid enters the inlet plenum chambers. If a high-velocity fluid stream enters a plenum chamber axially (Fig. I.2a), it is apparent that a high-velocity jet will shoot across the plenum chamber and impinge on the center of the heat-transfer matrix, thus the velocity through the center of the matrix will be higher than that through the outer annular zone. Flow distribution control devices such as those shown in Figs. I.2b and I.2c can be used to reduce the jet effect before the flow is discharged into the plenum. The central baffle design (Fig. I.2b) is simple and effective and has been employed by Escher-Wyss, Ltd. in their design of gas-to-gas recuperators. The apparent disadvantage of this arrangement is the creation of a stagnation region in the center as well as eddies behind the two outer edges of the baffle, with the consequent increase in pressure loss and pumping power. The louvered design (Fig. I.2c) would result in a more uniform flow distribution and lower flow holdup, and lower pressure loss at the expense of complexity and higher cost.

If the fluid is brought into the plenum of the heat exchanger from the side, significantly different effects may occur. The velocity distribution of this configuration is depicted in Fig. I.3a. This undesirable flow maldistribution can be avoided by re-designing the plenum chamber as shown in Figs. I.3b and I.3c, where the flow guide vanes as well as a torus entrance are being used. Because of the complexity and difficulty in design and installation of flow guide vanes, this concept has not been widely used. However, the torus entrance has been successfully used as the exchanger head in many air heater designs (Ref. 1.21) and other flow systems.

According to Ref. 1.11, the best flow pattern for a diffuser would be the one with a uniform velocity profile at the exit. In other words, the uniform velocity at the diffuser exit implies the lowest exit velocity attainable for a given flow rate and lowest rate of momentum outflow and thus maximum pressure rise. The use of vane systems for very-wide-angle diffusers (Ref. 1.22) has become a common practice in flow-distribution control to achieve high performance for diffusers. Even if the velocity distribution entering the diffuser is uniform, the flow will separate from the wall of a very wide-angle diffuser because of the strong adverse pressure gradient. When flow separation occurs, the diffuser efficiency drops significantly (see Fig. IV.17). To avoid flow separation, vane systems are used.

The design of a vane system normally depends on the specific flow conditions and other design constraints and requirements. For marine-gas-turbine waste-heat recovery applications, where the diffuser has to handle a highly-nonuniform turbulent-flow turbine exhaust gas within a very restricted space, a vaned, wide-angle diffuser would be more desirable. However, the design of such a diffuser system is more complicated. Figure 1.4 shows that such a system might have to incorporate non-symmetric diffuser angle and vane arrangements.

When the undesirable velocity distribution appears in a duct system (because of a bend, change in flow area, viscous effects, etc.), a set of screens is often used for obtaining a more uniformly distributed flow. The screens could be a woven wire mesh, a lattice of crossed rods, or perforated plates. The effectiveness of screens in flattening a highly-nonuniform velocity distribution depends on many factors such as the flow-passage geometry in the vicinity of the screen, the undisturbed velocity-distribution in the duct, and the flow-resistance characteristics of the screen. For example, in order to cut the difference between the peak velocity and the average velocity in half, the screen should impose enough resistance so that the pressure drop across the screen is equal to the dynamic head (based on averaged velocity) of the incident flow (Ref. 1.22). The increased pressure loss associated with the application of screens as a flow distribution control method could become a critical problem in certain flow systems.

The water/steam-side flow distribution in a marine boiler represents a special category of flow distribution problems. Inappropriate flow distribution would have significant impact on boiler performance, availability and reliability (Ref. 1.23). Because the amount of flow distributed to each tube of the heat-transfer matrix is governed by the porous walls of the manifolds, this is called "the manifold problem." Because only two important factors (inertia and friction), determine the distribution of the flow in and from the manifolds, flow distribution control methods are somewhat different from those discussed earlier. A more uniform flow distribution can be obtained by one of the following two methods: (1) keeping the cross-sectional area of the manifold constant and varying the diameter of the discharge holes (or the width of a continuous slot) along the manifold; (2) keeping the diameter of the discharge holes (or the width of the continuous slot) constant and varying the cross-sectional area of the manifold. Both methods have been adopted by many engineers with great success. Detailed studies of manifold problems are given in Refs. 1.23 to 1.25.

REFERENCES

- 1.1 Schlichting, H.: Boundary Layer Theory, McGraw-Hill Book Company, 1968.
- 1.2 Chiou, J. P.: The Effect of Nonuniform Fluid Flow Distribution on Thermal Performance of Crossflow Heat Exchanger, ASME paper 77-WA/HT-3, Nov. 27-Dec. 2, 1977.
- 1.3 Chiou, J. P.: Thermal Performance Deterioration in Crossflow Heat Exchanger Due to the Flow Nonuniformity, Trans. of ASME, J. of Heat Transfer, Nov. 1978, pp. 580-587.
- 1.4 Wilson, D. G.: A Method of Design for Heat-Exchanger Inlet Headers, ASME paper 66-WA/HT-41, Nov. 27-Dec. 1, 1966.
- 1.5 Kutchey, J. A. and H. L. Julian: The Measured Influence of Flow Distribution on Regenerator Performance, General Motors Research Labs. SAE Paper No. 740164, 1974.
- 1.6 Schwartz, C. E. and J. M. Smith: Flow Distribution in Packed Beds, Ind. and Eng. Chem., Vol. 45, No. 6, June 1953, pp. 1209-1218.
- 1.7 Mueller, A. C.: An Inquiry of Selected Topics on Heat Exchanger Design, Donald Q. Kern Award Lecture, 6th National Heat Transfer Conf., Chase-Park Plaza Hotel, St. Louis, Missouri. Aug. 1976.
- 1.8 Walters, H. H. and R. D. Mueller: Flow Distribution Study for a Rotary Regenerator, AiResearch Manufacturing Division, L-9492, Oct. 1965.
- 1.9 Frass, A. P. and M. N. Ozisik: Heat Exchanger Design, John Wiley & Sons, Inc., 1965.
- 1.10 Richard, C. C.: Flow Patterns and Velocity Measurements in a Power Plant Condenser Waterbox, Naval Systems Engineering Department, U. S. Naval Academy, Annapolis, MD, 1979.
- 1.11 Feil, O. G.: Vane Systems for Very-Wide-Angle Subsonic Diffusers, Trans. of the ASME, J. of Basic Engineering, Dec. 1964, pp. 759-764.
- 1.12 Wolf, S. and J. P. Johnston: Effects of Nonuniform Inlet Velocity Profiles on Flow Regimes and Performance in Two-Dimensional Diffusers. Trans. of the ASME, J. of Basic Engineering, Sept. 1969, pp. 462-474.
- 1.13 Graf, T. E. and J. E. Nagengast: DD-963 Class Waste Heat Recovery System Experience, ASME Paper 79-GT-159, March 1979.

REFERENCES (Cont'd)

- 1.14 Colombo, R. M.: TF4 Rectangular Exhaust Duct Investigation, UAC Report H233877-1, May 1969.
- 1.15 Rains, D. A.: DD963 Power Plant, Marine Technology, January 1975.
- 1.16 Bauver, W. P. II and J. G. McGowan: Modeling the Distribution and Effects of Steam Flow in Marine Superheaters, Combustion, March 1980, pp. 36-44.
- 1.17 Berman, P. A.: Combined Cycle Gas Turbine Systems for Marine Propulsion, PB179033, Westinghouse Electric Corporation, Pittsburgh, PA, 1963.
- 1.18 Giblon, R. P. and I. H. Rolih: COGAS, Marine Power Plant for Energy Savings, Marine Technology, July 1979, pp. 225-259.
- 1.19 Tanabe, K. and R. Okugawa: Evaluation of Improved Cycles for Marine Application of an Aircraft Derivative Gas Turbine, ASME paper 76-GT-114, March 1976.
- 1.20 Muench, R. K. et al.: A Study of Waste-Heat-Boiler Size and Performance of a Conceptual Marine COGAS System, DTNSRDC TM-27-80-19, Feb. 1980.
- 1.21 Rothemich, E. F. and G. Parmakian: Tubular Air-Heater Problems, Trans. of the ASME, Applied Mech. and Heat Transfer, July 1953.
- 1.22 Baines, W. D. and E. G. Peterson: An Investigation of Flow through Screens, Trans. of the ASME, Vol. 73, 1951, pp. 467.
- 1.23 Bauver, W. P. II and J. G. McGowan: Modeling the Distribution and Effects of Steam Flow in Marine Superheaters, Combustion, March 1980.
- 1.24 Bajura, R. A. and E. H. Jones, Jr.: Flow Distribution Manifolds, Trans. of the ASME, J. of Fluids Eng., Dec. 1976, pp. 654-666.
- 1.25 Keller, J. D.: The Manifold Problem, J. of Applied Mechanics, March 1949, pp. 77-85.

TABLE I.1
ORIGINS OF NONUNIFORM FLOW DISTRIBUTION

- . Viscous Effects
- . Body Force - Gravitational, Induced
- . Geometric Effects
 - Sudden Expansion
 - Sudden Contraction
 - Bends
 - Blockage
 - Non-Symmetric Flow Passage
 - Others
- . Flow Disturbances
 - Injection
 - Extraction
 - Bypass
- . Localized Heating and Cooling

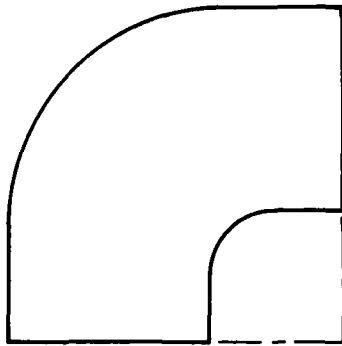
TABLE I.2
CONSEQUENCES OF FLOW MALDISTRIBUTION

1. Increased Pressure Loss - Higher Pumping Power or Loss of Flow Rate
2. Deterioration of Heat Exchanger Performance.
3. Thermal/Mechanical Stress Concentration - Cracks, Ruptures, or Buckling, etc.
4. Local Overheat, Dryout, or Freezing, etc.
5. Flow-Induced Vibration.
6. Flow-Induced Noise.

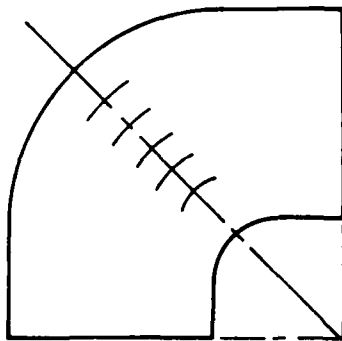
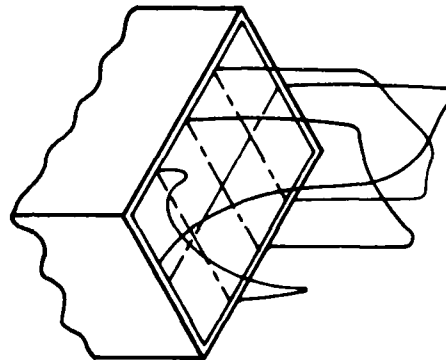
TABLE I.3
FLOW DISTRIBUTION CONTROL METHODS

1. Guide Vanes, Louvers, Baffles, or Screens.
2. Flow Wedges, Buffer Plates, or Agitator.
3. Variation of Flow Area.
4. Flow Injection, or Suction.
5. Local Heating, Cooling, or Shaking.

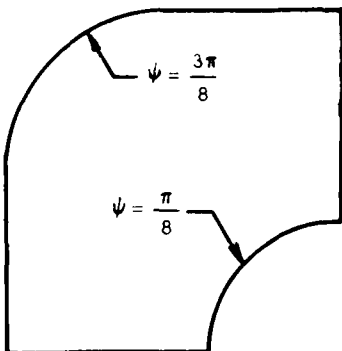
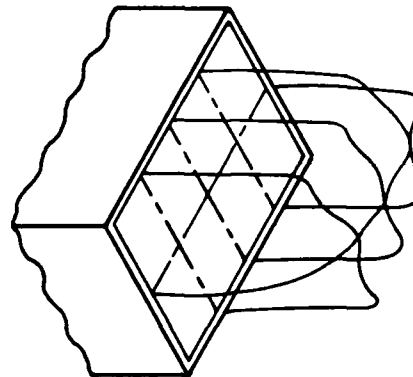
TYPICAL DOWNSTREAM VELOCITY DISTRIBUTION IN RECTANGULAR 90° BENDS



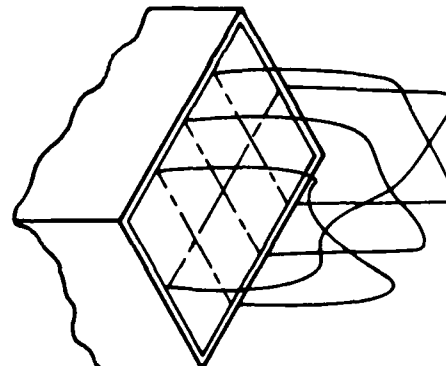
a) WITHOUT FLOW DISTRIBUTION CONTROL



b) WITH LOUVERS

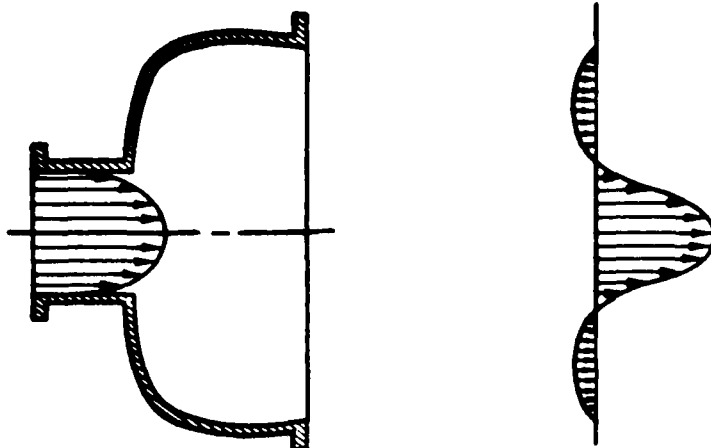


c) WITH STREAMLINE DUCT WALL

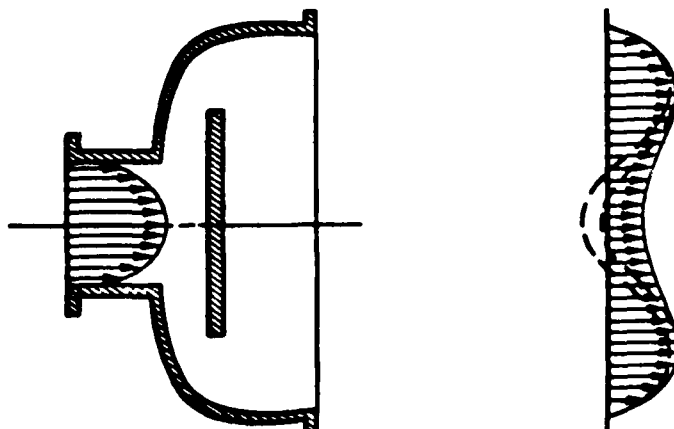


**JET EFFECT AND TYPICAL FLOW DISTRIBUTION BUFFLES
FOR AXIAL-FLOW INLET IN HEAT EXCHANGERS**

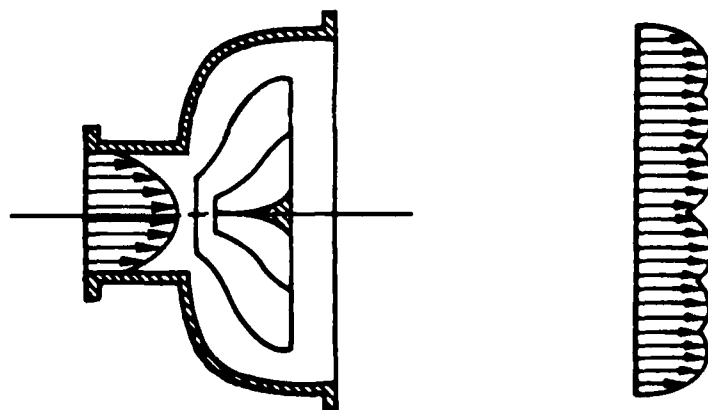
a)



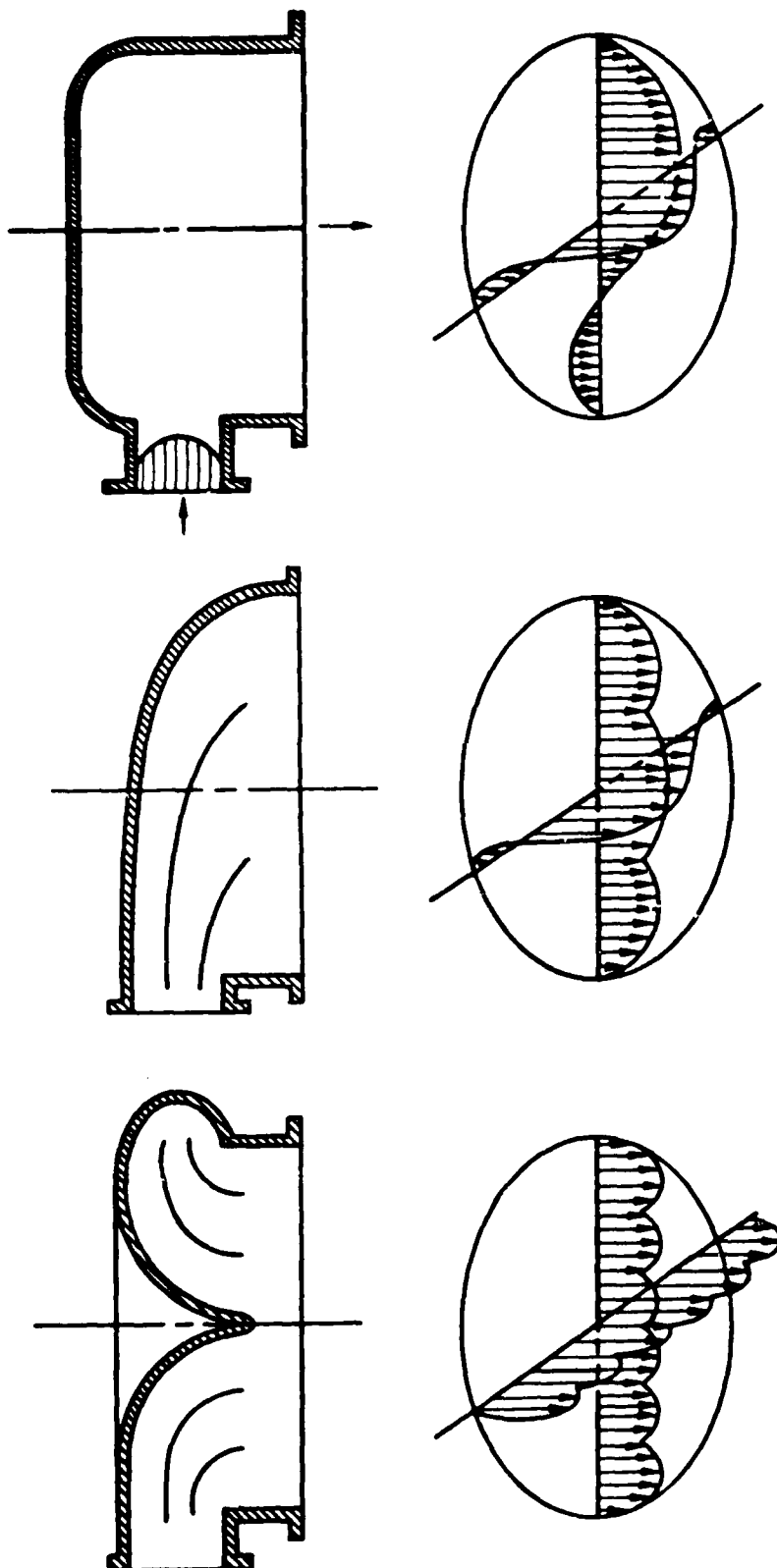
b)



c)



**JET EFFECT AND TYPICAL FLOW DISTRIBUTION EFFLES
FOR RADIAL-FLOW INLET IN HEAT EXCHANGERS**



80-11-56-3

TWO DIMENSIONAL DIFFUSER AND FLOW DISTRIBUTION BAFFLES FOR GAS TURBINE WASTE
HEAT RECOVERY SYSTEMS

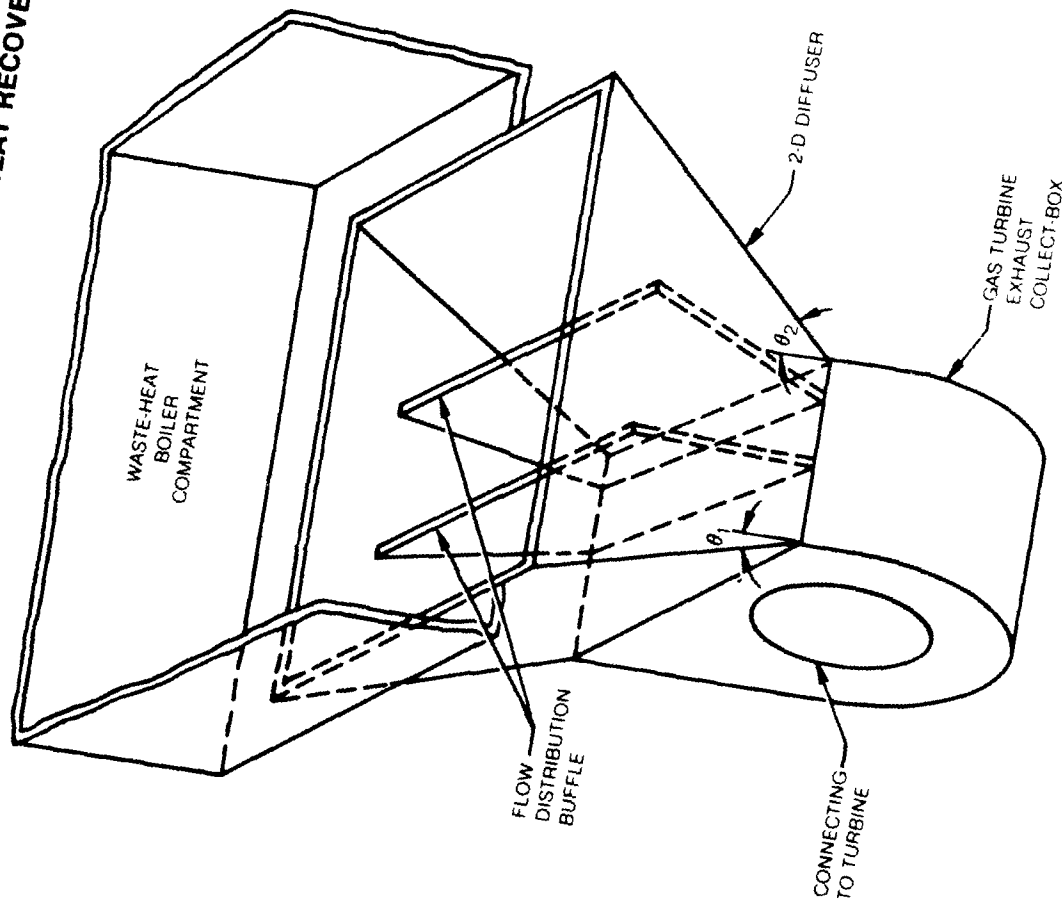
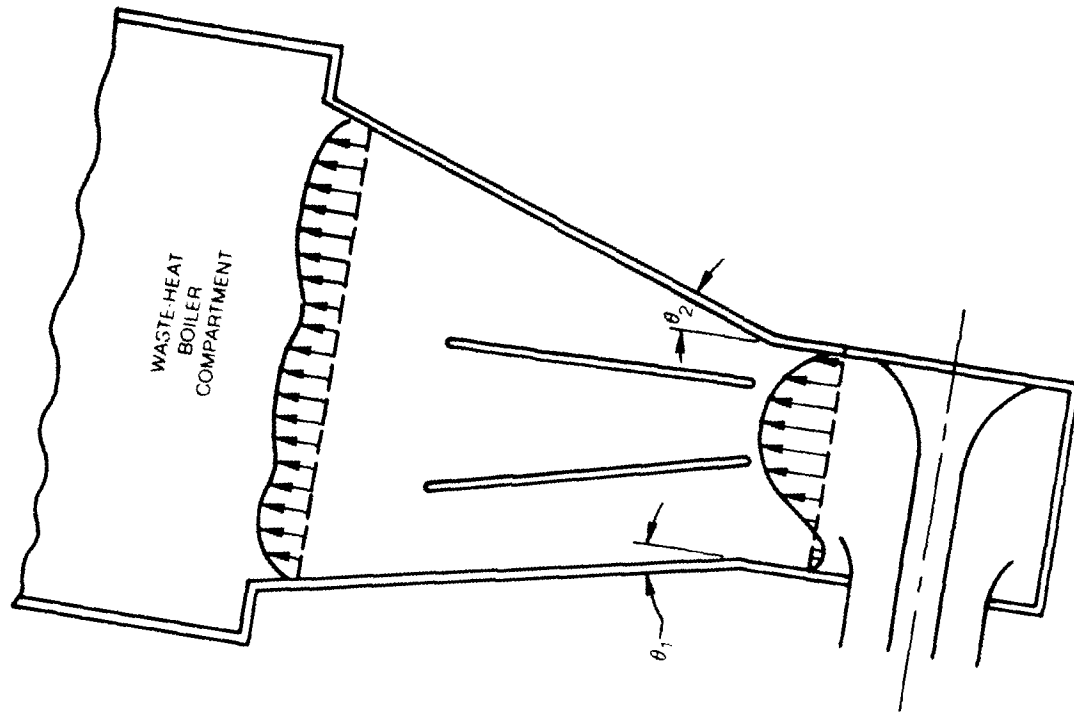


FIG 14



SECTION II

ACQUISITION OF GAS TURBINE EXHAUST VELOCITY DATA

The objective of this task was to acquire and evaluate actual marine gas turbine exhaust-velocity profiles under full-load and part-load operations. More than ten sets of flow distribution data have been acquired and evaluated. Four representative sets were selected for the flow-distribution control study. The thermodynamic conditions and physical properties of each candidate system have also been identified. The results are discussed in this section.

II.1 Acquisition of Turbine Exhaust Flow-Distribution Data

In an effort to acquire actual exhaust-velocity distribution data of marine gas turbines, three approaches were undertaken simultaneously. They were: (1) to request the Office of Naval Research (ONR) to supply test data from their previous sponsored studies; (2) to review UTC in-house reports on various marine gas turbine studies; and (3) to conduct a literature survey on other marine gas turbine models manufactured by other gas turbine manufacturers, such as General Electric Corporation, Westinghouse Electric Company, etc. The third approach has not been very fruitful, and our best understanding is that this kind of information is usually considered proprietary by most gas turbine manufacturers. Therefore, very little data has been released to the public. Another possible reason for the lack of such data is that the exhaust-gas-velocity distributions of marine gas turbines have not been appreciably investigated before. Therefore, the present study used the data provided by ONR and those available from UTC in-house studies. The data provided by ONR are shown in Figs. II.1 thru II.3 which were obtained from Ref. 2.1. Figure II.1 shows the configuration of propulsion engine combustion air and exhaust ducting system aboard DD963-Class destroyer and the locations where the flow distribution data were taken. Figures II.2 and II.3 show the exhaust pressure profiles for gas turbine modules 2A and 2B respectively. Figures II.2 and II.3 each contain three sets of flow distribution data measured at the diffuser inlet (location No. 8 of Fig. II.1) for three different power levels. The pressures are presented in terms of inches of water head which will be converted into pounds-per-square-foot later in this report. The gas temperatures were identified to be 837°F and 856°F, respectively for turbine module 2A and 2B under full-load operation. The part-load temperature was found to be approximately 790°F for both models. The dimensions of the diffuser inlet cross-section are approximately 5 ft by 7 ft.

In the area of in-house studies, the United Technologies Research Center (UTRC) has conducted extensive studies in the mid-60's of exhaust elbows in a scale model

of the UTC-FT4 marine gas turbine (Refs. 2.2 to 2.6). The objectives of these studies were to measure the flow distribution and to investigate the pressure loss characteristics in the exhaust elbows (i.e., collector box). Both circular and rectangular elbows were studied. For each type of exhaust elbow, geometric dimensions and shapes of inserts were varied to meet the study objectives. The air flow rate was also varied over a wide range to simulate the design and off-design conditions of actual engine operation. Figures II.4 and II.5 are two typical velocity-distribution maps for a rectangular exhaust elbow operated at two different flow rates, and Figs. II.6 and II.7 present similar data for a circular exhaust elbow. Both rectangular and circular geometries are of potential interest in naval applications.

II.2 Evaluation of Flow Distribution Data

The results presented in Figs. II.2 thru II.7 show a unique phenomena: the flow distributions at the exit of the exhaust elbow are highly irregular and nonuniform. The results also show that the majority of the flow was concentrated at the rear end of the elbow and that reversed flow was observed in the regions near the front end. No two similar velocity-distribution maps were found. Results presented in Refs. 2.2 thru 2.5 indicate that each flow nonuniformity in the exhaust elbow resulted in a different pressure loss.

Figures II.2 and II.3 show the total (stagnation) pressure and static pressure profiles along the center line of diffuser inlet cross section (or at station No. 8 of Fig. II.1) for DD963-Class prototype gas turbine models 2A and 2B. The three-dimensional flow distribution data were not available. Because the flow model to be developed in this study is two-dimensional, the two-dimensional flow distribution data acquired would satisfy the study objectives.

Because the prior study with the UTC-FT4 marine gas turbine models was conducted using a scale-model of a real engine, many important flow parameters needed for the present study were not documented. Re-examination of the laboratory test data became necessary in order to estimate the actual flow conditions expected of the full-scale engine.

The flow distribution data in Refs 2.2 through 2.5 was presented in terms of a velocity parameter, which was defined as $(P_t - P_s)/P_t$, where P_t and P_s represent the total and static pressures, respectively. The velocity parameter can easily be converted into velocity or mass flux using the isentropic relations and the principle of similarity (which includes Mach number similarity, Reynolds number similarity, and geometric similarity). Based on the descriptions of the test model, the static pressure was assumed to be uniformly distributed over the elbow-exit cross-section. The calculated velocity maps for the UTC-FT4 engine are shown in Figs. II.4 through II.7. In addition to those flow-distribution data, the exhaust gas flow rate and the gas temperature as a function of output-power rating were also obtained and are shown in Figs. II.8 and II.9. This information has also been incorporated into the data reduction.

The UTRC studies have prepared three-dimensional flow distribution maps at the exit of the exhaust elbow. However, the present study needs only two-dimensional flow distribution data. Because the pressure probes (marked as "+" in Figs. II.4 through II.7) were located to cover equal flow areas of the exhaust elbow, geometrically averaged values of the three pressure-rake measurements can be used as representative flow distribution data for the present study.

II.3 Selection of Baseline Diffuser Configuration

The selection of a baseline diffuser configuration depends on the geometric configuration of the engine exhaust elbow, the type of waste-heat boiler, and the space available for installation of the waste-heat recovery systems. Three possible diffuser configurations were considered. Their relative merits and potential applications are discussed in the following paragraphs.

Figure II.10 shows two possible diffuser configurations for integration with a circular engine exhaust elbow. Configuration 7a is a conical diffuser which employs several concentric annular vanes to control the flow distribution such that the flow would be distributed more uniformly over the first module of the heat transfer elements in the waste-heat boiler. This type of diffuser is commonly used for ceiling outlets in ventilating systems. It has the advantage of shortened diffuser length and provides relatively even distribution of air flow into a room. The only problem with the conical diffusers is that their passage length-to-diameter ratio is usually too small for good pressure recovery.

Configuration 7b employs the conical diffuser concept and properly distributes the conical louvers along the center line. This configuration has been used in the current DD-963 class waste-heat-boiler design (Fig. II.11 and Refs. 2.7 through 2.9). Because the heat transfer element will coil around the radially-discharged cylindrical diffuser, this type of diffuser could significantly shorten the overall length of the waste heat boiler. However, the coil geometry also introduces some inconveniences in designing the modular heat-transfer element. Furthermore, if the out-funnel or discharge-duct of the waste-heat boiler is not properly designed, the flow distribution could be unexpectedly distorted as discussed in Ref. 2.9.

Although the waste-heat recovery system in the existing DD-963 Class destroyer (USS Spruance) was designed for integration with the circular exhaust elbow of its service engine, current Navy interest in the waste-heat recovery system seems to be on the main propulsion engine (Ref. 2.10). If the flow distribution control model to be developed in this study is based on rectangular elbows, it should have more direct application for the Navy because most of the marine propulsion gas turbines also have rectangular exhaust elbows. It is also

known that the rectangular diffuser has some advantages of being simple and effective. Results for two-dimensional rectangular diffusers operating with uniform flow conditions are also available which can be used as reference to the present study. Therefore two-dimensional rectangular-cross-section diffusers were selected as the baseline configuration for this study.

Figure II.12 shows the potential layout of the combined-cycle gas and steam turbine system for a marine propulsion system which employs a rectangular diffuser. A more detailed illustration of the diffuser and boiler sections is given in Fig. II.13. Figure II.14 shows two existing marine-boiler/steam-generator types designed by Babcock and Wilcox and used to power the Liberty and Victory Ships, respectively. By removing their combustion chambers, these two boiler/steam-generators could offer potential for gas turbine waste-heat recovery applications if their geometric size and thermal capacity satisfy the performance requirements. This potential application will be investigated in the next phase of this study.

II.4 Identification of Flow Conditions and Properties

Based on the above discussions, Figure II.3, II.4, and II.5 were also selected as representative flow-distribution data for this study. The numerical values of the flow-distribution data for each probe location are tabulated in Table II.1 and the averaged flow conditions and flow properties are summarized in Table II.2. Item A of Table II.1 consists of two sets of data (designated as DATA-1 and DATA-2) representing the exhaust gas pressure-distribution data of the DD-963 class destroyer prototype marine gas turbine Module 2B under full-load and part-load operation, respectively. Item B, which also consists of two sets of data (designated as DATA-3 and DATA-4), shows the corresponding information for a typical UTC-FT4 engine.

In each data set, the first column gives the location of the pressure probes where the values were normalized by the diffuser width. Columns 2, 3, and 4 are values of total (stagnation) pressure, static pressure, and total temperature, respectively.

Table II.2 shows the averaged flow conditions and flow properties for the four candidate sets of flow distribution data. It should be noted that the total pressure and static pressure are the geometrically-averaged values which were obtained by dividing the sum of pressure values from each pressure probe by the number of pressure probes. The static temperatures were obtained from performance data of each gas turbine model. Based on the averaged pressures and temperatures, the flow density, molecular viscosity, specific heat at constant pressure and constant volume were calculated. Finally the Mach number, Prandtl number, and Reynolds number were computed. All these data will be used as references to normalize the flow parameters in the working model.

REFERENCES

- 2.1 Final Report - DD963 Class Destroyer Propulsion Subsystem Prototype Test at NAVSSES/PHILADIV(U), March 1976.
- 2.2 Jensen, R.: Scale Model Tests of FT4A Rectangular Exhaust Elbow, UARL Report UAR-D134, September 1965.
- 2.3 Basham, W. M.: FT4A Rectangular Exhaust Elbow Investigation, UARC Report UAR-F9, Jan. 1967.
- 2.4 Bashan, W. M.: FT4 Circular Exhaust Elbow Investigation, UARC Report F232520-1, Dec. 1967.
- 2.5 Colombo, R. M.: FT4 Rectangular Exhaust Duct Investigation UARC Report H233877-1, May 1969.
- 2.6 Brown, P.: An Experimental Investigation of Exhaust Duct Configurations for the FT4 Twin-Pac Installation, UARC Report L830116-1, May 1972.
- 2.7 Katz, Y and Boyen J. L.: Design Considerations for Heating Recovery System for DD-963 Class Ship, ASME Paper 77-GT-106, 1977.
- 2.8 Katz, Y.: Design Considerations for Future Heat Recovery Boilers Aboard Naval Vessels, ASME Paper 78-GT-162, 1978.
- 2.9 Graf, T. E. and J. E. Nagengast: DD-963 Class Waste Heat Recovery System Experience, ASME Paper 79-GT-159, 1979.
- 2.10 Muench, R. K. et. al.: A Study of Waste-Heat-Boiler Size and Performance of a Conceptual Marine COGAS System. David W. Taylor Naval Ship Research and Development Center, DTNSRDC TM-27-80-19, Feb. 1980.

TABLE II.1

ACTUAL FLOW DISTRIBUTION DATA

A. DD963 Class Destroyer Prototype Gas Turbine Module B

Probe Location	DATA - 1			DATA - 2		
	20,500 Shp, $N_s = 137$			10200 Shp, $N_s = 112$		
Y/W_r	P_t (psf)	P_s (psf)	T_t (R)	P_t (psf)	P_s (psf)	T_t (R)
0.045	2149.06	2144.89	1316	2136.57	2133.97	1250
0.136	2148.54	2143.85	1316	2136.05	2132.93	1250
0.227	2146.98	2142.81	1316	2135.01	2132.41	1250
0.318	2145.94	2142.29	1316	2131.37	2131.37	1250
0.409	2144.30	2140.21	1316	2130.33	2130.33	1250
0.500	2144.89	2137.61	1316	2133.97	2129.29	1250
0.591	2154.78	2140.73	1316	2142.81	2131.37	1250
0.682	2187.04	2152.70	1316	2158.42	2138.65	1250
0.773	2195.88	2139.17	1316	2162.58	2137.61	1250
0.864	2195.36	2142.81	1316	2144.37	2138.13	1250
0.955	2139.69	2132.93	1316	2134.49	2127.20	1250

B. UTC-FT4 Marine Gas Turbine

Probe Location	DATA - 3			DATA - 4		
	15,000 Shp			5,000 Shp		
Y/W_r	P_t (psf)	P_s (psf)	T_t (R)	P_t (psf)	P_s (psf)	T_t (R)
0.05	2129.41	2121.12	1345	2233.82	2229.12	1077
0.15	2129.41	2121.12	1345	2233.92	2229.12	1077
0.25	2129.78	2121.12	1345	2234.40	2229.12	1077
0.35	2135.13	2121.12	1345	2237.76	2229.12	1077
0.45	2144.92	2121.12	1345	2239.68	2229.12	1077
0.55	2159.52	2121.12	1345	2241.12	2229.12	1077
0.65	2180.16	2121.12	1345	2250.72	2229.12	1077
0.75	2196.48	2121.12	1345	2275.90	2229.12	1077
0.85	2211.36	2121.12	1345	2260.32	2229.12	1077
0.95	2211.36	2121.12	1345	2261.28	2229.12	1077

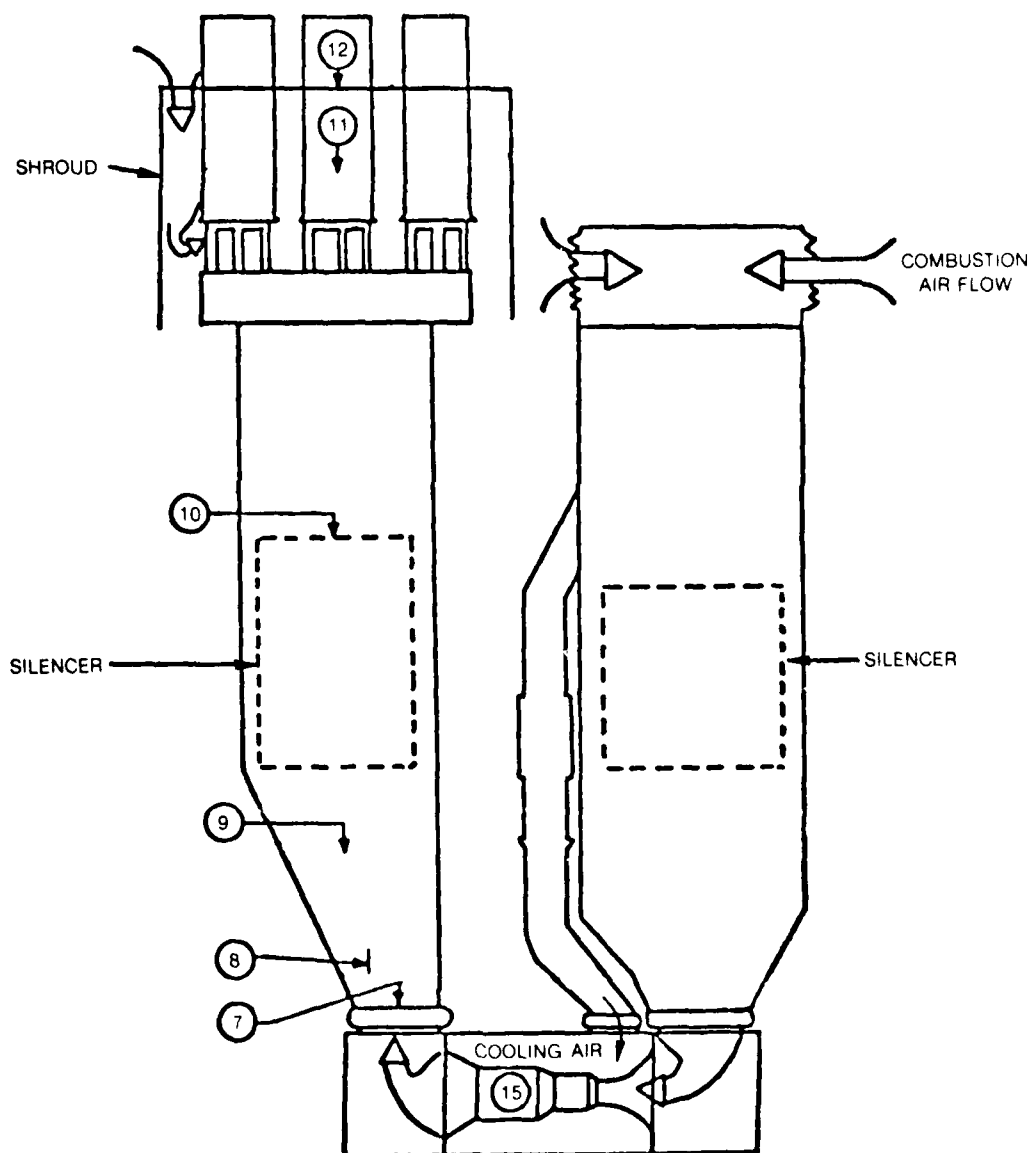
TABLE II.2

AVERAGED FLOW CONDITIONS AND FLOW PROPERTIES

Parameters or Properties	Units	DD963 Class Prototype Gas Turbine Module 2B		UTC-FT4 Marine Gas Turbine	
		Design	Off-Design	Design	Off-Design
Power Rating	Shp	20,500	10,200	27,500	9,000
Total Press.	lb/ft ²	2163.94	2140.52	2195	2179
Static Press.	lb/ft ²	2141.77	2133.03	2169	2169
Total Temp.	°R	1316	1250	1345	1075
Density	#/ft ³	.0305	.0320	.0320	.0378
Viscosity	lb/ft-hr	.0827	.0801	.0838	.0726
Sp. Heat, cp	Btu/#-R	.259	.256	.2587	.2501
Sp. Heat, Cv	Btu/#-R	.185	.183	.1843	.1786
Mach No.	-	.0843	.515	.131	.081
Prandtl No.	-	.691	.688	.693	.686
Reynold No.	-	.115x10 ⁷	.075x10 ⁷	.169x10 ⁷	.134x10 ⁷

**DD963-CLASS DESTROYER PROPULSION ENGINE COMBUSTION
AIR AND EXHAUST DUCTING SYSTEM**

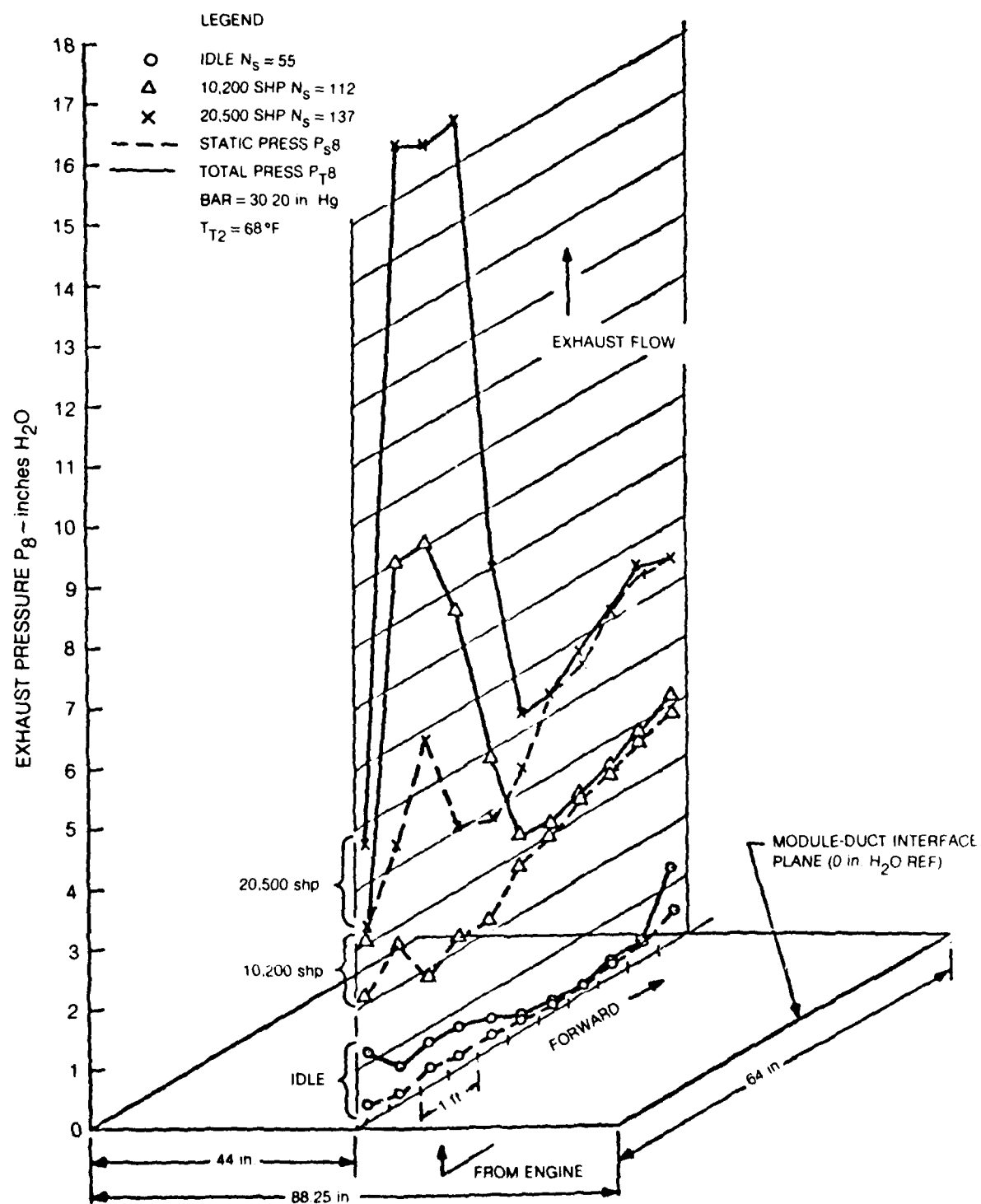
• PROVIDED BY THE OFFICE OF NAVAL RESEARCH FROM REF 2 1



81-6-95-8

EXHAUST PRESSURE MAP OF GAS TURBINE MODULE 2A

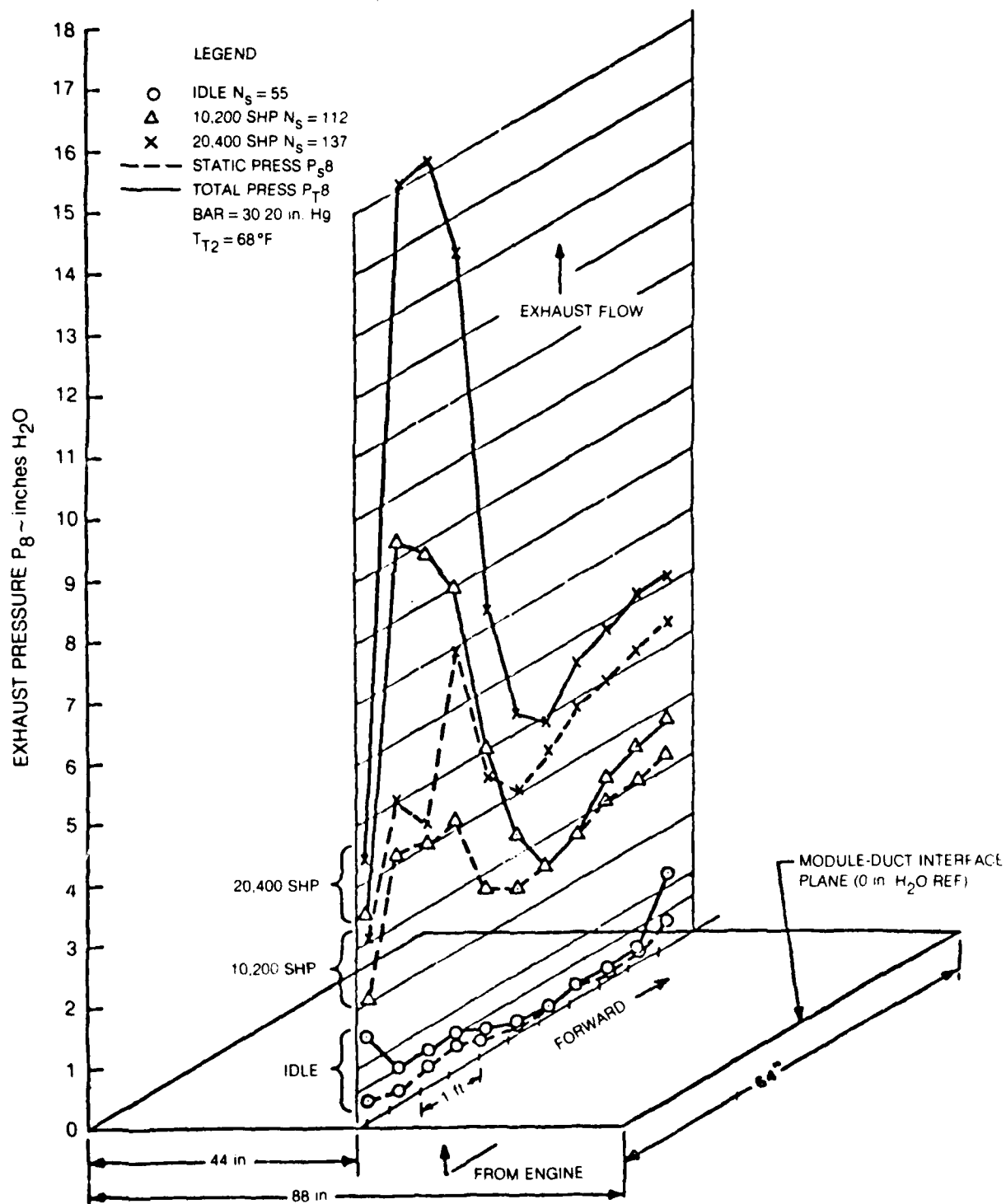
• PROVIDED BY THE OFFICE OF NAVAL RESEARCH FROM REF 21



81-6-95-9

EXHAUST PRESSURE MAP OF GAS TURBINE MODULE 2B

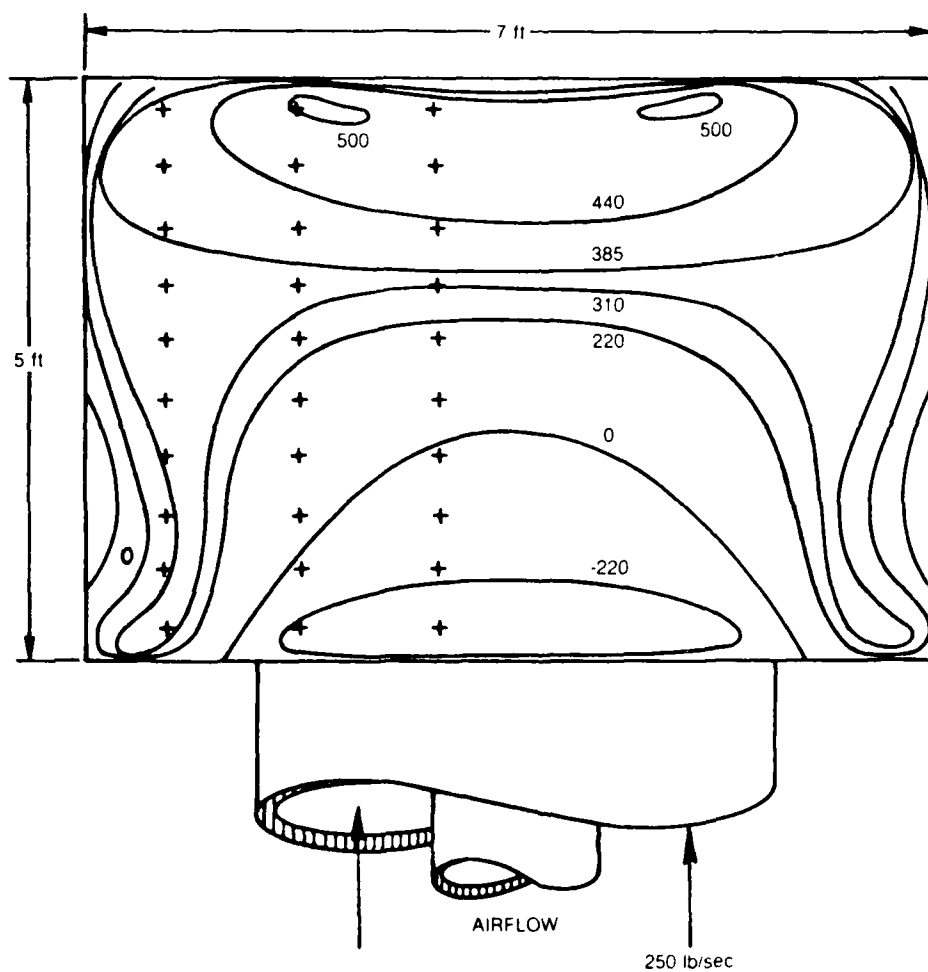
• PROVIDED BY THE OFFICE OF NAVAL RESEARCH FROM REF 21



81-6-95-10

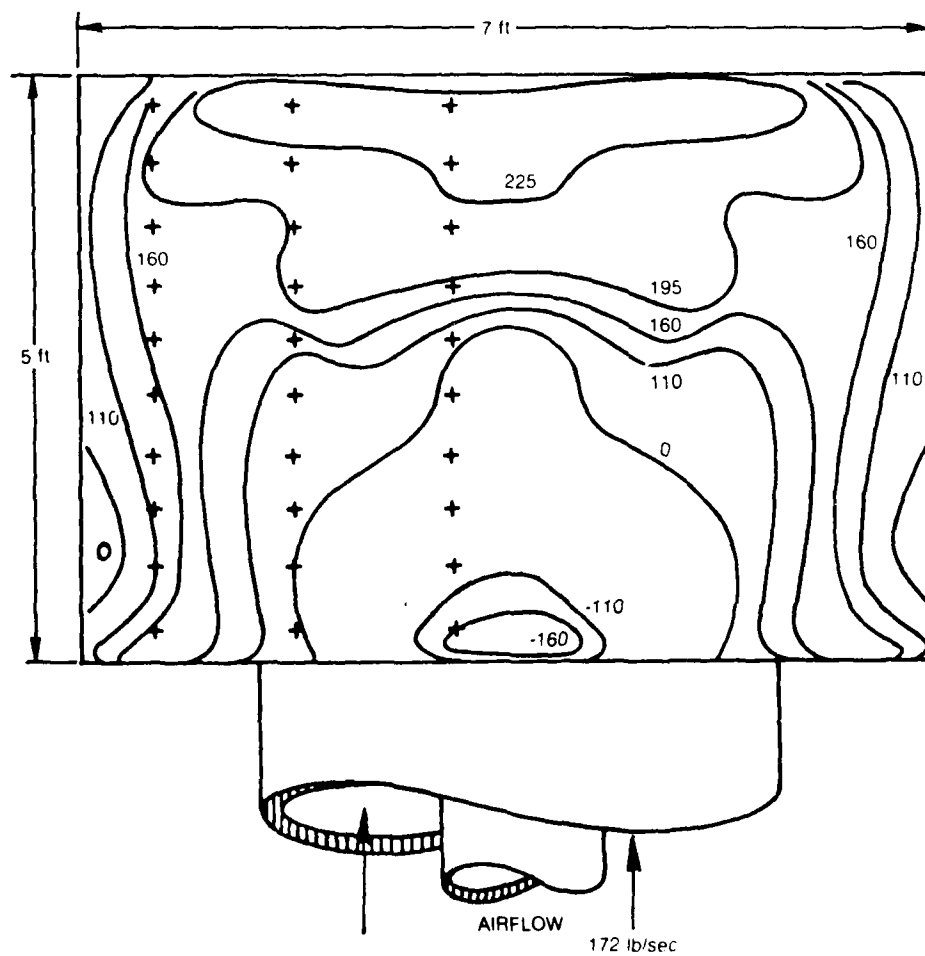
TYPICAL VELOCITY PROFILES AT THE EXIT OF GAS TURBINE

- RECTANGULAR ELBOW — DESIGN CONDITION
- VELOCITY IN ft/sec
- + INDICATES PROBE LOCATION



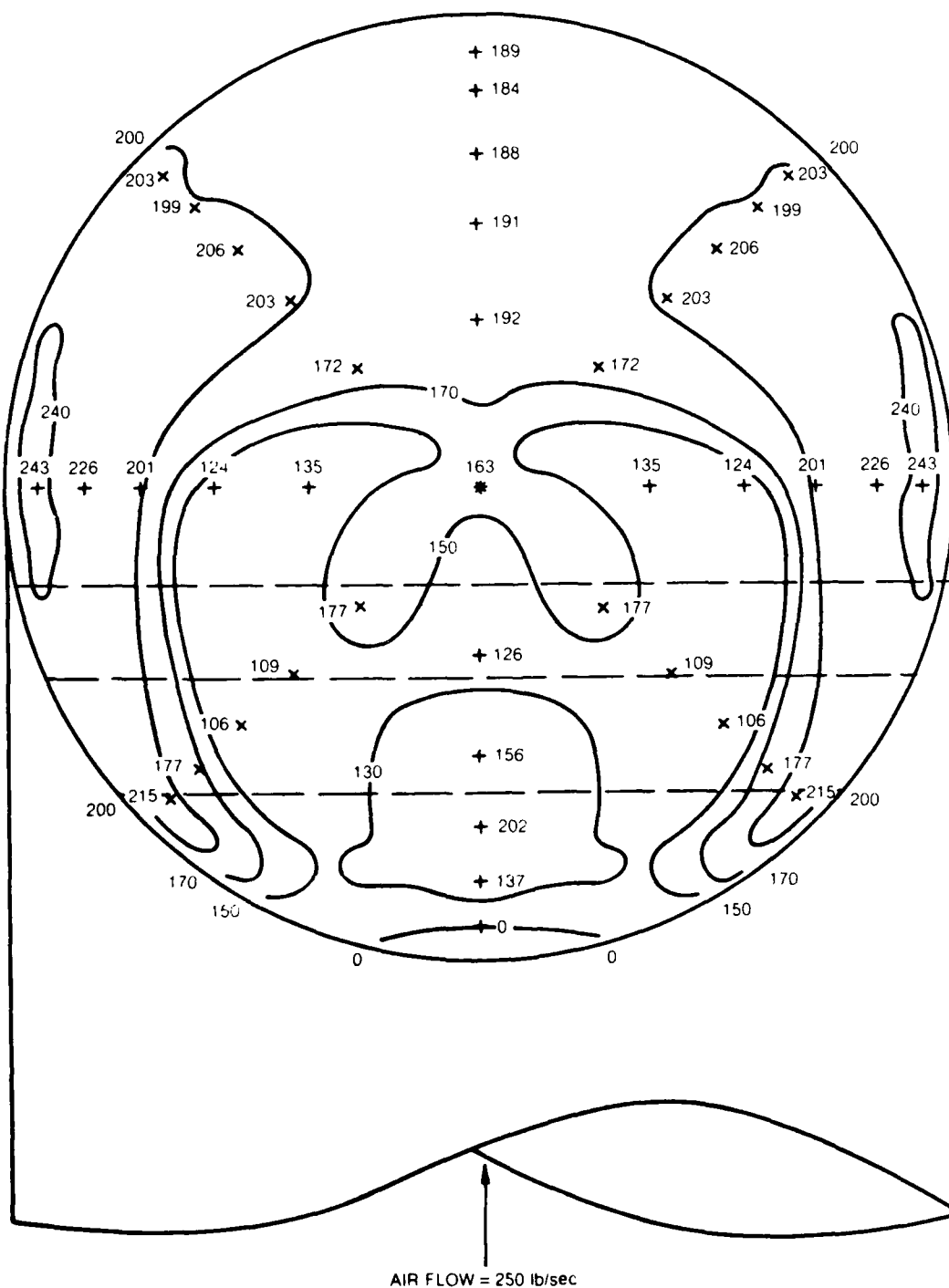
TYPICAL VELOCITY PROFILES AT THE EXIT OF GAS TURBINE

- RECTANGULAR ELBOW — OFF DESIGN CONDITION
- VELOCITY IN ft/sec



TYPICAL VELOCITY PROFILES AT THE EXIT OF GAS TURBINE CIRCULAR EXHAUST ELBOW — WITH TURNING VANES

+ INDICATES PROBE LOCATION
 — — — INDICATES TURNING VANE EXIT LOCATION

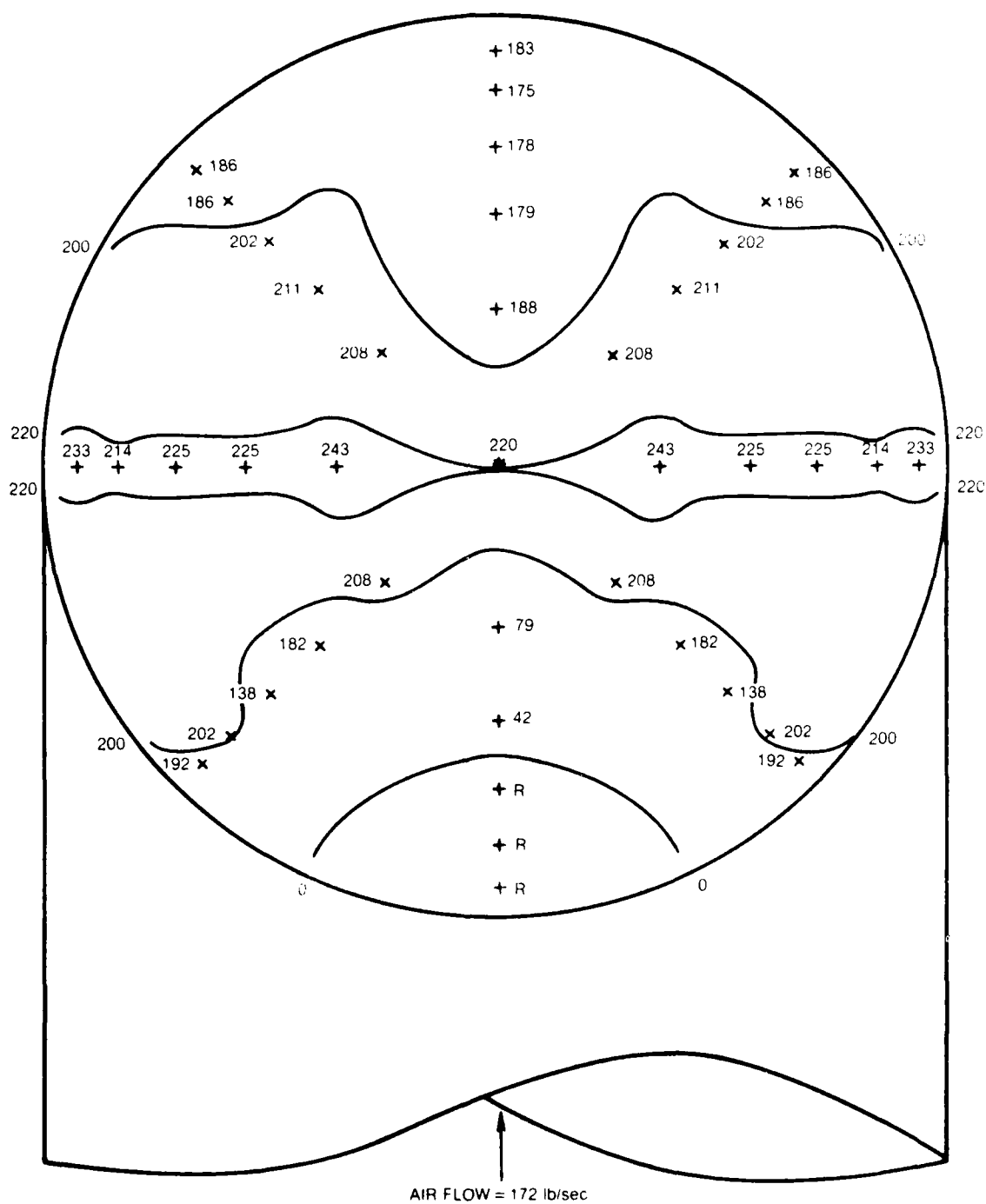


80-11-56-7

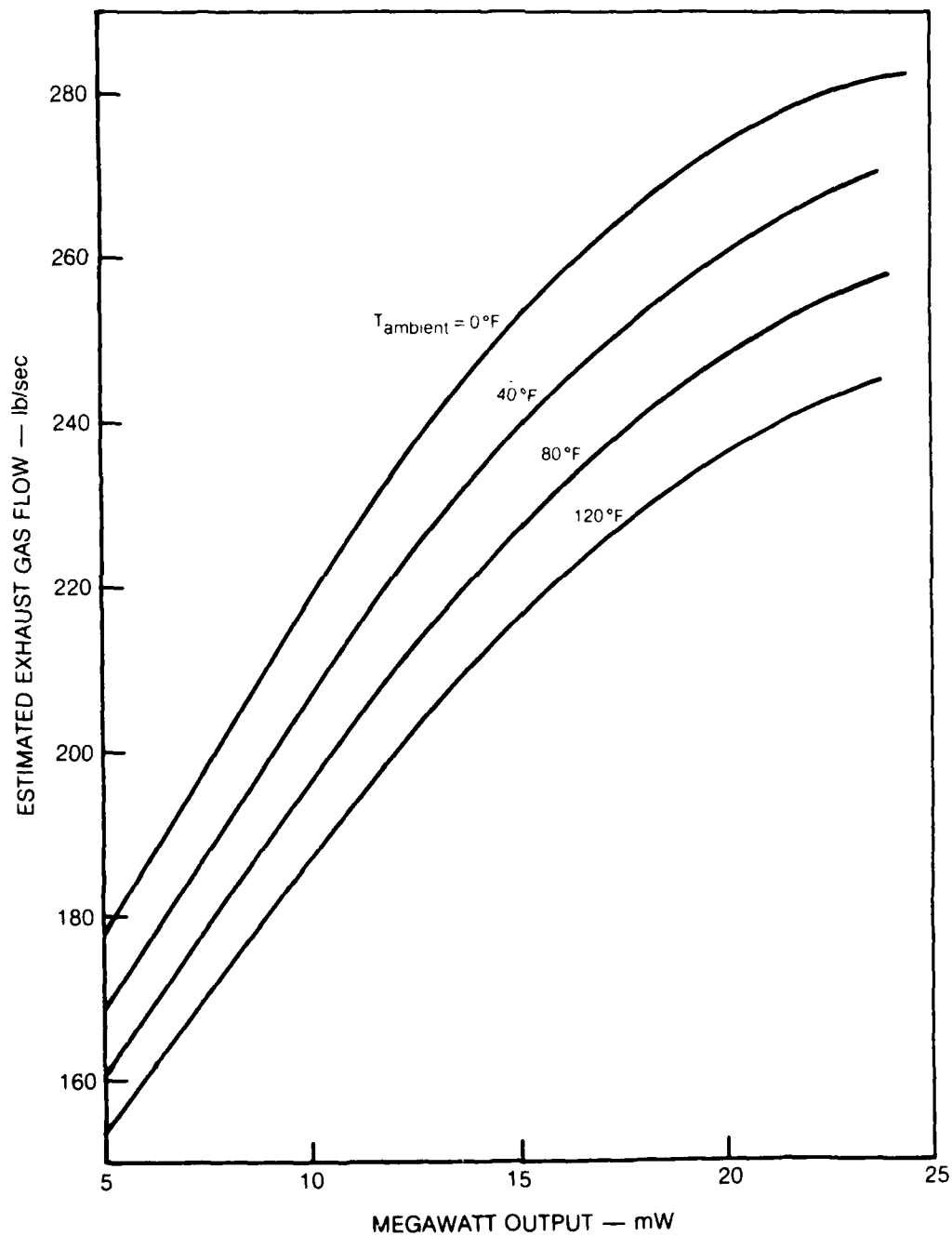
TYPICAL VELOCITY PROFILES AT THE EXIT OF GAS TURBINE CIRCULAR EXHAUST ELBOW — NO TURING VANES

+ INDICATES PROBE LOCATION

R INDICATES REVERSE FLOW



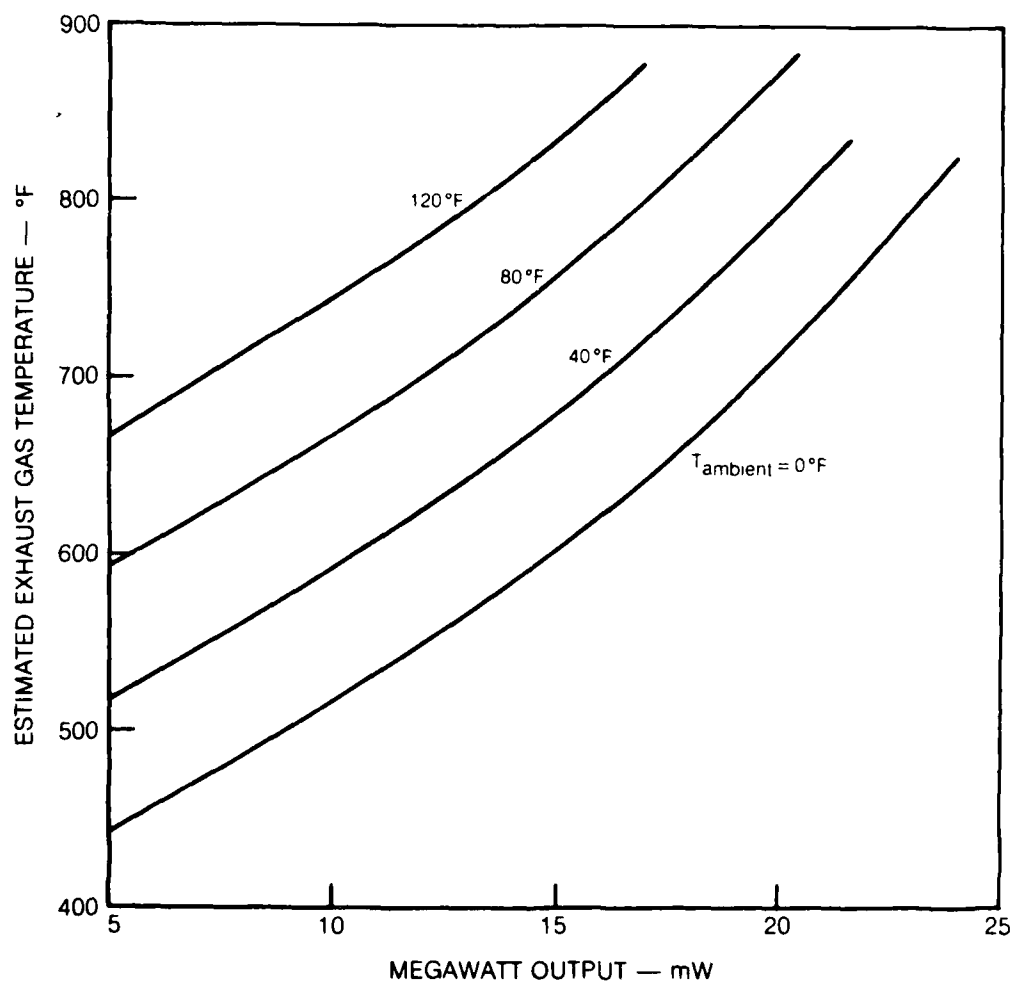
80-11-56-4

**ESTIMATED GAS FLOW vs POWER OUTPUT FOR
TYPICAL UTC-FT4 MARINE GAS TURBINE**BASED ON 4 in H_2O INLET AND 10 in H_2O EXHAUST DUCT PRESSURE LOSSES

80-11-56-10

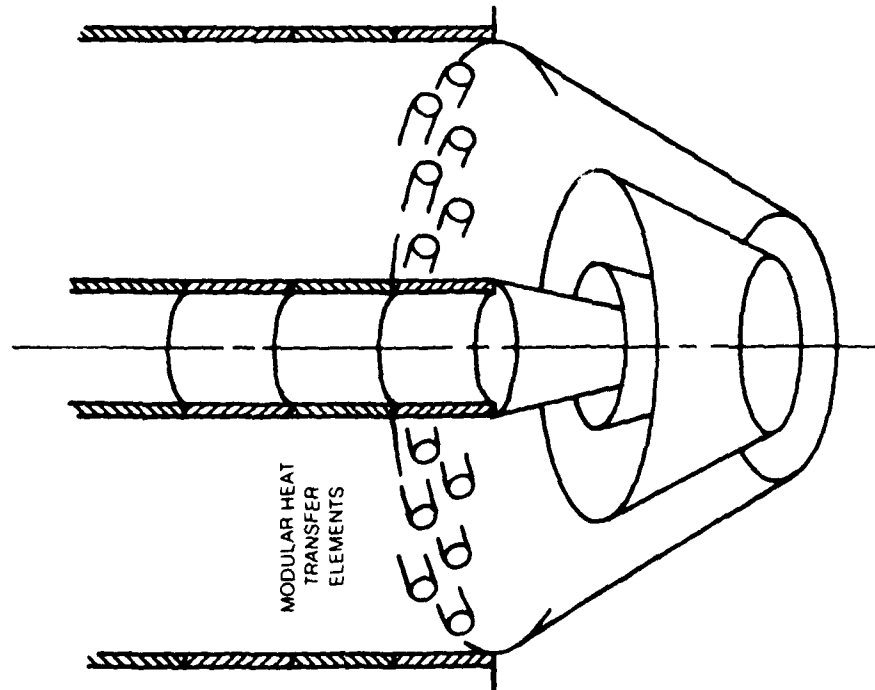
**ESTIMATED GAS TURBINE EXHAUST TEMPERATURE AT THE ELBOW EXIT
FOR TYPICAL UTC-FT4 MARINE GAS TURBINE**

BASED ON 4 in H₂O INLET & 10 in H₂O EXHAUST DUCT PRESSURE LOSSES

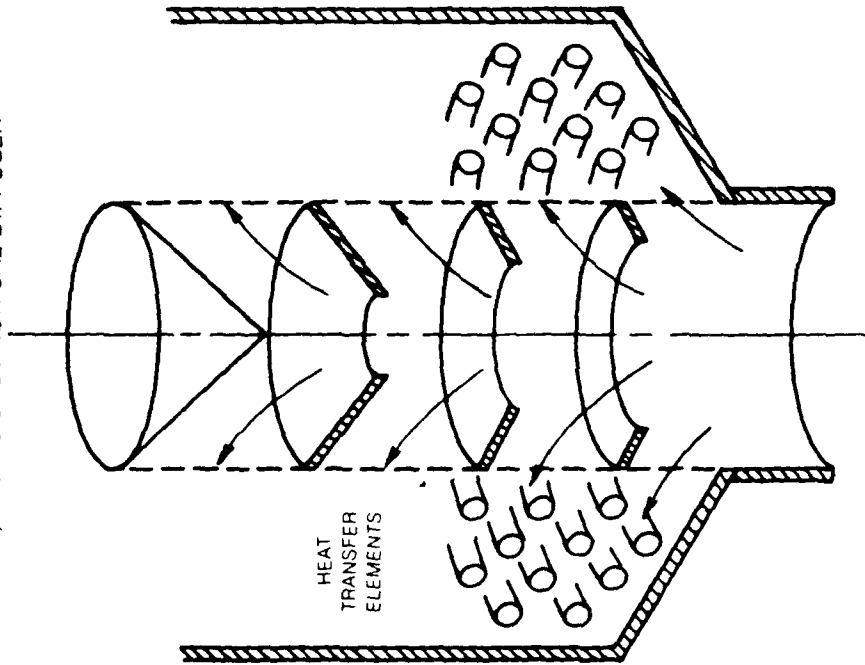


TWO-DIMENSIONAL RADIAL DIFFUSER FOR MARINE WASTE-HEAT RECOVERY SYSTEMS

a) RADIAL CONICAL DIFFUSER

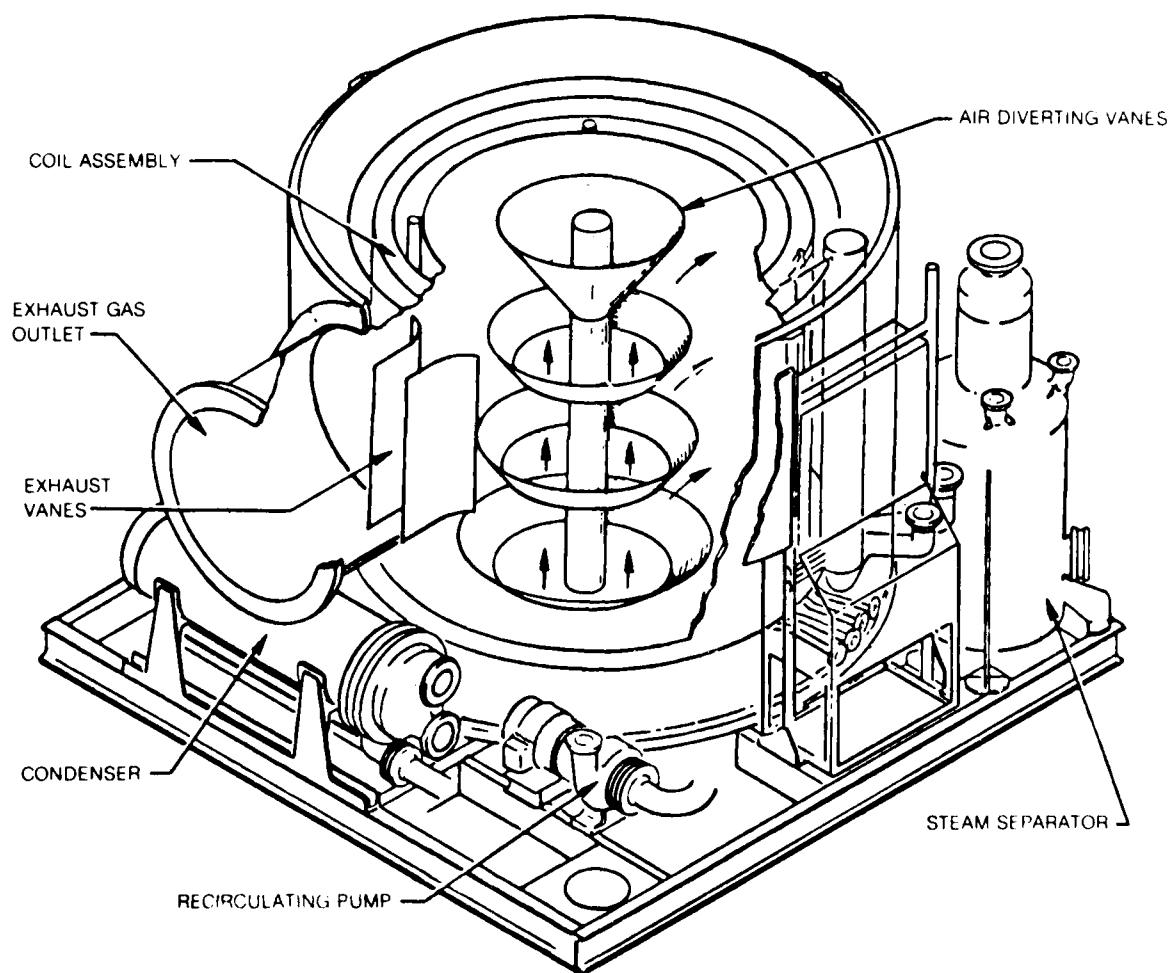


b) RADIAL CYLINDRICAL DIFFUSER



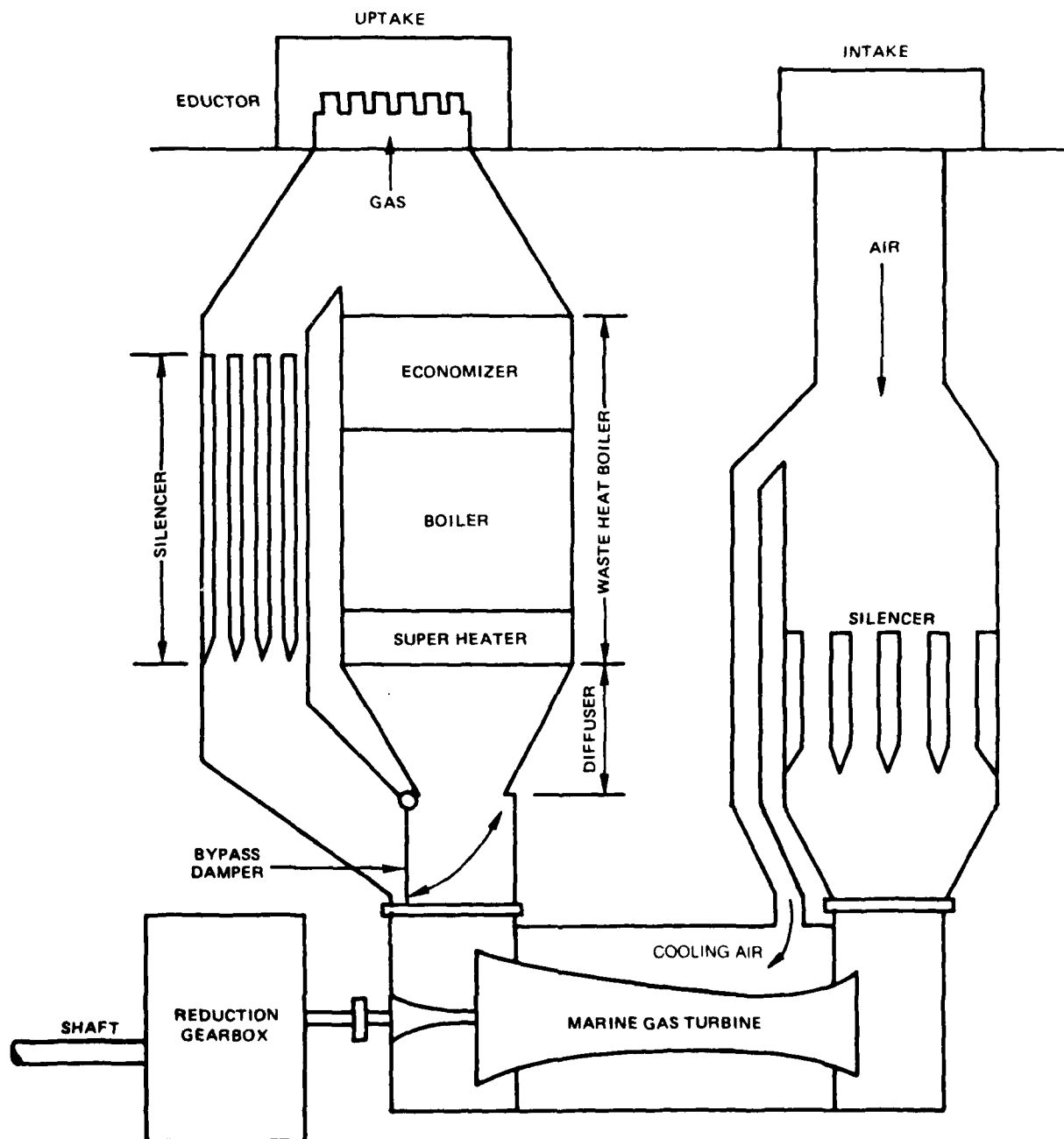
**CURRENT DESIGN CONFIGURATION OF GAS TURBINE
WASTE HEAT RECOVERY SYSTEM**

DD963 DESTROYER

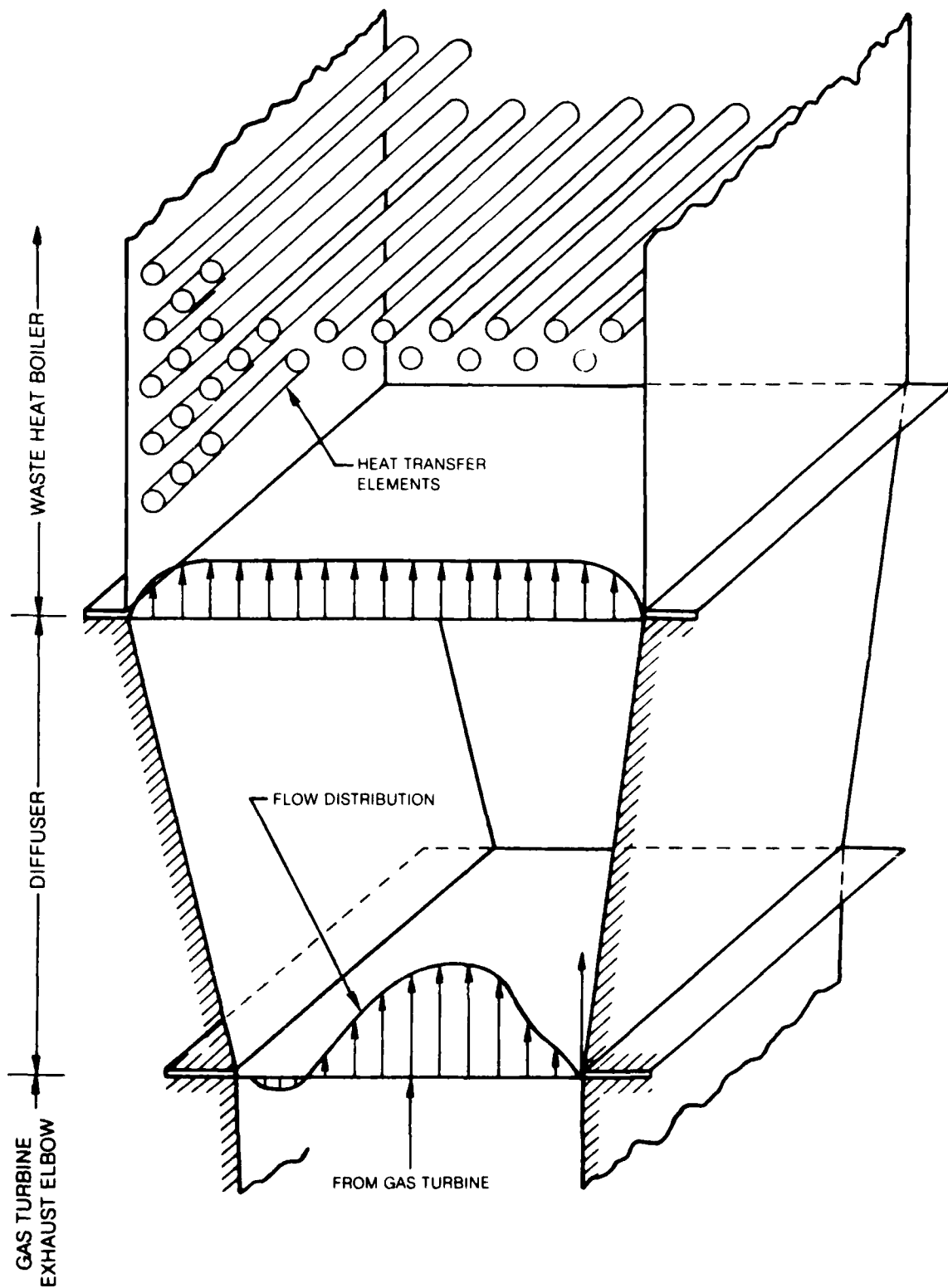


80-11-56-6

POTENTIAL LAYOUT OF COMBINED-CYCLE GAS TURBINES MARINE PROPULSION SYSTEM

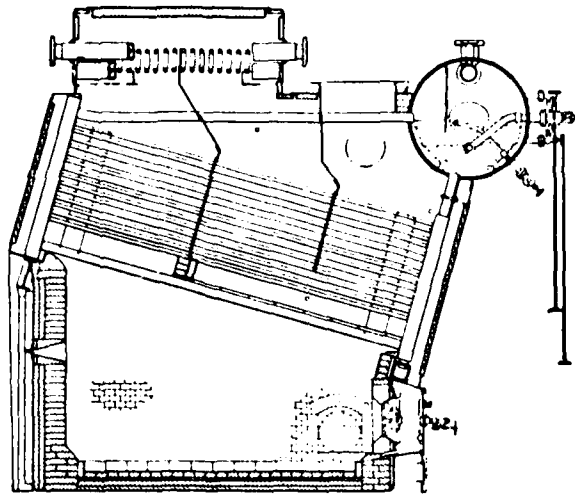


TWO-DIMENSIONAL RECTANGULAR DIFFUSER FOR MARINE WASTE-HEAT RECOVERY SYSTEM

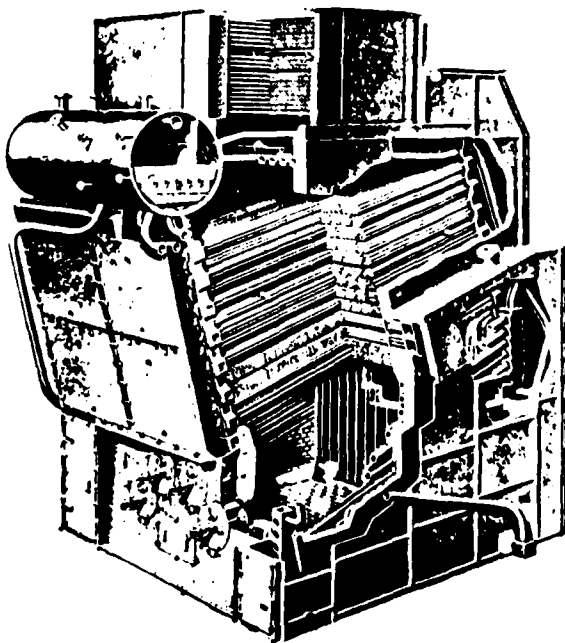


81-6-96-5

**POTENTIAL USE OF EXISTING MARINE BOILER/STEAM GENERATOR
FOR WASTE HEAT RECOVERY SYSTEM**



a) SECTIONAL-HEADER TYPE OF BOILER
DESIGNED BY B&W — SELECTED FOR ALL
LIBERTY SHIPS, WORLD WAR II



b) SINGLE-PASS HEADER-TYPE BOILER (B&W
DESIGN). THIS GENERAL TYPE WAS
INSTALLED IN THE VICTORY SHIPS

SECTION III

FORMULATION OF TWO-DIMENSIONAL TURBULENT
FLOW MODEL FOR DIFFUSERS

The unstalled or slightly stalled flow processes in two-dimensional diffusers can be represented by a set of non-linear partial differential equations derived from conservation of mass, momentum, and energy and the equation of state. The procedures of manipulating these partial differential equations into an analytical model for analyzing the flow distribution characteristics and diffuser performance of two-dimensional diffusers are presented in this section. The flow-distribution characteristics to be investigated are the velocity, the mass flux, the pressure and the temperature. The diffuser performance characteristics are presented in terms of the pressure recovery coefficient, which is defined as the ratio of the static-pressure rise to the inlet dynamic-head. The study was conducted for the nonuniform inlet flow conditions and the diffuser geometries identified in Section II.

The procedure of formulating a working model for studying flow distribution characteristics in two-dimensional diffusers consisted of three steps:

- (1) constructing an orthogonal curvilinear coordinate system for two-dimensional diffusers;
- (2) formulating a two-dimensional turbulent flow model based on orthogonal curvilinear coordinate systems;
- (3) manipulating the analytical model to obtain a set of equations that can be solved numerically by computer.

The results of this study can be plotted using either Tektronix Interactive Terminals for quick evaluation or a CALCOMP plotter for final documentation.

III.1 Streamline Orthogonal Curvilinear Coordinate System

Before a useful working model was developed, an appropriate coordinate system was chosen. It was known that the choice of coordinate system has significant importance in the calculation procedure of solving the non-linear partial differential equations for the fluid system. As mentioned earlier, the diffuser geometry for this study is arbitrary. It could be straight-wall or curved-wall annular diffusers or diffusers with a rectangular cross-section. The working model which could provide this flexibility must be based on a streamline orthogonal curvilinear coordinate system. The other advantages of using streamline coordinates can also be seen in Patankar and Spalding's book (Ref. 3.1).

There are many ways of constructing a streamline coordinate for given flow system configurations. The one used in this study was developed by Anderson (Ref. 3.2). This approach not only preserved the nature of the boundary value problem but also provided accurate, efficient, and stable numerical computations for flows at moderate to high Reynolds number in curved or straight-wall diffusers. The model has been extensively used for many in-house research projects as well as outside contract studies (Refs. 3.3 and 3.4).

However, it should be mentioned that the original program was developed for analyzing axisymmetric diffusers only. During the current study, an additional option for analyzing rectangular-cross section diffusers was added to the program. Because the program has been described in detail in Ref. 3.2, only a brief discussion is given below.

The coordinate system used in this study is expressed by "s" and "n" which stand for the velocity potential in the streamwise direction and the stream function in the normal direction, respectively. These (s, n) coordinates are related to the physical coordinate (x, y, see Fig. III.1) through LaPlace's transformation as:

$$\frac{\partial^2 n}{\partial x^2} + \frac{\partial^2 n}{\partial y^2} = 0 \quad (1)$$

$$\frac{\partial^2 s}{\partial x^2} + \frac{\partial^2 s}{\partial y^2} = 0 \quad (2)$$

The boundary conditions for Equations (1) and (2) are: 1) $n = 0$ and 1 along the two divergent walls; 2) the normal pressure gradient at the inlet and exit of the diffuser is equal to zero.

The metric scale coefficient is the same in both directions and is equal to the inverse of the magnitude of the potential flow velocity, V , which is defined as:

$$V^2 = \left(\frac{\partial n}{\partial x} \right)^2 + \left(\frac{\partial n}{\partial y} \right)^2 = \left(\frac{\partial s}{\partial x} \right)^2 + \left(\frac{\partial s}{\partial y} \right)^2 \quad (3)$$

Lengths along the streamlines and potential lines are given by:

$$ds = V dx \quad (4)$$

$$dn = V dy \quad (5)$$

and the radii of curvature of streamlines and potential lines are given by:

$$R_s = \frac{1}{V^2} \frac{\partial s}{\partial V} \quad (6)$$

$$R_n = \frac{1}{V^2} \frac{\partial n}{\partial V} \quad (7)$$

In this coordinate system, (n, s) are independent variables and (x, y) are dependent variables. Solution of the inverse problem $(x(n, s), y(n, s))$ can be obtained by conformal mapping using the Schwartz-Christoffel transformation (Ref. 3.5). If a curved-wall duct is approximately represented by straight line segments in the W -plane to form a many-sided polygon, the Schwartz-Christoffel transformation may be used to transform the interior of this polygon into the upper half of the ζ -plane (Fig. II.2). Then a point source at the origin of the ζ -plane transforms into the potential flow through the duct in the W -plane. The only approximation used in this approach involves the segmentation of the geometry, which would occur in any finite-difference solutions of Eqns (1) and (2).

III.2 Governing Equations for Two-Dimensional Diffusers

The equations of motion for a steady-state compressible flow in the (s, n) coordinates can be obtained by replacing the metric scalar coefficients h_1, h_2, h_3 by $1/V, 1/V, w$ from general orthogonal curvilinear coordinates and by making use of Eqs. (6) and (7). The resulting equations become:

Continuity Equation

$$\frac{\partial}{\partial s} \left(\frac{w \rho u_s}{V} \right) + \frac{\partial}{\partial n} \left(\frac{w \rho u_n}{V} \right) = 0 \quad (8)$$

s-Momentum Equation

$$\begin{aligned} & \rho \left[u_s V \frac{\partial}{\partial s} \left(\frac{u_s}{V} \right) + u_n V \frac{\partial}{\partial n} \left(\frac{u_n}{V} \right) - \frac{u_n^2}{R_n} + \frac{u_s u_n}{R_s} \right] \\ & = - \frac{V}{w} \frac{\partial}{\partial s} \left(\frac{\rho P}{V} \right) + \frac{V^2}{w} \left[\frac{\partial}{\partial s} \left(\frac{w \sigma'_{ss}}{V} \right) + \frac{\partial}{\partial n} \left(\frac{w \sigma'_{ns}}{V} \right) + \frac{w \sigma'_{sn}}{R_s} - \frac{w \sigma'_{nn}}{R_n} \right] \end{aligned} \quad (9)$$

n-Momentum Equation

$$\rho \left[u_s v \frac{\partial}{\partial s} (u_n) + u_n v \frac{\partial}{\partial n} (u_n) + \frac{u_s u_n}{R_n} - \frac{u_s^2}{R_s} \right] \\ = - \frac{v}{w} \frac{\partial}{\partial n} \left(\frac{w P}{v} \right) + \frac{v^2}{w} \left[\frac{\partial}{\partial s} \left(\frac{w \sigma_{sn}}{v} \right) + \frac{\partial}{\partial n} \left(\frac{w \sigma'_{nn}}{v} \right) + \frac{w \sigma_{sn}}{R_n} - \frac{w \sigma'_{ss}}{R_s} \right] \quad (10)$$

Energy Equation

$$\rho \left[u_s v \frac{\partial}{\partial s} (C_p T) + u_n v \frac{\partial}{\partial n} (C_p T) \right] = \frac{v^2}{w} \left[\frac{\partial}{\partial s} \left(\frac{w q_s}{v} \right) + \frac{\partial}{\partial n} \left(\frac{w q_n}{v} \right) \right] + \phi \quad (11)$$

Equation of State

$$P = \rho RT \quad (12)$$

where the stress tensor, σ 's strain tensors e 's, heat flux q 's, and dissipation function ϕ are defined as

$$\left. \begin{aligned} \sigma'_{ss} &= 2\mu e_{ss} - \overline{\rho u'_s u'_s} + \frac{\lambda v^2}{r} \left[\frac{\partial}{\partial s} \left(\frac{r u_s}{v} \right) + \frac{\partial}{\partial n} \left(\frac{r u_n}{v} \right) \right] \\ \sigma'_{nn} &= 2\mu e_{nn} - \overline{\rho u'_n u'_n} + \frac{\lambda v^2}{r} \left[\frac{\partial}{\partial s} \left(\frac{r u_s}{v} \right) + \frac{\partial}{\partial n} \left(\frac{r u_n}{v} \right) \right] \\ \sigma_{ns} &= \sigma_{sn} = 2\mu e_{ns} - \overline{\rho u'_s u'_n} \end{aligned} \right\} \quad (13)$$

$$\left. \begin{aligned} e_{ss} &= v \frac{\partial u_s}{\partial s} + \frac{u_n v^2}{R_s} \\ e_{nn} &= v \frac{\partial u_n}{\partial n} + \frac{u_s v^2}{R_n} \\ e_{ns} &= e_{sn} = \frac{1}{2} \left[\frac{\partial}{\partial s} (v u_n) + \frac{\partial}{\partial n} (v u_s) \right] \end{aligned} \right\} \quad (14)$$

$$\left. \begin{aligned} q_s &= KV \frac{\partial T}{\partial s} \\ q_n &= KV \frac{\partial T}{\partial n} \end{aligned} \right\} \quad (15)$$

$$\begin{aligned} \phi &= 2\mu (e_{ss}^2 + e_{nn}^2 + 2e_{sn}^2) + 2(\overline{\rho u'_s u'_s} e_{ss} + \overline{\rho u'_n u'_n} e_{nn} + 2\overline{\rho u'_s u'_n} e_{sn}) \\ &\quad + \lambda (e_{ss} + e_{nn})^2 \end{aligned} \quad (16)$$

Equations (8) to (12) form a set of governing equations which may be used to solve for five unknowns, ρ , u_s , u_n , P , and T which stand for density, velocity components along the s - and n -coordinates, static pressure and temperature, respectively. Mathematically, this set of equations is classified as elliptic and can be solved if all the boundary conditions at the inlet, the exit and the walls of diffusers are provided. However, the computation procedure would require extremely large data storage and computational time. A set of simplified governing equations was then obtained by parabolizing Eqs. (8) to (12) to facilitate the numerical computations.

The parabolization process was accomplished by employing the so-called thin-channel assumption. This is a well-justified assumption particularly when the streamline coordinate system is used. The thin-channel assumption implies that the velocity component u_n is much smaller than u_s . It also implies that the normal components of shear stress and strain tensors σ_{ss} , σ_{nn} , e_{ss} , e_{nn} are negligibly small as compared with the others. This assumption should reduce the original Navier-Stokes equations (8) to (12) to a set of parabolic equations which can be solved by a numerical forward-marching method. The parabolized governing equations are then written in non-dimensional form as:

$$\frac{\partial}{\partial S} \left(\frac{WPU_n}{V} \right) - \frac{\partial}{\partial N} \left(\frac{\partial \psi}{\partial S} \right) = 0 \quad (17)$$

$$\begin{aligned}
& PU_S \frac{\partial}{\partial S} \left(U_S \right) - \frac{V}{W} \frac{\partial U_S}{\partial N} \frac{\partial \psi}{\partial S} + \frac{1}{\gamma M_r^2} \frac{\partial \pi}{\partial S} \\
& = \frac{V}{W} \frac{\partial}{\partial N} \left\{ \frac{W}{V} \left[\frac{1}{N_R} \frac{\mu_{eff}}{\mu_r} \frac{\partial}{\partial N} (V U_S) \right] \right\} + \frac{V}{R_S} \left[\frac{1}{N_R} \frac{\mu_{eff}}{\mu_r} \frac{\partial}{\partial N} (V U_S) \right]
\end{aligned} \quad (18)$$

$$\frac{1}{\gamma M_r^2} \frac{\partial \pi}{\partial N} - \frac{P U_S^2}{V R_n} = 0 \quad (19)$$

$$\begin{aligned}
& PU_S \frac{\partial \theta}{\partial S} - \frac{V}{W} \frac{\partial \psi}{\partial S} \frac{\partial \theta}{\partial N} \\
& = \frac{V}{W} \frac{\partial}{\partial N} \left[\frac{1}{N_R N_{PT}} \left(\frac{W}{V} \right) \left(\frac{\mu_{eff}}{\mu_r} \right) \frac{\partial \theta}{\partial N} \right] + \frac{(\gamma - 1) M_r^2}{N_R} \frac{\mu_{eff}}{\mu_r} \left[\frac{\partial}{\partial N} (V U_S) \right]^2
\end{aligned} \quad (20)$$

$$\pi - P R \theta = 0 \quad (21)$$

where

$$\left. \begin{aligned}
S &= s/w_r, & N &= n/w_r, & W &= w/w_r, \\
P &= \rho/\rho_r, & U_S &= U_S/\bar{U}_r, & U_n &= U_n/\bar{U}_r, \\
\pi &= P/P_r, & \theta &= T/T_r, & N_{PT} &= \mu_{eff} c_p/k \\
N_R &= \rho_r \bar{U}_r w_r / M_r, & M_r^2 &= \rho_r \bar{U}_r^2 / P_r = \bar{U}_r^2 / \gamma R T
\end{aligned} \right\} \quad (22)$$

and the stream function, which satisfies the continuity equation, was defined as:

$$\left. \begin{aligned} \frac{\partial \psi}{\partial S} &= - \frac{PRU_n}{V} \\ \frac{\partial \psi}{\partial N} &= \frac{PRU_s}{V} \end{aligned} \right\} \quad (23)$$

In Eq. (22), the reference quantities (with subscript r) of all thermodynamic quantities are based on standard sea-level atmosphere conditions (at a pressure of 2117 lbf/ft² and a temperature of 540°R), w_r and \bar{u}_r represent the diffuser inlet width and mean inlet velocity, respectively. The effective turbulent viscosity, μ_{eff} , was defined as:

$$\mu_{eff} = \left[\nu \frac{\partial}{\partial n} (v_{us}) - \overline{cu'_s u'_n} \right] / \frac{\partial}{\partial n} (v_{us}) \quad (24)$$

which will be determined in the next section when the turbulence model is selected. The boundary conditions for Eqs. (17) through (21) are given as:

$$\left. \begin{aligned} U_s = U_n = 0, \quad T = T_w \text{ at } N = 0 \text{ and } N = 1 \\ U_s, P, T \text{ as function of } N \text{ are specified at } S = 0 \end{aligned} \right\} \quad (25)$$

Before Eqns. (17) through (21) are put into finite-difference form, two important facts about this parabolization process should be mentioned. The first one concerns the feasibility of the parabolized Navier-Stokes Equations. As indicated in Ref. 3.2, the parabolization process did not actually change the original elliptic nature of the flow system because of the choice of streamline coordinates. These streamline coordinates were actually obtained by solving the elliptic Eqns (1) and (2) based on potential flow theory. Secondly, the parabolized governing equations imposed certain restrictions if it is desired to set the downstream static pressure conditions. Because the objective of the parabolization process was to manipulate the governing equations such that they can be solved by forward-marching methods, therefore not all initial conditions can satisfy the pre-specified downstream conditions. A practical procedure to solve this problem is to fix the inlet stagnation pressure and temperature and vary the inlet static pressure until downstream static pressure conditions are satisfied. The purpose of this procedure is to let the downstream static pressure set the mass flow rate.

III.3 Turbulent Flow Model

In order to solve Eqs. (17) through (21), the effective viscosity, μ_{eff} , must first be determined. If the flow is laminar, μ_{eff} becomes the same as laminar viscosity which can then be calculated easily. For turbulent flow, precise knowledge regarding μ_{eff} is not available, so a well-justified semi-empirical model is to be chosen for this study.

More than a dozen turbulence models have been proposed so far (Ref. 3.6), and what constitutes the "best" model of turbulence will differ according to the problem under consideration. The turbulent flow model used in the present study is the same as that used by Smith (Ref. 3.7) who assumed that the inner layer region of the turbulent flow is governed by Prandtl's mixing length theory with a Van Driest damping factor and that the outer-layer region is governed by an eddy model proposed by Clauser (Ref. 3.8). Based on this assumption, the effective viscosity for the inner and outer region of the flow fields are given respectively as:

$$\mu_{eff} = \mu \left\{ 1 + 0.16 y_t \left[1 - \exp(-y_t \sqrt{\tau_t} / 26) \right]^2 \frac{du_t}{dy_t} \right\} \quad (26)$$

$$\mu_{eff} = .008 \mu N_R \rho w (u_\infty - \bar{u}) \quad (27)$$

where μ represents the molecular viscosity and u_t , y_t are defined as

$$\left. \begin{aligned} u_t &= u / \sqrt{\tau_w} / \rho \\ y_t &= n \sqrt{\tau_w} \rho / \mu \\ \tau_t &= \tau / \tau_w \end{aligned} \right\} \quad (28)$$

The subscript ∞ and w represent the maximum and wall values at a given streamline station. \bar{u} represents the averaged velocity across the diffuser width, w . N_R stands for Reynolds number which is calculated based on averaged flow properties. The empirical constants, 0.16, 26 and 0.008 which appear in Eqs. (26) and (27) are the values suggested in Ref. 3.2.

In the region near the wall, the independent variables and their derivatives change rapidly and numerical solution is difficult without using a large number of closely spaced mesh points. This is done by using an exponential transformation (also called Robert's Transformation) given by:

$$\eta = \frac{(C+0.5) \exp \left[(2\eta-1) \ln \left(\frac{C+0.5}{C-0.5} \right) \right] - (C-0.5)}{1 + \exp \left[(2\eta+1) \ln \left(\frac{C+0.5}{C-0.5} \right) \right]} \quad (29)$$

where $\eta = nk/k_L$, $k = 1, 2, 3 \dots k_L$ represents the number of points to be placed across the diffuser height. The parameter C is chosen so as to place the first mesh point at approximately $y_t = 1$.

III.4 Method of Solution

Equations (17) through (21) were solved by the explicit numerical method as described in Refs. 3.9 and 3.10. This method has been used with success in many previous studies (Ref. 3.9 to 3.11). With this method, the solution for the dependent variables (P , ψ , U_s , π , ϕ) and their normal derivatives are presumed known from previous calculations for input data up to station S . Using the forward-marching numerical method, the solutions of the equations for the next station are obtained and the process is continued until it reaches the exit of the diffuser, or until flow separation or reverse-flow conditions occur.

Mach-Number Transformation

To solve Eqs. (17) through (21) numerically, experience indicated that, at low Mach number, a small variation of pressure and temperature within the diffuser could lead to large errors in the results if the actual pressure (π) and temperature (ϕ) were used. Therefore, new dependent variables for pressure and temperature ($\bar{\pi}$, $\bar{\phi}$) were introduced using the so-called Mach number transformation defined as follows:

$$\left. \begin{aligned} \pi &= \bar{\pi} + \gamma M_r^2 \tilde{\pi} \\ \theta &= \bar{\theta} + (\gamma-1) M_r^2 \tilde{\theta} \end{aligned} \right\} \quad (30)$$

where $\bar{\pi}$ and $\bar{\phi}$ are the mean pressure and temperature at the diffuser inlet. After substitution of Eqs. (29), (30), and (23) and after some rearrangements, Eqs. (17) through (21) become:

$$\frac{\partial \psi}{\partial N} - \frac{P W U_s}{V} = 0 \quad (31)$$

$$\frac{\partial \Sigma}{\partial N} + \frac{V \Sigma}{R_s} - \frac{W}{V} \frac{\partial \tilde{\pi}}{\partial S} - \frac{\partial \psi}{\partial N} \frac{\partial U_s}{\partial S} + \frac{\partial \psi}{\partial S} \frac{\partial U_s}{\partial N} = 0 \quad (32)$$

$$\frac{\partial \tilde{\pi}}{\partial N} \frac{P U_s^2}{V R_s} = 0 \quad (33)$$

$$\frac{\partial Q}{\partial N} - \frac{\partial \psi}{\partial N} \frac{\partial \tilde{\theta}}{\partial S} + \frac{\partial \psi}{\partial S} \frac{\partial \tilde{\theta}}{\partial N} + \Sigma \frac{\partial (V U_s)}{\partial N} = 0 \quad (34)$$

$$\tilde{\pi} = \frac{\gamma-1}{\gamma} P R \tilde{\theta} \quad (35)$$

where

$$\Sigma = \frac{W}{V} \frac{\mu_{eff}}{\mu_r} \frac{1}{N_R} \frac{\partial (V U_s)}{\partial N} \quad (36)$$

$$Q = \frac{W}{V} \frac{\mu_{eff}}{\mu_r} \frac{1}{N_R N_{PT}} \frac{\partial \tilde{\theta}}{\partial N} \quad (37)$$

Finite Difference Equations

Equations (31) through (37) are further reduced to finite-difference form so that they can be solved by computer. The finite-differencing process is essentially a linearization process which can be accomplished by making use of the Taylor series expansion formula and the backward difference approximation. As suggested by Briley and McDonald (Refs. 3.9 and 3.10), we first introduce the following notation and product rules:

$$\Delta S = \Delta S^j = S^j - S^{j-1}$$

$$\Delta N = \Delta N_k = N_k - N_{k-1}$$

$$S^{j-1/2} = \frac{1}{2} (S^j - S^{j-1})$$

$$N_{k-1/2} = \frac{1}{2} (N_k - N_{k-1})$$

$$F^{j-1/2} = \frac{1}{2} (F^j + F^{j-1})$$

$$F_{k-1/2} = \frac{1}{2} (F_k + F_{k-1})$$

$$\left(\frac{\partial F}{\partial S} \right)_k^j = \frac{F_k^j - F_k^{j-1}}{\Delta S^j}$$

$$\left(\frac{\partial F}{\partial N} \right)_k^j = \frac{F_k^j - F_{k-1}^j}{\Delta N_k}$$

(38)

$$(FG)^j = F^j G^{j-1} + F^{j-1} G^j - (FG)^{j-1}$$

$$(FG)^{j-1/2} = \frac{1}{2} (F^j G^{j-1} + F^{j-1} G^j)$$

$$(FGH)^j = F^{j-1} G^{j-1} H^j + F^j G^{j-1} H^{j-1} + F^{j-1} G^j H^{j-1} - 2F^j G^j H^j$$

(39)

$$\left(F \frac{\partial G}{\partial S} \right)_k^{j-1/2} = F_k^{j-1} \frac{G^j - G^{j-1}}{\Delta S^j}$$

where j represents the streamwise mesh-point number which varies from 2 to j_L and k represents the transverse mesh point which varies from 2 to k_L . F , which is a function of (S, N) , stands for independent variables ψ , U_s , etc. The product rules presented in Eq. (39) were obtained by Taylor series expansion and three-point, second-order finite approximation.

With Eqs. (38) and (39) in hand, we can reduce the governing equations (31) through (37) into finite-difference form. After replacing U_s by U for easy typing, and rearranging the explicit terms such that the unknown quantities are kept on the left-hand side of the equation and the known quantities are moved to the right-hand side, the governing equations become:

$$\begin{aligned} \psi_k^j - \psi_{k-1}^j - \frac{\Delta N}{2} \left(\frac{W}{V} \right)_{k-1/2}^j & \left[\left(P_k^j - P_{k-1}^j \right) U_{k-1/2}^{j-1} + P_{k-1/2}^{j-1} \left(U_k^j - U_{k-1}^j \right) \right] \\ & = - \Delta N \left(\frac{W}{V} \right)_{k-1/2}^j (PU)_{k-1/2}^{j-1} \end{aligned} \quad (40)$$

$$\begin{aligned} & \left[1 + \frac{\Delta N}{2} \left(\frac{V}{R_s} \right)_{k-1/2}^j \right] \Sigma_k^j - \left[1 - \frac{\Delta N}{2} \left(\frac{V}{R_s} \right)_{k-1/2}^j \right] \Sigma_{k-1}^j - \frac{\Delta N}{\Delta S} \left(\frac{W}{V} \right)_{k-1/2}^j \left(\tilde{\pi}_k^j + \tilde{\pi}_{k-1}^j \right) \\ & - \frac{1}{\Delta S} \left(\psi_k^{j-1} - \psi_{k-1}^{j-1} \right) \left(U_k^j + U_{k-1}^j \right) + \frac{1}{\Delta S} \left(U_k^{j-1} - U_{k-1}^{j-1} \right) \left(\psi_k^j + \psi_{k-1}^j \right) \\ & = - \left[1 + \frac{\Delta N}{2} \left(\frac{V}{R_s} \right)_{k-1/2}^j \right] \Sigma_k^{j-1} + \left[1 - \frac{\Delta N}{2} \left(\frac{V}{R_s} \right)_{k-1/2}^j \right] \Sigma_{k-1}^{j-1} + \frac{\Delta N}{\Delta S} \left(\frac{W}{V} \right)_{k-1/2}^j \left(\tilde{\pi}_k^{j-1} + \tilde{\pi}_{k-1}^{j-1} \right) \\ & - \frac{1}{\Delta S} \left(\psi_k^{j-1} - \psi_{k-1}^{j-1} \right) \left(U_k^{j-1} + U_{k-1}^{j-1} \right) + \frac{1}{\Delta S} \left(U_k^{j-1} - U_{k-1}^{j-1} \right) \left(\psi_k^{j-1} + \psi_{k-1}^{j-1} \right) \end{aligned} \quad (41)$$

$$\begin{aligned}
\tilde{\pi}_k^j - \tilde{\pi}_{k-1}^j - \frac{\Delta N}{2} \left(\frac{1}{VR_S} \right)^j_{k-1/2} \left[2 \left(PU \right)_{k-1/2}^{j-1} \left(U_k^j + U_{k-1}^j \right) + \left(UU \right)_{k-1/2}^{j-1} \left(P_k^j - P_{k-1}^j \right) \right] \\
= - 2\Delta N \left(\frac{1}{VR_S} \right)^j_{k-1/2} \left(PU^2 \right)_{k-1/2}^{j-1}
\end{aligned} \tag{42}$$

$$\begin{aligned}
Q_k^j - Q_{k-1}^j - \frac{1}{\Delta S} \left[\left(\psi_k^{j-1} - \psi_{k-1}^{j-1} \right) \left(\theta_k^j + \theta_{k-1}^j \right) + \left(\theta_k^{j-1} - \theta_{k-1}^{j-1} \right) \left(\psi_k^j + \psi_{k-1}^j \right) \right] \\
+ \Sigma_{k-1/2}^{j-1} \left[\left(VU \right)_k^j - \left(VU \right)_{k-1}^j \right] \\
= Q_k^{j-1} - Q_{k-1}^{j-1} - \frac{1}{\Delta S} \left[\left(\psi_k^{j-1} - \psi_{k-1}^{j-1} \right) \left(\theta_k^{j-1} + \theta_{k-1}^{j-1} \right) + \left(\theta_k^{j-1} - \theta_{k-1}^{j-1} \right) \left(\psi_k^{j-1} + \psi_{k-1}^{j-1} \right) \right] \\
+ \Sigma_{k-1/2}^{j-1} \left[\left(VU \right)_k^{j-1} - \left(VU \right)_{k-1}^{j-1} \right]
\end{aligned} \tag{43}$$

$$\pi_k^j = \frac{\gamma-1}{r} R \left[\tilde{\theta}_k^{j-1} \tilde{p}_k^j + p_k^{j-1} \tilde{\theta}_k^j \right] = - \frac{\gamma-1}{\gamma} R \left[P \tilde{\theta} \right]_k^{j-1} \tag{44}$$

$$\Sigma_k^j + \Sigma_{k-1}^j - \frac{2}{\Delta N} \left[\frac{W}{V} \frac{\mu_{eff}}{\mu_r} \frac{1}{N_R} \right]_{k-1/2}^{j-1} \left[\left(VU \right)_k^j - \left(VU \right)_{k-1}^j \right] = 0 \tag{45}$$

$$Q_k^j + Q_{k-1}^j - \frac{2}{\Delta N} \left[\frac{W}{V} \frac{\mu_{eff}}{\mu_r} \frac{1}{N_R N_{PT}} \right]_{k-1/2}^{j-1} \left[\theta_k^j - \theta_{k-1}^j \right] = 0 \tag{46}$$

The boundary conditions of Eqs (23) and (29) can also be written in finite-difference form as

$$\psi_1^j = \psi_{w1}^j, \quad U_1^j = 0, \quad \tilde{\theta}_1^j = (\theta_w^j - \bar{\theta}_r)/(\gamma-1) M_r^2 \quad (47)$$

$$\psi_{k_\ell}^j = \psi_{k_\ell}^j, \quad U_{k_\ell}^j = 0, \quad \tilde{\theta}_{k_\ell}^j = (\theta_w^j - \bar{\theta}_r)/(\gamma-1) M_r^2$$

Note that Eq. (44) involves only k^{th} mesh point, but this equation can also be used to represent the boundary conditions if the subscripts of k are replaced by 1, and k_ℓ . The resulting boundary condition equations become:

$$\tilde{\pi}_1^j - \left(\frac{\gamma-1}{\gamma} R Q_1^{j-1} \right) P_1^j - \left(\frac{\gamma-1}{\gamma} R P_1^{j-1} \right) \tilde{\theta}_1^j = - \frac{\gamma-1}{\gamma} R (P \tilde{\theta})_1^{j-1} \quad (48)$$

$$\tilde{\pi}_{k_\ell}^j - \left(\frac{\gamma-1}{\gamma} R \tilde{\theta}_{k_\ell}^{j-1} \right) P_{k_\ell}^j - \left(\frac{\gamma-1}{\gamma} R P_{k_\ell}^{j-1} \right) \tilde{\theta}_{k_\ell}^j = - \frac{\gamma-1}{\gamma} R (P \tilde{\theta})_{k_\ell}^{j-1} \quad (48)$$

Matrix Equations

Now Eqs. (40) through (46) contain seven unknowns. If we let them be expressed by a column matrix \bar{F}^j as:

$$\bar{F}_k^j = \left(\psi_k^j, U_k^j, \tilde{\pi}_k^j, \tilde{\theta}_k^j, P_k^j, \Sigma_k^j, Q_k^j \right)^T \quad (49)$$

Then the finite-difference equations in matrix form become:

$$\bar{G}_k^{j-1} \bar{F}_k^j - \bar{H}_k^{j-1} \bar{F}_{k-1}^j = \bar{I}_k^{j-1} \quad (50)$$

where \bar{G}_k^{j-1} and \bar{H}_k^{j-1} are 7×7 matrices representing the coefficients of the dependent variables and \bar{I}_k^{j-1} is also a 7×7 matrix representing the known quantities either from the initial condition (Eq. 23) or from results of previous calculations. The boundary conditions, Eqs. (47) and (48) are 4×7 matrices and are expressed as

$$\left. \begin{aligned} \bar{B}_1 \bar{F}_1 &= \bar{C}_1 \\ \bar{B}_{k_\ell} \bar{F}_{k_\ell} &= \bar{C}_{k_\ell} \end{aligned} \right\} \quad (51)$$

Combining Eqs. (50) and (51), we have a complete set of matrix equations as:

$$\bar{A} \bar{F} = \bar{Q} \quad (52)$$

$$\bar{A} = \left\{ \begin{array}{ccccccc} \bar{B}_1 & 0 & 0 & & & & 0 \\ 0 & -\bar{H}_1 & \bar{G}_1 & 0 & & & \\ & 0 & -\bar{H}_2 & \bar{G}_2 & 0 & & \\ & & 0 & -\bar{H}_k & \bar{G}_k & 0 & \\ 0 & & & 0 & -\bar{H}_{k_\ell} & \bar{G}_{k_\ell} & 0 \\ & & & & 0 & 0 & \bar{B}_{k_\ell} \end{array} \right\} \quad (53)$$

$$\bar{Q} = \left(\bar{C}_1, \bar{I}_k, \bar{C}_{k_\ell} \right)^T \quad (54)$$

Equation (52) can be solved efficiently using a standard block-elimination method such as the matrix factorization method discussed by Isaacson and Keller (Ref. 3.12), and Varah (Ref. 3.13).

Pressure-Recovery Coefficient

Following the standard definition of the pressure-recovery coefficient, we have:

$$C_p = \frac{\bar{P} - \bar{P}_r}{\rho \bar{u} / 2} \quad (55)$$

If the fluid flows through the diffuser were incompressible, inviscid, and of uniform distribution, then Eq. (55), with the application of continuity and Bernoulli's equations, can be reduced to the following form:

$$(C_p)_i = 1 - \left(\frac{A_r}{A} \right)^2 \quad (56)$$

where A and A_r represent the local and inlet area of the diffuser, respectively, and the subscript, i , indicates that C_p is calculated based on a one-dimensional,

ideal-flow assumption. In reality, because of the effects of friction and the flow blockage appearing in the boundary layer, the velocity distribution is rarely uniform. The calculated C_p will never be the same as $(C_p)_i$.

Wall Stress Calculation

If the boundary layer displacement thickness at the diffuser inlet were given, the values of shear stress along the two divergent walls can be computed with the two-dimensional flow model discussed in Sections III.2, III.3, and III.4. The drag force along these two walls can then be determined by summing up the calculated shear stress.

However, the shear stress along the two parallel walls is not available because of the assumed two-dimensional flow model. In order to include the shear stress on the two parallel walls of the flow field, a simplified correction procedure was established based on the following two assumptions: 1) the growth of the boundary layer thickness along the two parallel walls is much smaller than that along the two divergent walls; and 2) the local drag coefficient along the two parallel walls can be represented by the 1/7-th-power velocity-distribution law. With these two assumptions, Eqs. (21.6) and (21.2) of Ref. 3.14 can be used for calculating the boundary layer displacement thickness and local drag force for the two parallel walls. When written in finite-difference form, they become:

$$\delta_k^j = \left[\left(\delta_k^{j-1} \right)^{5/4} + .289 (\Delta s) \left(\frac{u_k^{j-1}}{p_k^{j-1} u_k^{j-1}} \right)^{1/4} \right]^{4/5} \quad (57)$$

$$D_k^j = \frac{\Delta N}{72} p_k^{j-1} (u_k^{j-1})^2 \left[\delta_k^j - \delta_k^{j-1} \right] \quad (58)$$

The pressure and velocity distribution profiles obtained from matrix equation, (Eq. 52), are then corrected locally using Eqs. (57) and (58). The diffuser performance characteristics were calculated by mass-flow-weighted integration methods.

III.5 Flow Distribution Computer Program

The two-dimensional turbulent flow model discussed above has been implemented in FORTRAN language on a UNIVAC 1110/80 computer system to facilitate

the diffuser performance analysis. Many existing subroutines developed by Anderson (Ref. 3.4) were used to minimize the program development effort. The structure and capabilities of the program and format of input data are presented in the sections which follow.

Structure

The overall structure of the computer programs for the flow distribution control study can be depicted by Fig. III.3. Located in the far left center of the figure is the main program which reads, checks, and interprets the input data and sets up the common block for the subroutines which are then called by the main program to perform specific tasks. Based on the two-dimensional potential flow theory, inviscid flow theory, and turbulent flow theory discussed earlier, three major subroutines called COORST, CALINV, and CALVIS are used to compute the flow-field coordinate system, the flow-distribution characteristics (velocity, density, pressure, and temperature, etc.) based on inviscid flow assumptions and turbulent viscous-flow assumptions, respectively. To reduce unnecessary repetition of computation, the program was structured such that it can be stopped at the end of each subroutine. The results computed by each subroutine are stored on a catalogued storage file, called units 8, 9, 12 and 22, respectively. In addition, the program also prints information on the status of the execution process as well as the computed results through a high-speed printer.

Unit-9 which is a storage file created by subroutine COORST, contains the flow field coordinate systems. It can be read either by subroutine CALINV or CALVIS. Using the coordinate system data and the inlet-flow conditions, the subroutine CALINV will calculate the inviscid-flow solution and store the results on unit 22, and similarly the subroutine CALVIS will store the viscous-flow results on unit 8. The mass-flow-weighted diffuser performance characteristics computed by both CALINV and CALVIS routines are stored in unit 12.

An independent program, which is not shown in Fig. III.3, was also developed to read those output data files and either print the results using a high-speed printer or plot them on a Tetronix Interactive Terminal or a CALCOM plotter.

Capability

Although the program was developed with allowance for expansion to analyze any compressible gas, the working fluid for the present study is assumed to be air. The flow is subsonic and turbulent. The flow can be uniformly or nonuniformly distributed in the transverse direction but is generally flowing in the axial direction along the diffusers with a moderate to high Reynolds number.

The program can analyze both annular and rectangular cross-section diffusers. The rectangular-cross-section diffuser must be formed by two divergent and two parallel walls so that it can be treated as a two-dimensional flow system. The shape of the two divergent walls can be straight, curved, or zig-zag. For an annular diffuser with no centerbody, a zero radius must be specified.

An important restriction to the computer program is that the inlet and exit flow must have no normal pressure-gradients produced by streamline curvature. To analyze diffusers which do not satisfy this requirement, one must properly extend the diffuser walls at the inlet or exit to approximate the streamline curvatures so that the normal pressure gradient can be maintained.

The maximum number of grid points (k_l) across the diffuser is 130 and the maximum number of streamline stations (j_l) along the diffuser is 100. To reduce the truncation error associated with the finite-differencing process of the governing equations, the increment between the two streamlines (Δk_i and/or between the two streamlined station (Δj_i) can be further divided into several substeps through a built-in parameter in group-3 of the input data. The flow-field coordinate system, the first- and second-order derivatives of coordinate systems, and the flow properties and parameters, are calculated for each grid point and stored on the output data storage files. However, the results calculated for the substeps are used as input to the next station only, and are not stored.

Input Data

Because the program was implemented on UNIVAC 1110/80 computer systems, UNIVAC EXEC-8 job control languages (JCL) are used for running the program. The program file and the output data files (units 8, 9, 12 and 22) must be catalogued beforehand and must be assigned each time when the program is being executed. A typical runstream is shown in Fig. III.4 where the first 10 statements with a special prefixed character, @, are the JCL cards and the rest of the runstream are the input-data cards. The input data are punched on standard 80-column BCD cards to provide the vital information for the program. These input data are divided into six groups:

- Group 1: which is punched on one BCD card and contains up to 72 characters to be used as the job title.
- Group 2: which consists of six option parameters and is also punched on one BCD card. These option parameters are used for selecting: 1) diffuser types, annular or rectangular cross-section diffusers; 2) solution print of streamline station; 3) execution of subroutines; 4) starting station number; and 5) ending station number to provide a high degree of flexibility and efficiency in running the program.

- Group 3: which consists of eight input parameters to provide the normal and streamwise grid-point information and is also punched on one BCD card.
- Group 4: which is used to provide the diffuser geometry, five BCD cards are needed for this group.
- Group 5: which consists of sixteen parameters regarding the reference flow properties (determined based on standard sea-level atmospheric conditions) and the averaged flow parameters at the diffuser inlet. Two BCD cards are needed for this group.
- Group 6: Actual flow distribution data at the diffuser inlet are given by this group. Each BCD card contains four values describing the location, the total pressure, the static pressure and the total temperature, respectively, for a testing rake. Therefore, Group 6 consists of as many BCD cards as the number of test data points.

All the flow distribution data and the diffuser geometry identified in Section II are tabulated in this format. The results of the parametric diffuser performance analyses are presented in Sections IV and V.

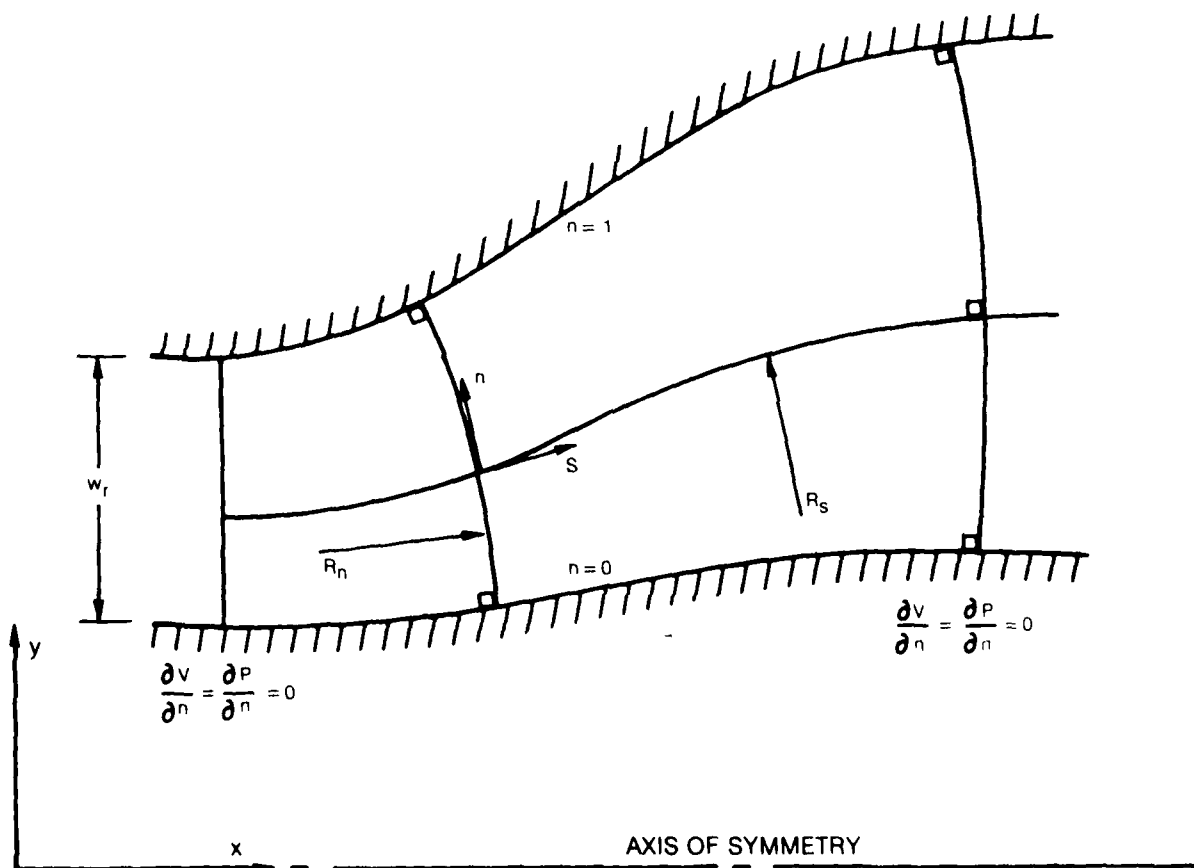
REFERENCES

- 3.1 Patankar, S. V. and D. B. Spalding: Heat and Mass Transfer in Boundary Layers, Morgan-Grampian Book, 1967.
- 3.2 Anderson, O. L.: Calculation of Internal Viscous Flows in Axisymmetric Ducts at Moderate to High Reynolds Number, Computers and Fluids, Vol. 8. pp. 391-411, 1980.
- 3.3 Anderson, O. L.: A Comparison of Theory and Experiment for Incompressible, Turbulent, Swirling Flows. AIAA 10th Aerospace Sciences Meeting, San Diego, California, January 17-19, 1972.
- 3.4. Anderson, O. L.: Finite Difference Solution for Turbulent Swirling Compressible Flow in Axisymmetric Ducts with Struts. NASA CR-2365, February 1974.
- 3.5 Kober, H.: Dictionary of Conformal Representations. Dover Publications, Inc., 1957.
- 3.6 Launder, B. E. and D. B. Spalding: Mathematical Models of Turbulence, Academic Press London and New York, 1972.
- 3.7 Smith, A. M. O. and T. Cebici: Numerical Solutions to the Turbulent Boundary Layer Equations. Douglas Aircraft Report No. DAC 33735, May 1967.
- 3.8 Clauser, F.: The Turbulent Boundary Layer. Advanced Applied Mathematics, Vol. 4, 1956, pp. 1-51.
- 3.9 Briley, W. R., and H. McDonald: An Implicit Numerical Method for the Multi-Dimensional Compressible Navier-Stokes Equations. United Aircraft Research Laboratories Report M911363-6, November 1973.
- 3.10 Briley, W. R., H. McDonald, and H. J. Gibeling: Solution of the Multi-Dimensional Compressible Navier-Stokes Equations by a Generalized Implicit Method. United Technologies Research Center Report R75-911363-15, 1976.
- 3.11 Briley, W. R.: A Numerical Method for Predicting Three-Dimensional Steady Viscous Flow in Ducts. Journal of Computational Physics, Vol. 14, No. 1, 1974, pp 8-28. Also, United Aircraft Research Laboratories Report L110888-1, November 1972. Also, paper presented at Third International Conference on Numerical Methods in Fluid Dynamics, Paris, 1972.

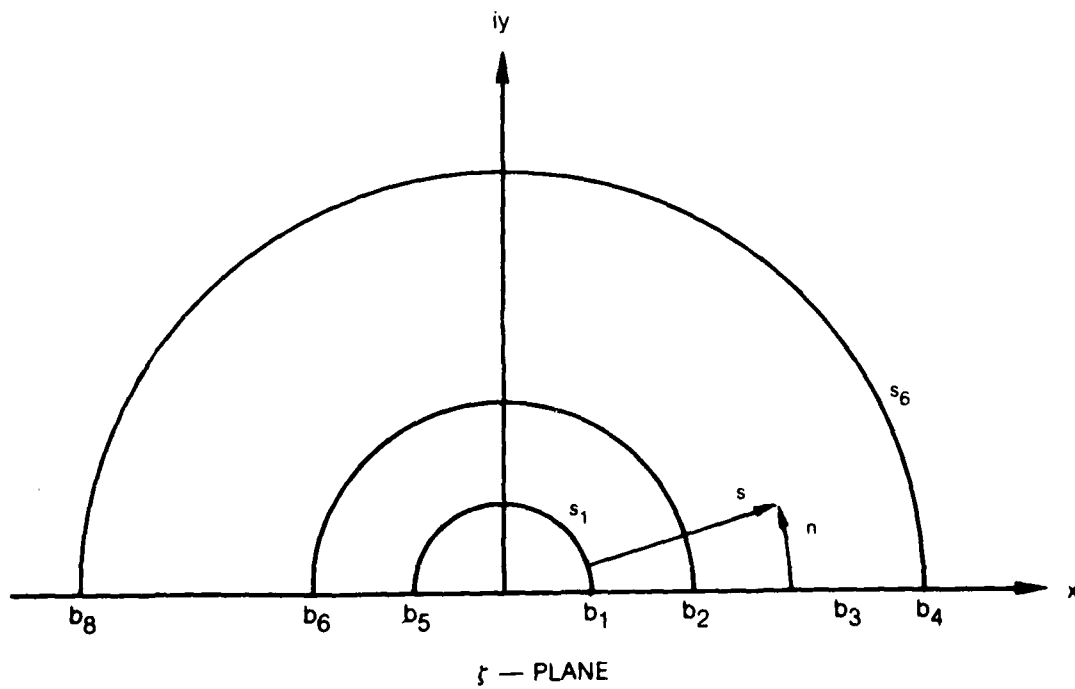
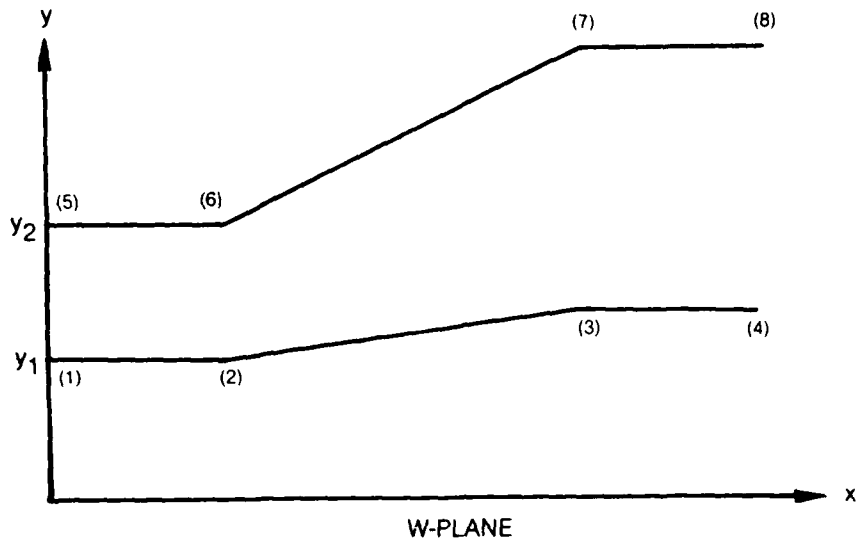
REFERENCES (Cont'd)

- 3.12 Isaacson, E. and H. B. Keller: Analysis of Numerical Methods. John Wiley & Sons, Inc., New York, New York 1966.
- 3.13 Varah, J. M.: On the Solution of Block-Tridiagonal Systems Arising From Certain Finite-Difference Equations. Mathematics of Computation, Vol. 26, No. 120, October 1972.
- 3.14 Schlichting, H.: Boundary Layer Theory. McGraw-Hill Book Co., Inc., New York, New York, 1955.
- 3.15 Anderson, O. L.: User's Manual for a Finite-Difference Calculation of Turbulent Swirling Compressible Flow In Axisymmetric Ducts with Struts and Slot Cooled Walls, Vol. 2, USAAMRDL-TR-74-50, 1974.

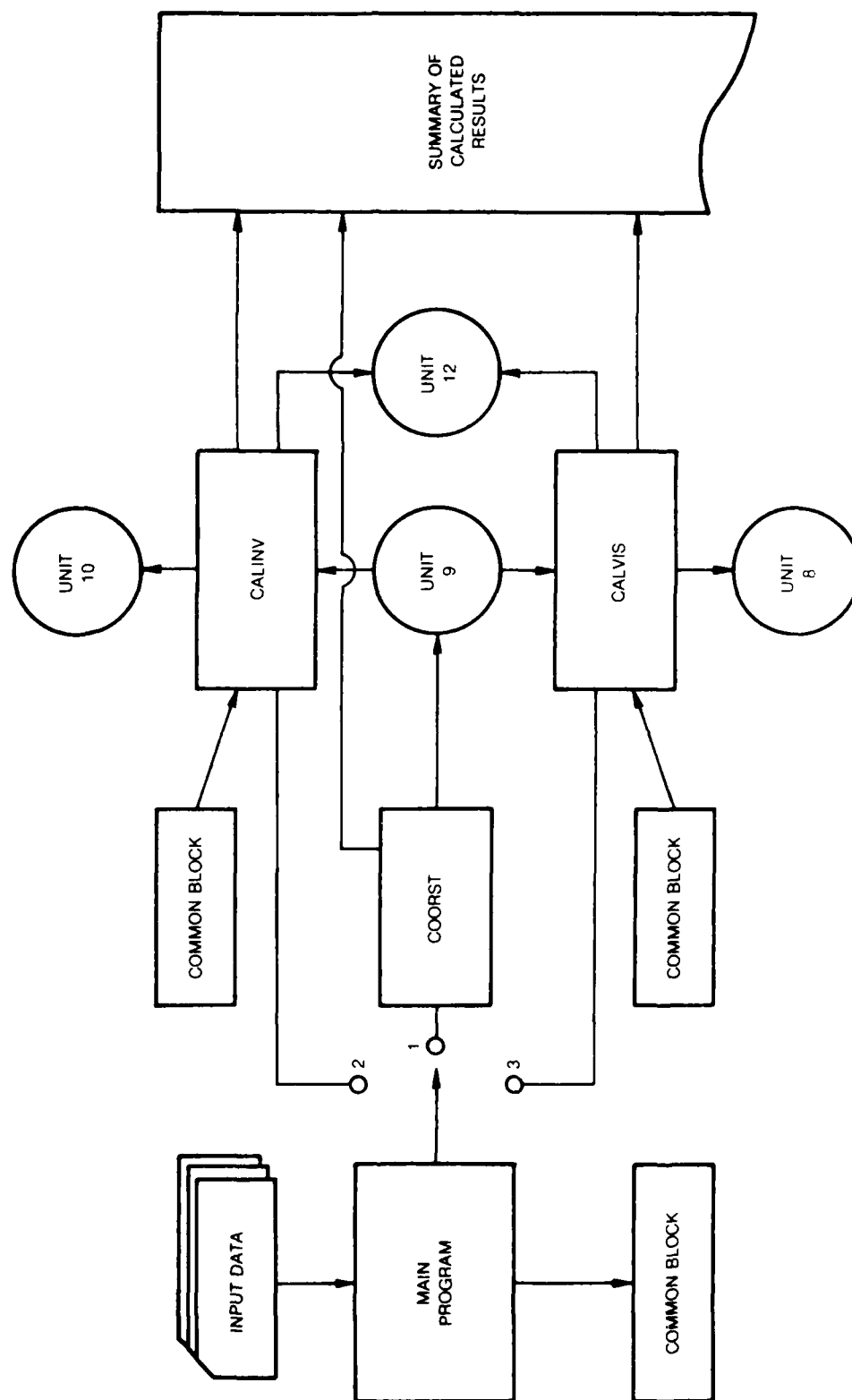
ORTHOGONAL STREAMLINE COORDINATE SYSTEM



CONFORMAL MAPPING OF 2-D DIFFUSERS



STRUCTURE OF FLOW DISTRIBUTION COMPUTER PROGRAMS



RUNSTREAM FOR FLOW DISTRIBUTION CONTROL PROGRAM

@RUN,/B Users ID, ACC NO, etc.
@ASG,AX EIGHT.,D
@ASG,AX NINE.,D
@ASG,AX TWELVE.
@ASG,AX TWOTWO.,D
@USE 8,EIGHT.
@USE 9,NINE.
@USE 12,TWELVE.
@USE 22,TWOTWO.
@XQT file name.FDCP

Input Data Group 1 - Title

Input Data Group 2 - Option Parameters RUNOPT, DIFOPT, FSTOPT, LSTOPT, PRTOPT, PLTOPT

Input Data Group 3 - Mesh Parameters DDS, KL, JL, KDS, KLL, JLAST, JLPTS, LFIN

Input Data Group 4 - Diffuser Geometry Parameters

Input Data Group 5 - Reference and Averaged Flow Parameters

Input Data Group 6 - Inlet Flow distribution data

@FIN

SECTION IV

PARAMETRIC ANALYSIS OF DIFFUSER PERFORMANCE

Parametric design and performance analyses of unstalled or slightly stalled, two-dimensional diffusers were analyzed using the actual flow-distribution data acquired as described in Section II and the analytical model developed in Section III. Four sets of representative flow distribution data of marine gas turbines selected for this study were presented in Tables II.1 and II.2. In addition to those four sets of actual flow distribution data, an idealized set of uniform-flow data was also selected to provide a basis for computing reference results needed for studying the effect of flow nonuniformity on diffuser design and performance. This idealized flow-distribution data was based on the averaged values of DATA-1. Therefore, five sets of flow-distribution data were included in this parametric analysis.

Although the flow-distribution computer program (FDCP) developed in Section III is capable of analyzing many complex diffusers, a candidate diffuser for marine gas turbine waste-heat-recovery system applications must be compatible with the propulsion system requirements and the ship structure. For instance, the diffuser-inlet cross-section must have the same dimensions as that of the gas turbine exhaust box for easy installation. The length of the diffuser must be either 9 feet or 18 ft for easy installation on the ship. It was found that, for the marine gas turbine models considered in this study, the exhaust collecting box has a 5-ft by 7-ft exit cross-section. These dimensions were then used as the inlet of the diffusers. The length of the diffuser was assumed to be either 9 ft or 18 ft. The diffuser angles were varied for investigating its impact on diffuser performance with different flow distributions.

Figure IV.1 shows the twenty-five cases that were analyzed: these cases result from combining five different diffuser configurations with five sets of flow distribution data. The left column of Fig. IV.1 shows the diffuser configurations and the other columns are the case numbers for each combination of the given diffuser and a specific set of flow distribution data.

IV.1 Preliminary Analysis of Diffuser Performance

To run the flow-distribution computer program, all the flow-distribution data and diffuser geometries identified earlier must be arranged in accordance to the specifications discussed in Section III.5. Such an arrangement is shown in Fig. IV.2 for case No. 6.

Before the extensive parametric analyses were undertaken, the flow-field coordinates of diffusers were first established and the actual flow distribution data were then checked. To establish the flow-field coordinates, the run-option parameter was set equal to two. The flow-field coordinates were then calculated by the COORST program shown Fig. III.3 and the results were stored on disk Unit-9. These results have also been plotted, as shown in Fig. IV.3 thru IV.7 for the five candidate diffusers. It should be mentioned that the flow-field coordinates stored on the catalog file of unit-9 can be retrieved as many times as needed for analyzing different flow-distribution data.

The actual flow-distribution data acquired as shown in Section II for two major marine gas turbine models were used in this study. However, if the test data acquired do not satisfy the basic flow theory on which the analytical model was developed, proper modification of input data becomes necessary. For instance, if the input stagnation pressure is smaller than static pressure at a given point, then those conditions violate the isentropic relationship. An error message will be printed and computation is terminated. On the other hand when the inputs of static pressure do not satisfy the normal component momentum equation, theoretical values will be used and computation process is continued without interruption.

Figure IV.8 compares the measured static pressure profiles from the test data with the calculated data which satisfy the momentum equations. The test data fluctuate, while the calculated data are much smoother. The disagreement between the two sets of data can be attributed to the fact that the test data might not be taken along the same streamline surface, or might not be taken in steady-state engine operation. In order to use the analytical model, the calculated pressure profiles have to be used. Based on these calculated static-pressure profiles and the total pressure distribution data presented in Table II.1, the velocity profiles were calculated and presented in Fig. IV.9 and IV.10 for the two candidate gas turbine models.

Because the actual velocity-distribution data near the walls were not available, Cole's turbulent boundary layer model (Ref. 4.1) was used to provide the initial profiles for the boundary layer region (shown in dotted lines in Figs. IV.9 and IV.10). It is expected that the initial velocity profile assumed for the boundary layer region will have certain effects on the results (Ref. 4.2). The results of this analysis can be easily modified when more reliable test data become available.

IV.2 Discussion of Results

Flow-distribution characteristics (which include the velocity profiles, the mass flux distribution, the pressure-recovery and temperature profiles) were calculated at each streamline station of the flow-field coordinates. These results were selectively plotted for discussions. Figure IV.11 thru IV.14 show these results for Cases No. 6 and No. 22. The results for other cases are similar in nature and will not be shown. Only comparative results are discussed herein.

The results are plotted using the scale factor given in the lower left corner of each figure. The arrows represent the magnitude of the flow-distribution data, and the dash lines represent the actual location of the streamline station. Figures IV.11 and IV.12 show that without implementing an effective flow-distribution control device, the flow-distribution nonuniformity remains almost unchanged throughout the flow field. Boundary-layer separation exists in all the non-uniform flow cases and the separation always occurs on the wall of the lower velocity side. Both Figs. IV.11 and IV.12 also show that the sluggish flow, which appears near the centerline region of the diffuser in the initial profile, has become more uniform as the fluid flows along the diffuser. This is due to the viscosity effect which would slow down the fast-moving fluid elements and speed up the slow-moving elements. Figure IV.13 shows that the pressure recovery profiles at each streamline station are not uniform. The pressure recovery is higher on the higher-velocity side where the initial static pressure is lower (Fig. IV.8). Therefore, one would expect a rather uniformly distributed static-pressure profile at the exit of the diffuser.

Shown in Fig. IV.14 are the calculated temperature profiles which remain rather uniform and constant throughout the diffusion process, because the initial temperature profile was assumed uniform and the wall condition was assumed to be adiabatic. The results of uniformly distributed pressure and temperature identified from this study should be beneficial to the design of waste-heat-recovery systems.

The parametric performance analysis of diffuser configuration No. 5 has not been very successful, because of the very large diffuser angle. Boundary layer separation occurs almost immediately after the fluid passes the diffuser throat. Figure IV.15 shows the typical results of this study. This diffuser will be studied further in Section V.

Figure IV.16 shows the velocity ratio and pressure-recovery coefficient as a function of diffuser length. The results were obtained by integrating the velocity profile and pressure-recovery profiles along the velocity-potential line at each streamline station and then weighted by the mass-flow rate. It was found that most kinetic energy has been converted into pressure in the first half (approximately 10 ft) of the diffuser length. In the second half of the diffuser, because boundary layer separation occurred, diffuser efficiency remains constant. This phenomenon was seen in all non-uniform flow cases. Figure IV.16 also presents the pressure-recovery-coefficient calculated from inviscid-flow theory and also from the Bernoulli theory. The difference between these two curves represents the effect of nonuniform-flow distribution on the diffuser performance.

Comparisons of two-dimensional diffuser efficiencies for Cases No. 1 thru 20 are shown in Fig. IV.17 where the solid lines and dotted line represent the results obtained based on turbulent-flow theory and inviscid-flow theory, respectively. These results can be classified into two groups: the upper group is for uniform-flow cases No. 1 thru 4, and the lower one is for the nonuniform-flow cases No. 5 thru 20. For the uniform-flow cases, the results from the inviscid-flow models fall on top of each other, and the values are found to be almost equal to those obtained from the Bernoulli equation. The results obtained from turbulent-flow models varied among the four diffusers, and the values are significantly lower than those from the inviscid-flow model.

For the nonuniform-flow cases, the performance results of the inviscid-flow model are computed only up to an area ratio of approximately 1.3. Beyond that point, reverse-flow developed in the core region and the governing equations are not valid. On the other hand, the turbulent-flow model does provide performance results up to an area ratio as high as 2.0. The results of this study indicated that the diffuser efficiency based on the actual flow-distribution data of marine gas turbine exhaust is approximately 50 percent lower than that based on an assumption of uniform flow.

IV.3 Improvement of the Analytical Model

In carrying out parametric analyses of diffusers, one major difficulty was to deal with the problem of boundary-layer separation. The phenomenon of boundary-layer separation seems intimately connected with the operation of diffusers. It is known that in the far-away-from-the-wall region, there is a transformation of kinetic energy into pressure as the fluid travels along the diffuser. Therefore, the static pressure increases as the diffusion process continues. This is generally referred to as external pressure and will impress on the boundary layer locally according to boundary-layer theory. On the other

hand, a fluid particle which moves in the immediate vicinity of the wall in the boundary layer remains under the influence of both the local external pressure and the wall friction. Owing to the large friction force in the thin boundary layer such a particle consumes so much of its kinetic energy on its path along the diffuser wall that it will eventually reach a separation point which is defined as $(\partial u / \partial y)_w = 0$. Beyond that point, the external pressure would cause the fluid particles near the wall to move in the opposite direction, commonly known as separated flow.

Because the integration of boundary layer equations is known to be unstable in the region of separated flow, special efforts must be made to modify the flow-distribution program. This effort includes the adoption of Reyhner and Flugg-Lotz's approximation method (Ref. 4.3) and the global iteration procedure invented by Carter, and Cebeci et al (Refs. 4.4 and 4.5). Details of this program modification and the example study are presented in Ref. 4.5.

Several control options and diagnoses were incorporated in the program as methods to check the input data and also to improve computational accuracy and numerical stability. For instance, the input data were first checked by a CKINPT program to ensure that they are compatible with each other. When the calculated value of temperature, pressure or density becomes negative, a numerical-instability diagnosis and the pertinent information associated with the flow field is printed, and then the computer analysis is stopped. Using the printed information, one can take appropriate action to improve the numerical results.

IV.4 Impact of Flow Nonuniformity on Design of Diffusers and Waste-Heat Boilers

General technical problems which can be attributed to nonuniform flow in heat exchangers or flow-equipment systems have been reviewed in Section I. Only the impact of flow-distribution nonuniformity on diffuser and waste-heat boiler performance and design are discussed in this section.

The effects of nonuniform flow at the diffuser inlet on flow regimes and diffuser performance have been studied by many researchers (Ref. 4.7 thru 4.9). The results of these studies have shown that the flow-distribution nonuniformity at the diffuser inlet can reduce the diffuser efficiency significantly. Based on the actual flow-distribution data of marine gas turbine exhaust flows, the results of this study (seen earlier in Fig. IV.17) show that the diffuser efficiency drops as much as 50 percent as compared to the efficiency with uniform-flow conditions.

As far as the effect of flow-distribution nonuniformity on the design of two-dimensional diffusers is concerned, the results of these parametric design and performance analyses indicate that the method of using non-symmetric diffuser angles would not improve either the flow distribution or the diffuser efficiency. The problems associated with boundary-layer separation and reverse flow for the nonuniform flow cases are found to be worse than those in symmetric diffusers with uniform flow. To achieve the objectives of this flow-distribution control study, a combination of a flow-distribution control method and some means of preventing boundary-layer separation must be considered. In addition, the results of this study would also reveal that most existing diffusers designed for gas turbine waste-heat recovery systems might have been oversized. It would appear that these existing diffusers can be modified, if necessary, with well-planned and carefully performed flow-modeling studies in order to reduce their sizes.

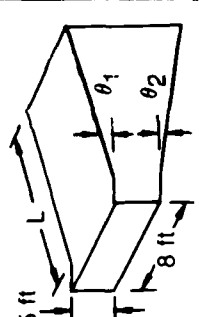
The detrimental effect of flow maldistribution to the thermal performance and life expectancy of heat exchangers is well known (Ref. 3.10). As much as a 30 percent degradation of heat transfer effectiveness could be ascribed to the poor flow distribution through the exchanger core (Ref. 3.11). Differential dynamic head in an exchanger core due to nonuniform-flow distribution might cause some difficulties in designing a waste-heat boiler. In addition, in order to avoid problems of flue gas condensation (or corrosion problems), the exit gas temperature from a gas turbine waste-heat boiler must be kept above 300F. This temperature limitation implies that the heat transfer element of a waste-heat boiler might have to be shaped in accordance with the flow distribution profile. To avoid these problems in the design of gas turbine waste-heat boilers, feasible means for controlling the flow distribution to achieve a more uniformly distributed flow will be investigated in the next section.

REFERENCES

- 4.1 Coles, D. E. and E. A. Hirst: Proceedings Computation of Turbulent Boundary Layer 1968. AFOSR-IFP-Stanford Conference, August 1968.
- 4.2 Reneau, L. R., J. P. Johnston, and S. J. Kline: Performance and Design of Straight, Two-Dimensional Diffusers, J. of Basic Engineering, March 1967, pp 141-150.
- 4.3 Reyhner, T. A. and I. Klugg-Lotz: The Interaction of a Shock Wave with a Laminar Boundary Layer, Int. J. of Non-Linear Mechanics, Vol. 3 No. 2, 1968, pp 173.
- 4.4 Carter, J. E.: Inverse Solutions for Laminar Boundary Layer Flows with Separation and Reattachment. NASA TR R-447, Nov. 1975.
- 4.5 Cebeci, T., H. B. Keller and P. G. Williams: Separating Boundary Flow Calculations: J. Computational Physics, Vol. 31, 1979.
- 4.6 Anderson, O. L. and D. E. Edwards: Extensions to an Analysis of Turbulent Swirling Compressible Flow in Axisymmetric Ducts, NASA CR NAS3-21853, Feb. 1981.
- 4.7 Wolf, S. and J. P. Johnston: Effects of Nonuniform Inlet Velocity Profiles on Flow Regimes and Performance in Two-Dimensional Diffusers, J. of Basic Eng. Trans of the ASME, Sept. 1969 pp 462-474.
- 4.8 Johnston, I. H.: The Effect of Inlet Conditions on the Flow in Annular Diffusers, National Gas Turbine Establishment, C. P. No. 178, Memorandum No. M.167, Jan. 1953.
- 4.9 Waitman, B. A. et. al.: Effects of Inlet Conditions on Performance of Two-Dimensional Diffusers, J. of Basic Eng. Trans ASME, Series D, Vol. 83, No. 3, Sept. 1961.
- 4.10 Chiou, J. P.: Thermal Performance Deterioration in Crossflow Heat Exchanger Due to the Flow Nonuniformity, J. of Heat Transfer, Trans ASME, Vol. 100, Nov. 1978, pp 580-587.
- 4.11 Wilson, D. G.: A Method of Design for Heat-Exchanger Inlet Headers, ASME Paper 66-WA/HT-41, Sept. 1967.

CASES FOR DIFFUSER PERFORMANCE ANALYSES

* PROVIDED BY ONR FROM REFERENCE 2.1

DIFFUSER CONFIGURATION		DIFFUSER INLET FLOW DISTRIBUTION DATA AND CASES					
		UNIFORM FLOW	DD963 PROPULSION SUBSYSTEM PROTOTYPE GT MODULE 2A*		UTC-FT4 MARINE GAS TURBINE MODEL C		
			FULL LOAD	PART LOAD	FULL LOAD	PART LOAD	
CONF. 1	L = 18 ft $\theta_1 = 11.0^\circ$ $\theta_2 = -11.0^\circ$	CASE 1	CASE 5	CASE 9	CASE 13	CASE 17	
CONF. 2	L = 18 ft $\theta_1 = 22.0^\circ$ $\theta_2 = 0.0^\circ$	CASE 2	CASE 6	CASE 10	CASE 14	CASE 18	
CONF. 3	L = 18 ft $\theta_1 = 15.5^\circ$ $\theta_2 = 0.0^\circ$	CASE 3	CASE 7	CASE 11	CASE 15	CASE 19	
CONF. 4	L = 18 ft $\theta_1 = 26.5^\circ$ $\theta_2 = 6.5^\circ$	CASE 4	CASE 8	CASE 12	CASE 16	CASE 20	
CONF. 5	L = 9 ft $\theta_1 = 32^\circ$ $\theta_2 = -32^\circ$	CASE 21	CASE 22	CASE 23	CASE 34	CASE 25	

EXAMPLE RUN-STREAM FOR FLOW-DISTRIBUTION COMPUTER PROGRAM

@RUN CARD

@ASG,AX EIGHT (1), D

@ASG,AX NINE (1), D

@ASG,AX TWELVE (1)

@ASG,AX TWOTWO (1), D

@ASG,T 10,D

@ASG,T 11,D

@ASG,T 14,D

@USE 8,EIGHT (1)

@USE 9,NINE (1)

@USE 12,TWELVE (1).

@USE 22,TWOTWO (1)

@XQT SPCS.MAPFDCS

FLOW DISTRIBUTION CONTROL STUDY CASE-6

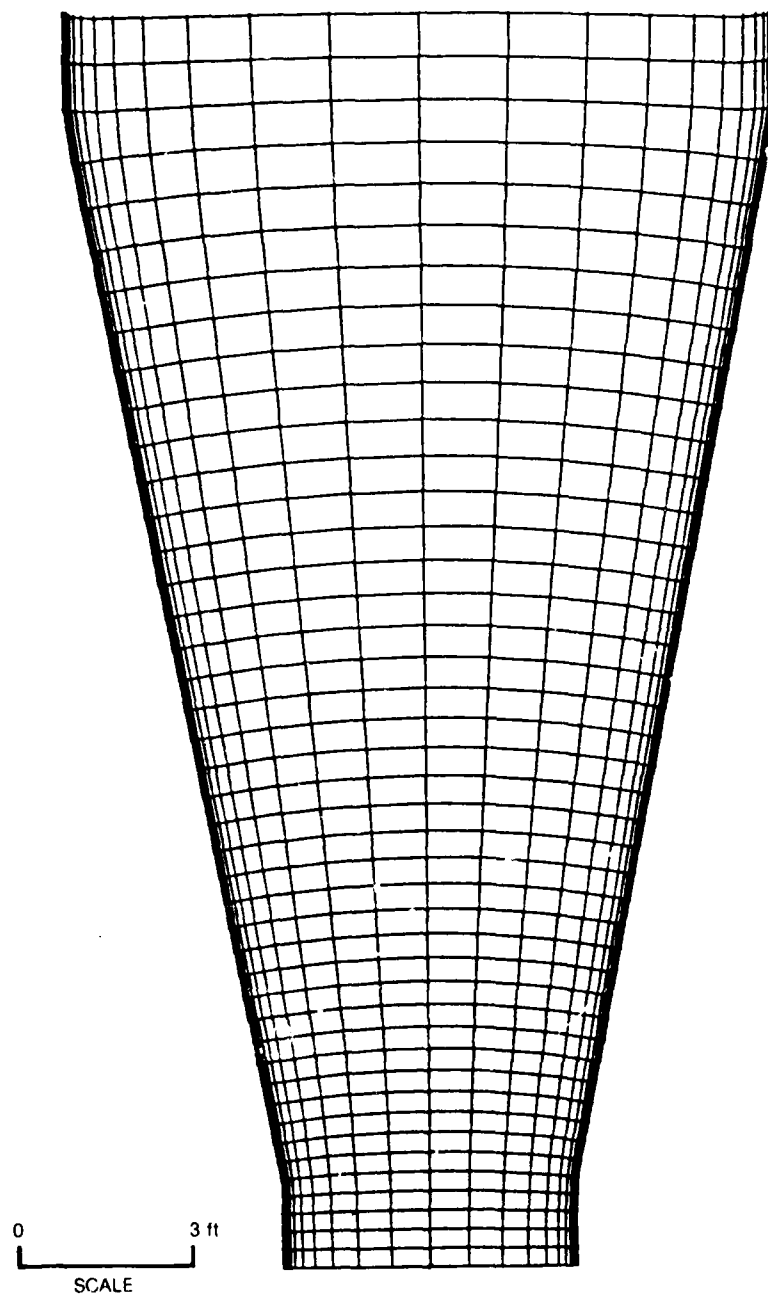
5 8 950 1 0

41 50 5 13 0 4 0

25.0	1.20	0.0	7.0					
12.0	12.0	19.30	19.0					
0.0	2.0	20.0	25.0					
7.0	7.0	7.0	7.0					
0.0	2.0	20.0	25.0					
2163.94	1316.00	.016	.41	26.0	.44	.750	5997.60	4283.70 .713E-80
.0843	0.0	.0341	.0341		7.0	7.0		
.000	2149.06	2140.89	1316.00					
.045	2149.06	2144.89	1316.00					
.136	2148.54	2143.85	1316.00					
.277	2146.98	2142.81	1316.00					
.318	2145.94	2142.29	1316.00					
.409	2144.30	2140.21	1316.00					
.500	2144.89	2137.61	1316.00					
.591	2154.78	2140.73	1316.00					
.682	2187.04	2152.70	1316.00					
.773	2195.88	2139.17	1316.00					
.864	2195.36	2142.81	1316.00					
.955	2139.69	2132.93	1316.00					
1.000	2139.69	2132.93	1297.00					

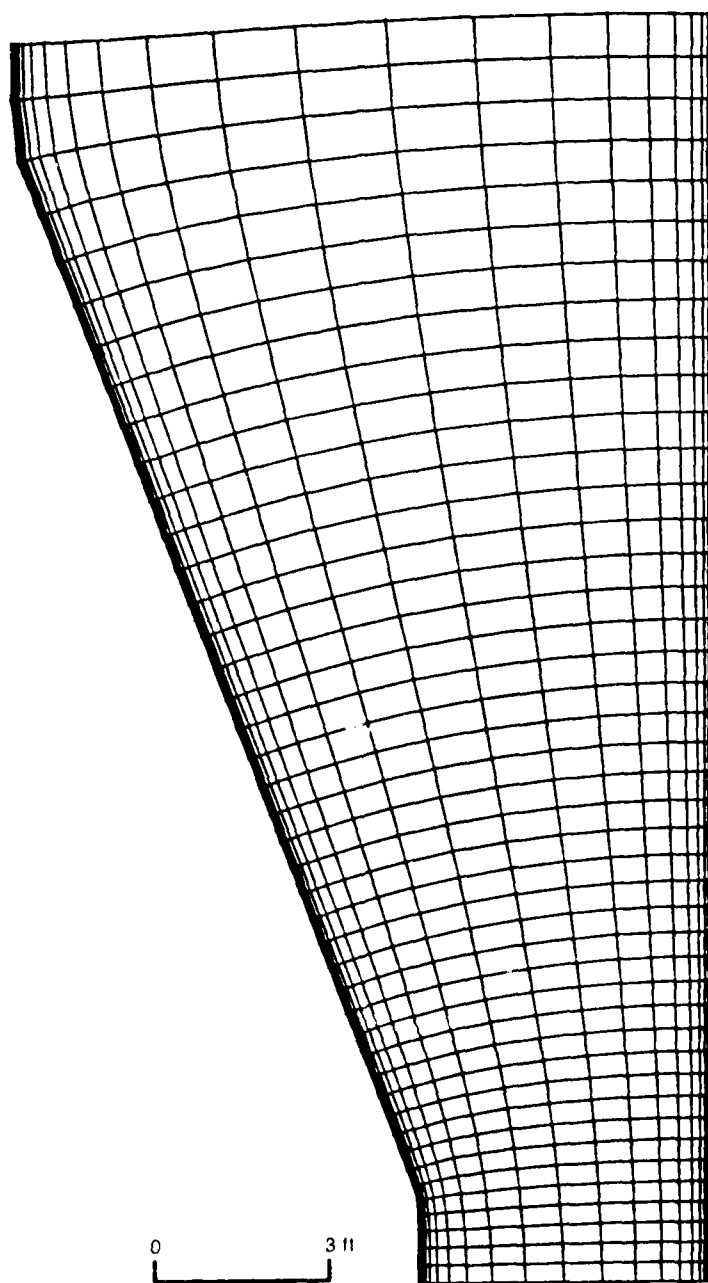
@FIN

FLOW FIELD COORDINATES FOR DIFFUSER CONFIGURATION NO. 1



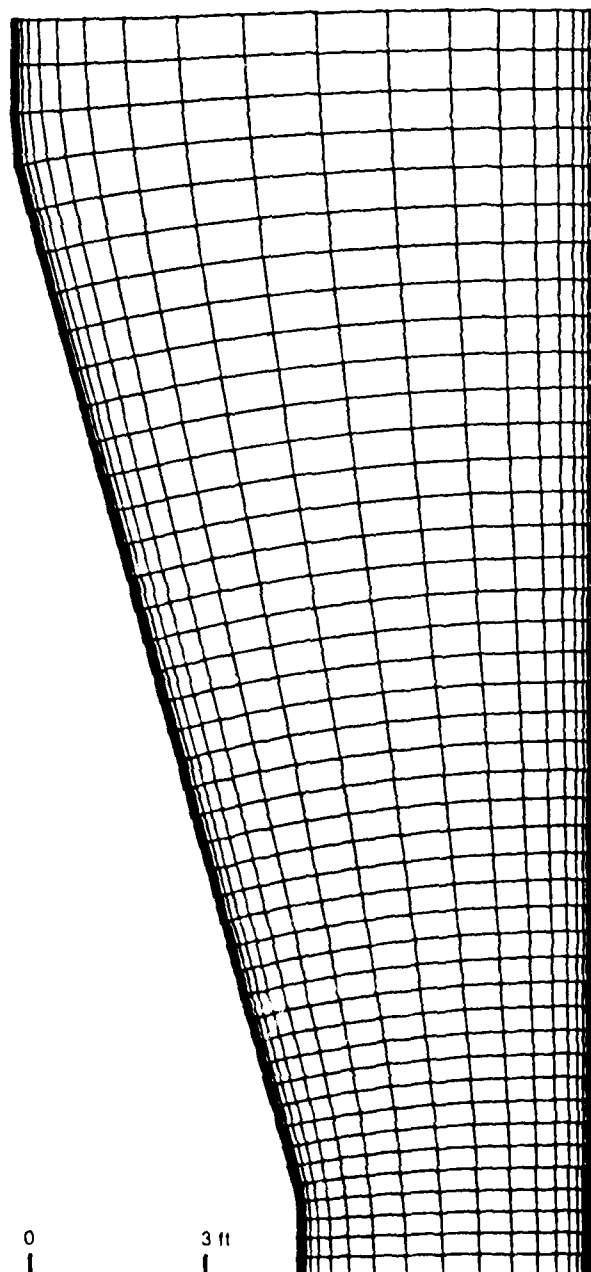
81-6-95-11

FLOW FIELD COORDINATES FOR DIFFUSER CONFIGURATION NO. 2



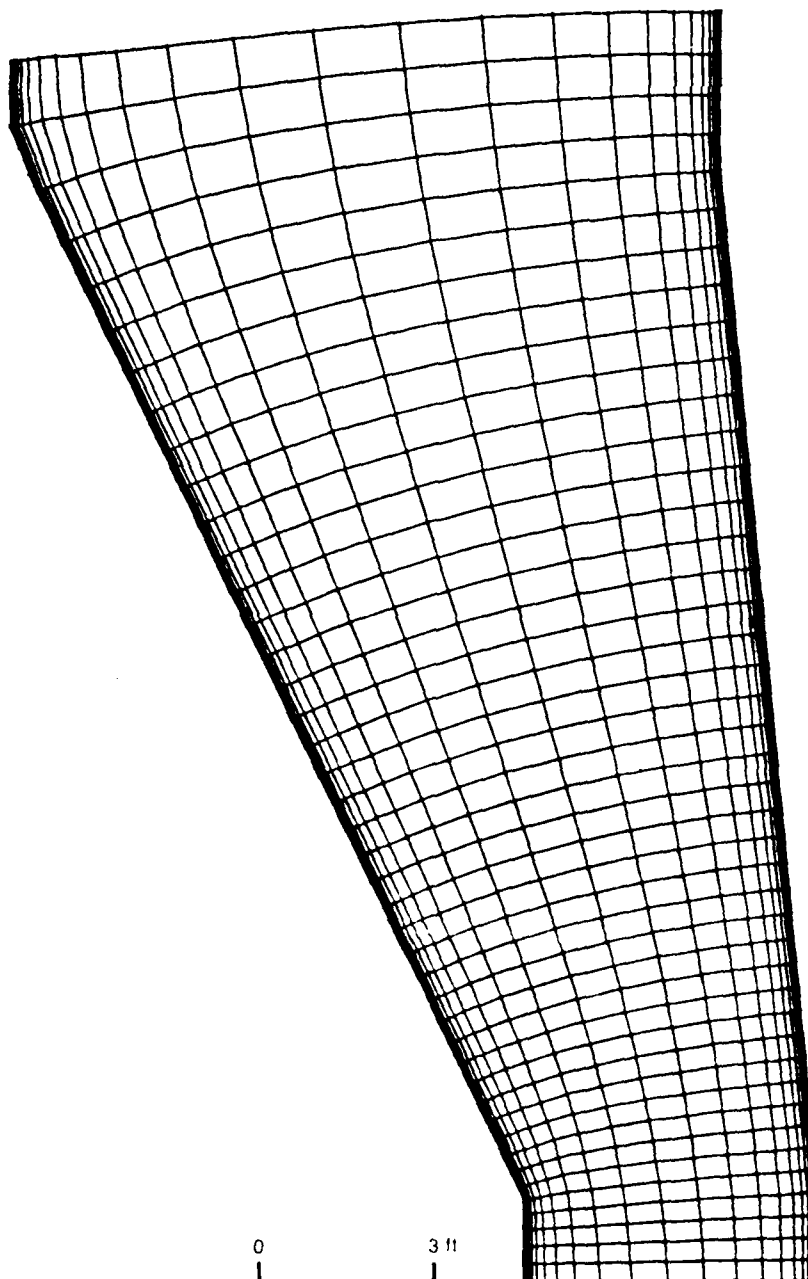
0 3 11
SCALE

FLOW FIELD COORDINATES FOR DIFFUSER CONFIGURATION NO. 3



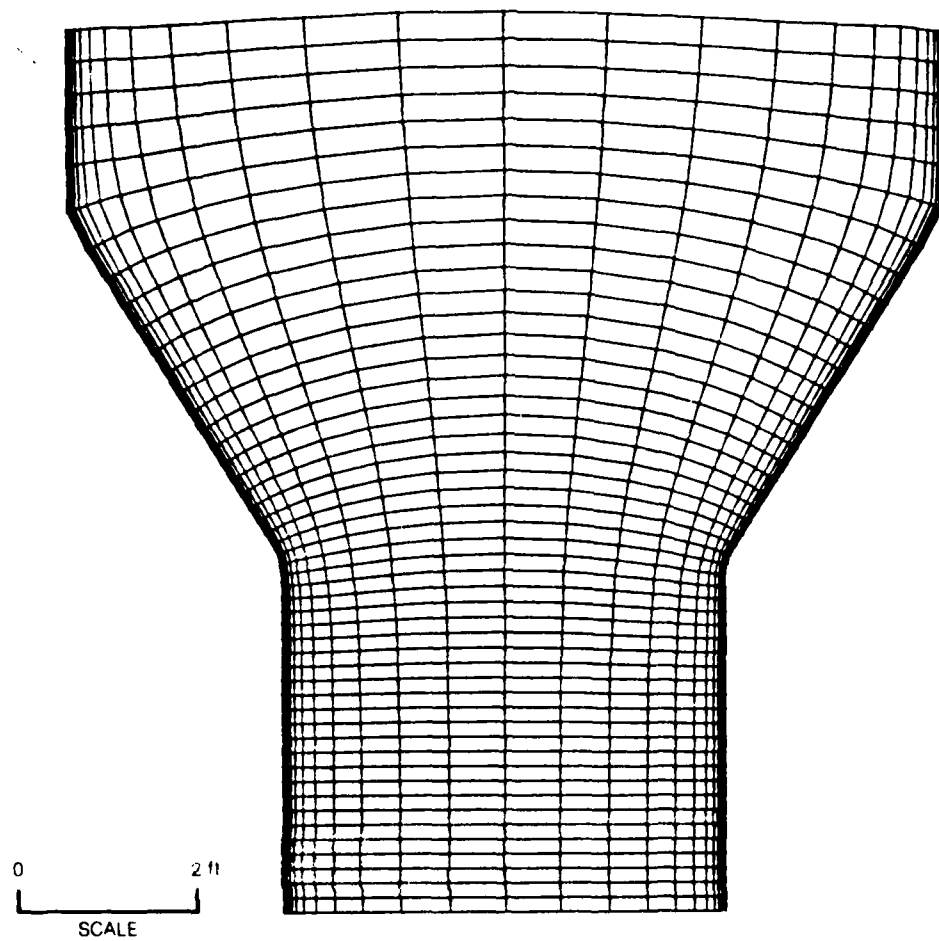
61-6-95-13

FLOW FIELD COORDINATES FOR DIFFUSER CONFIGURATION NO. 4

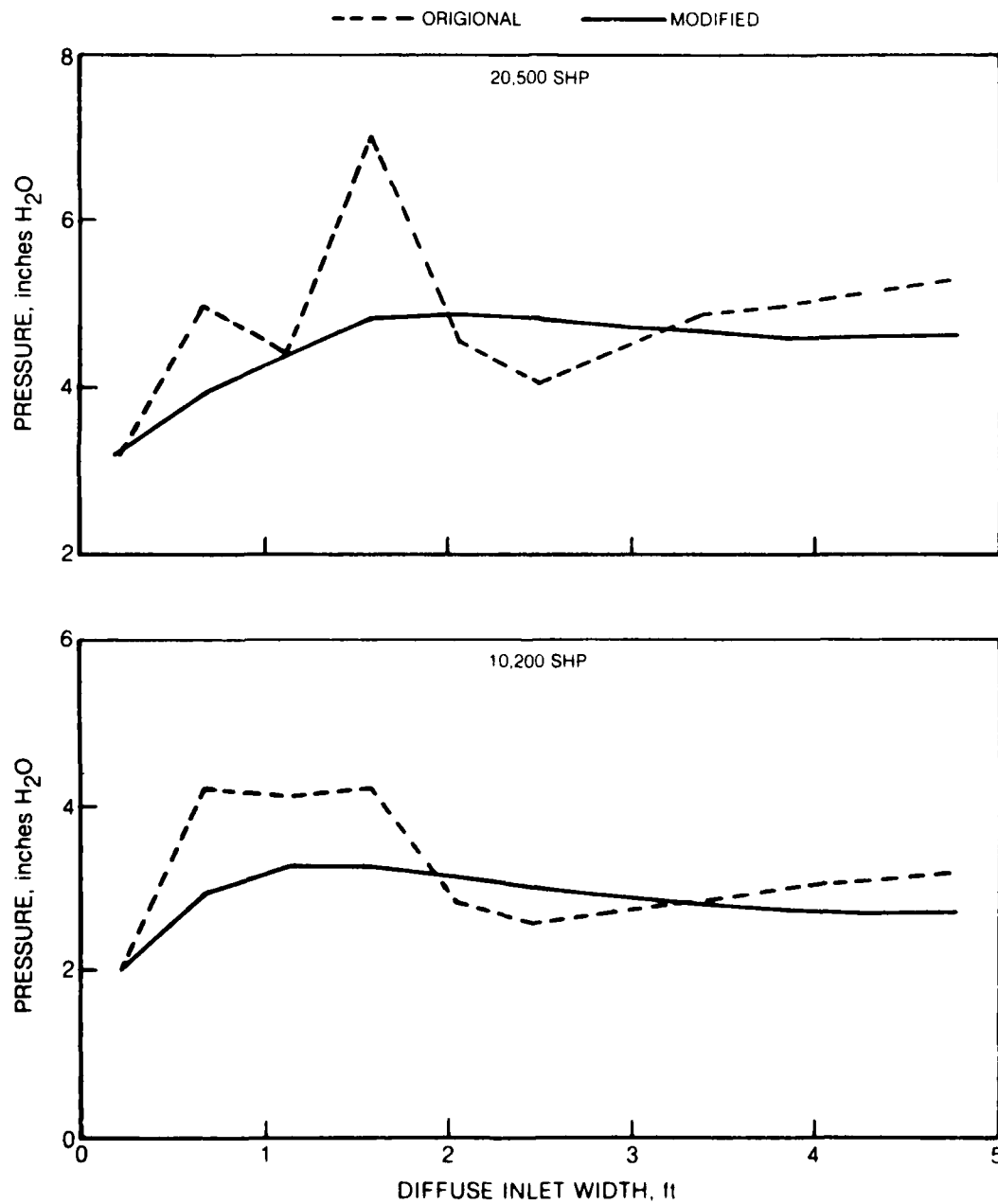


0 3 ft
SCALE

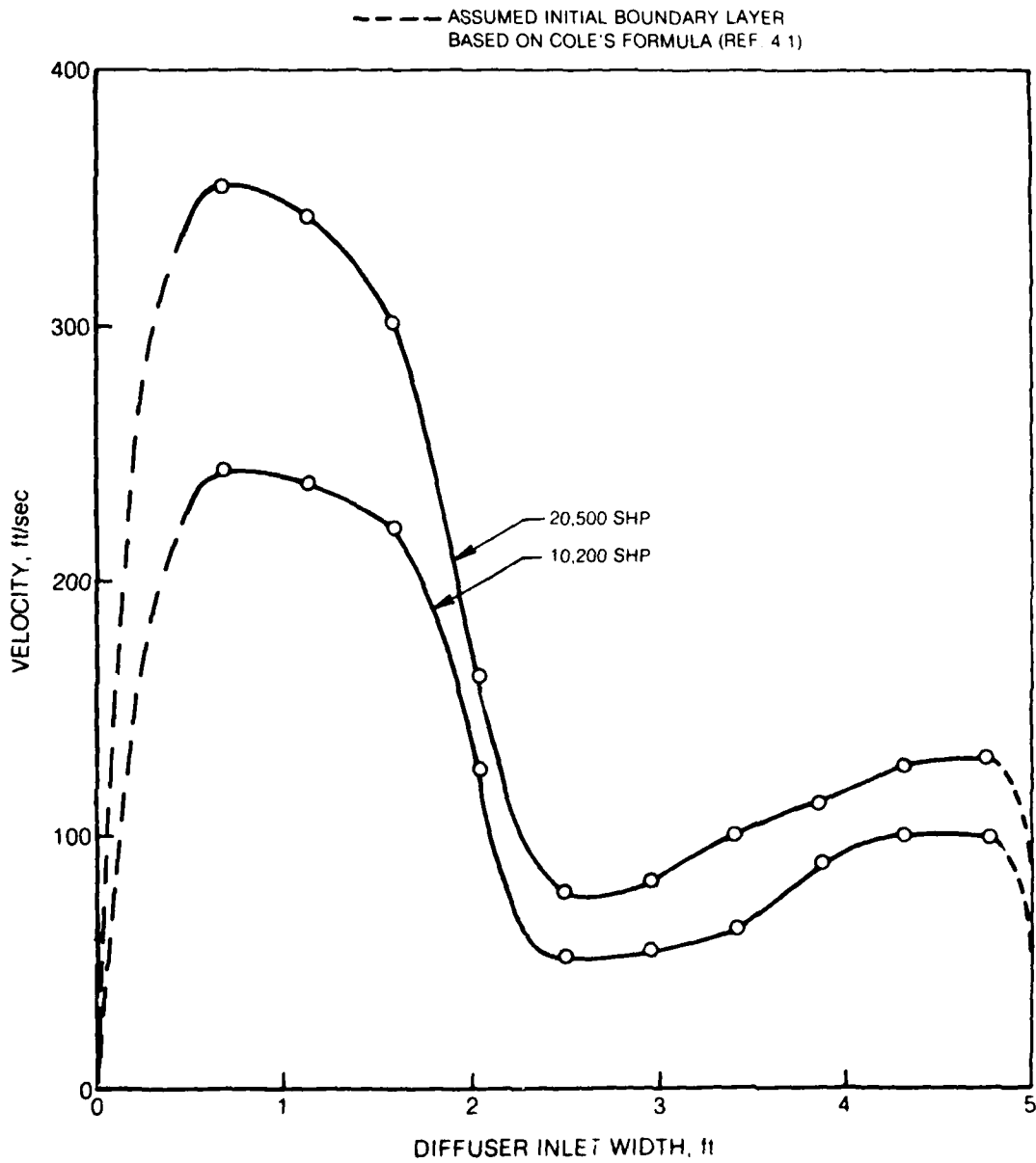
FLOW FIELD COORDINATES FOR DIFFUSER CONFIGURATION NO. 5



**MODIFICATION OF STATIC PRESSURE DATA OF DD-963 CLASS GAS TURBINE
MODULE-2B TO SATISFY MOMENTUM EQUATIONS**

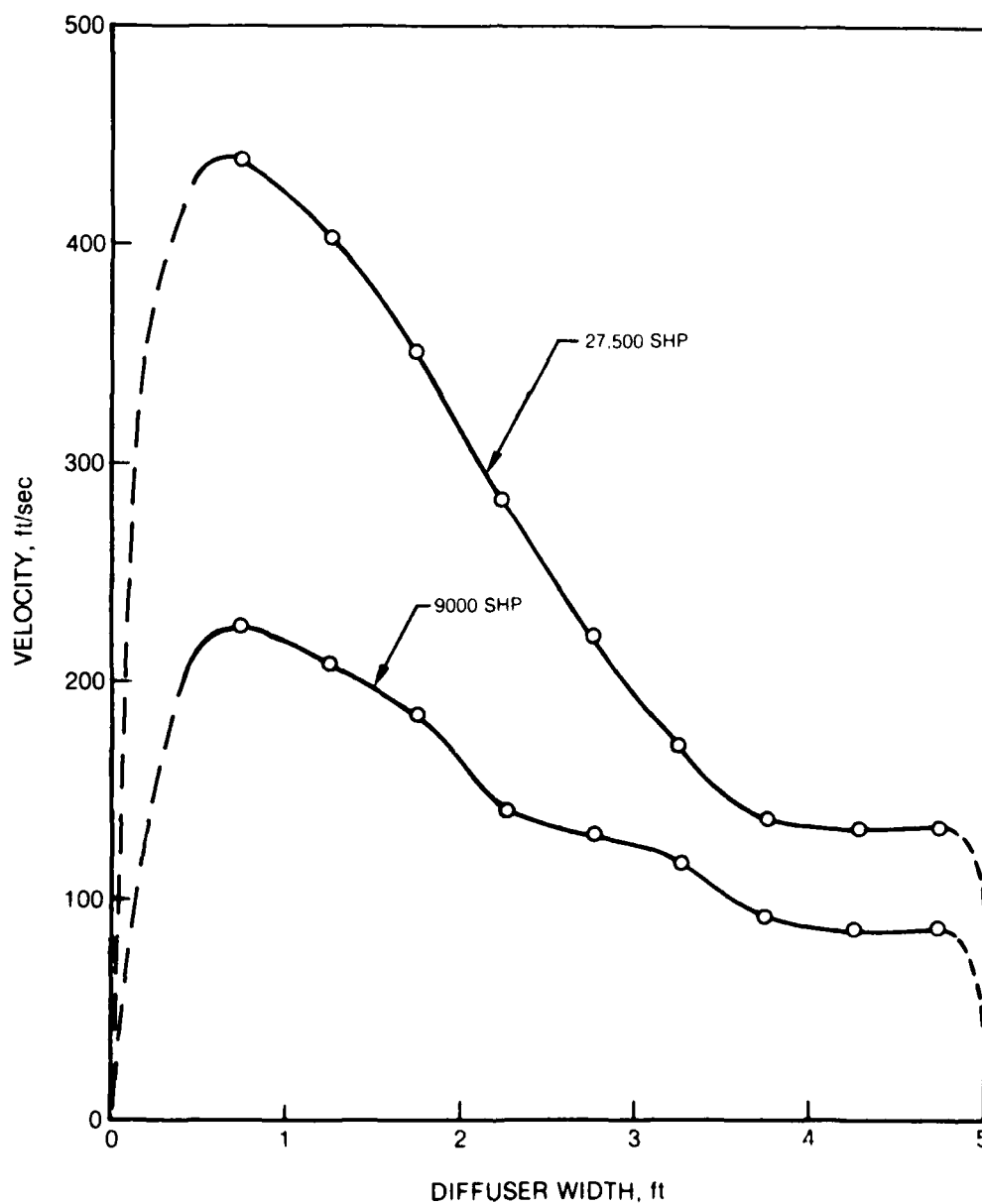


**CALCULATED EXHAUST GAS VELOCITY PROFILES FOR DD-963 CLASS
PROTOTYPE GAS TURBINE MODULE-2B**

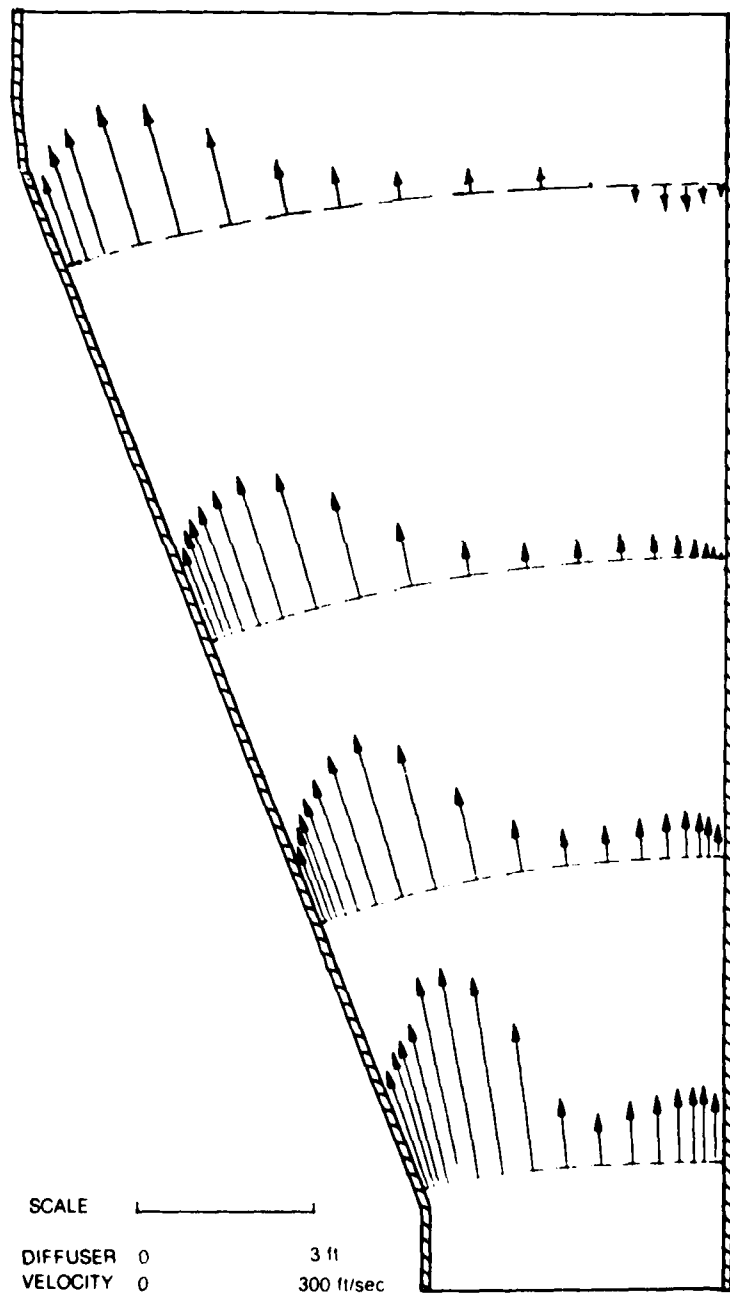


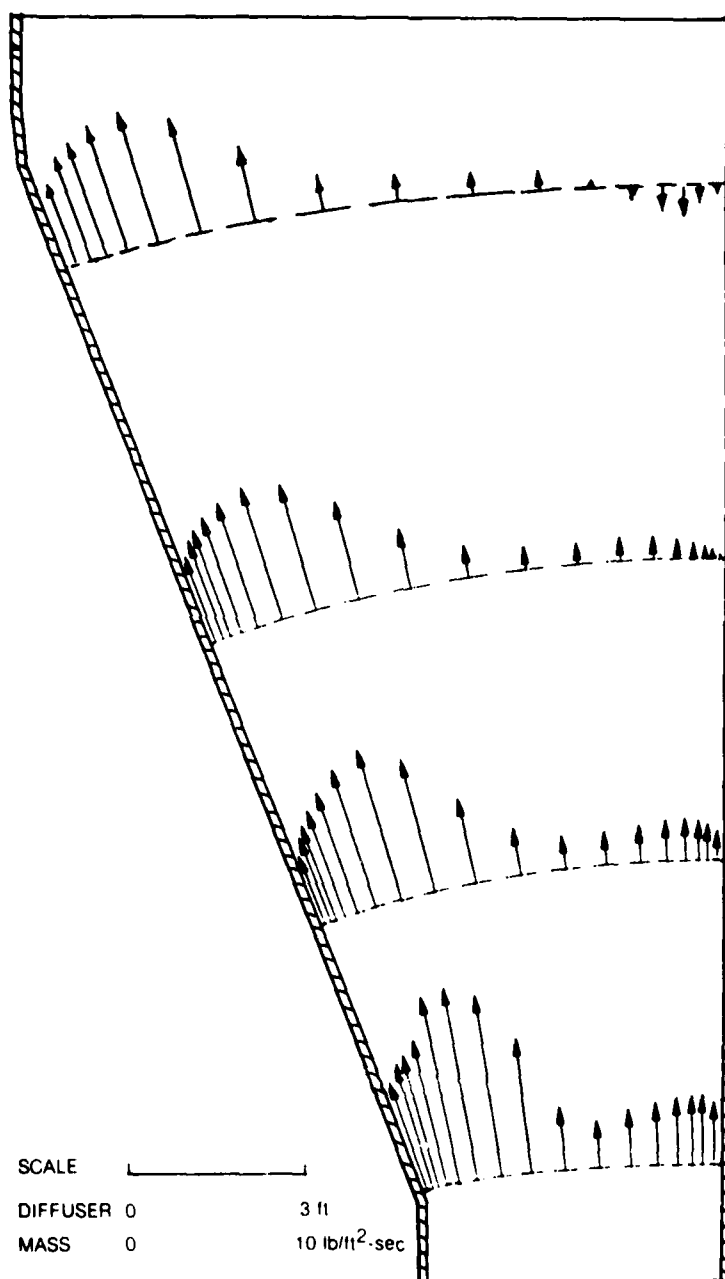
**CALCULATED EXHAUST GAS VELOCITY PROFILES FOR
UTC-FT4 MARINE GAS TURBINE**

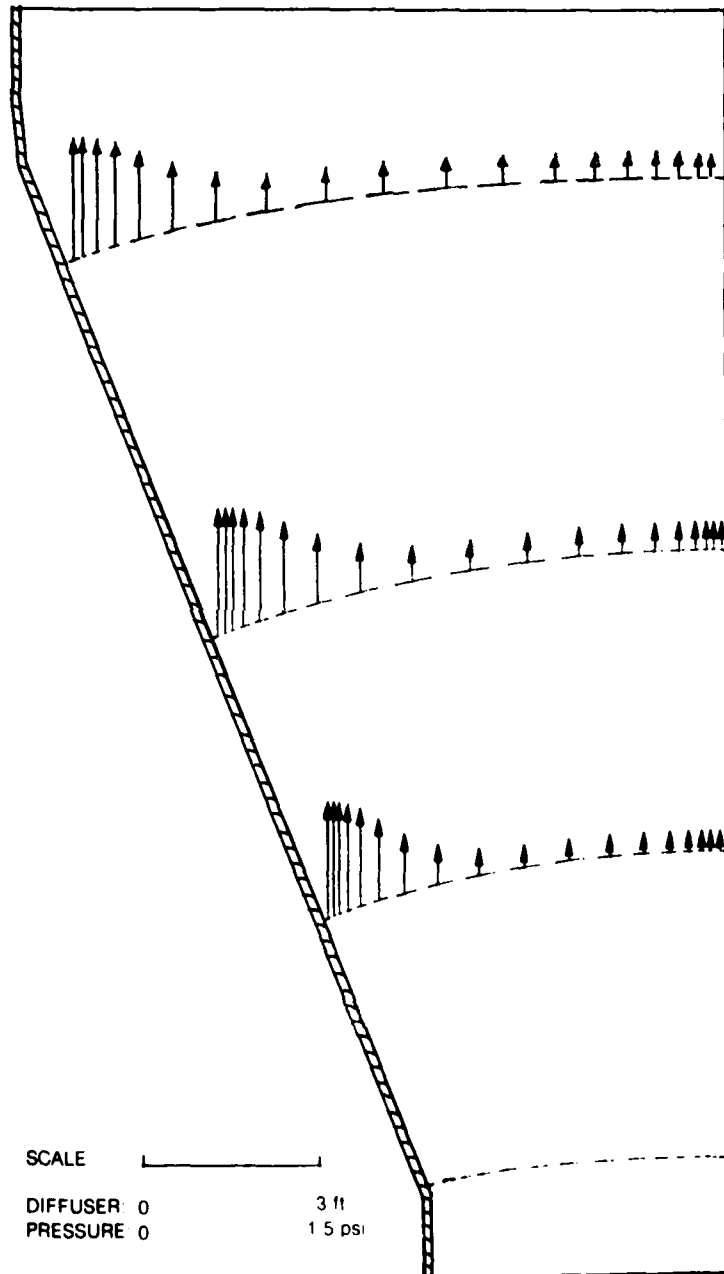
--- ASSUMED INITIAL BOUNDARY LAYER
BASED ON COLE'S FORMULA (REF 4 1)



VELOCITY DISTRIBUTION CHARACTERISTICS FOR CASE NO. 6

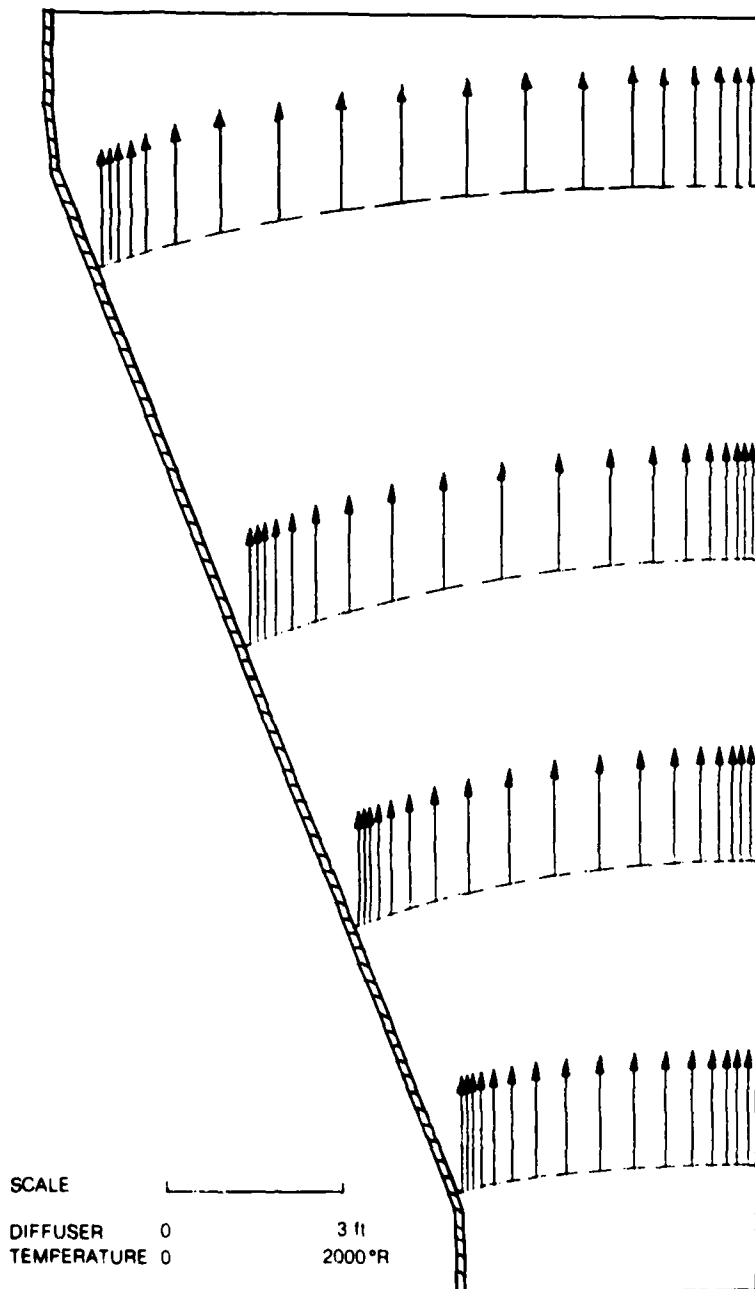


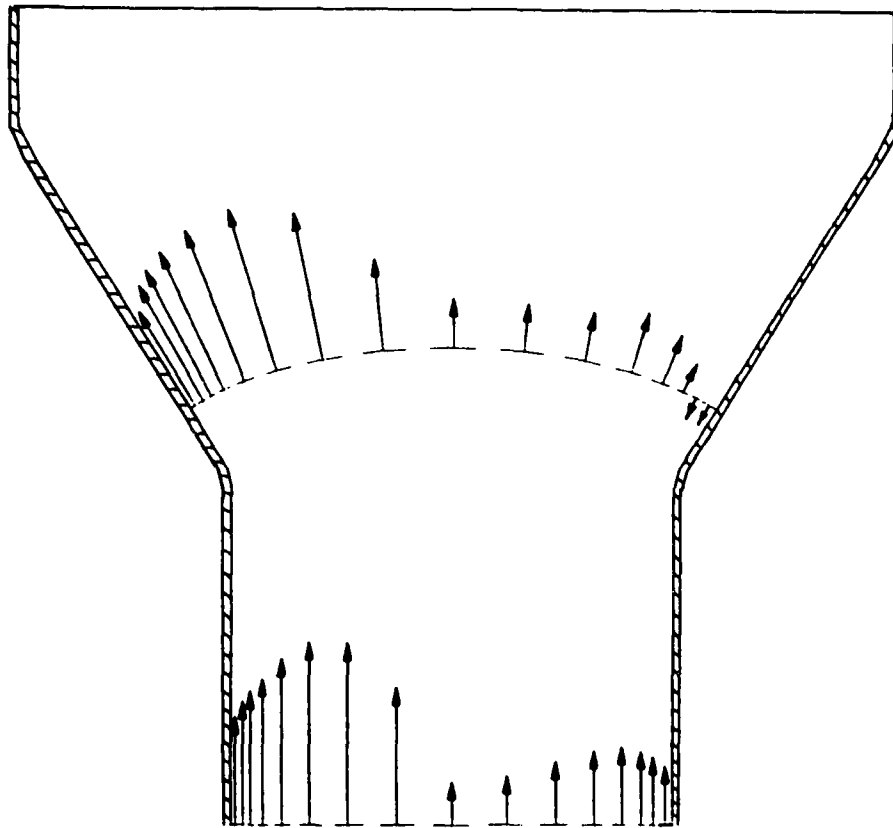
MASS FLUX DISTRIBUTION CHARACTERISTICS FOR CASE NO. 6

PRESSURE RECOVERY PROFILES FOR CASE NO. 6

81-6-95-21

TEMPERATURE PROFILES FOR CASE NO. 6

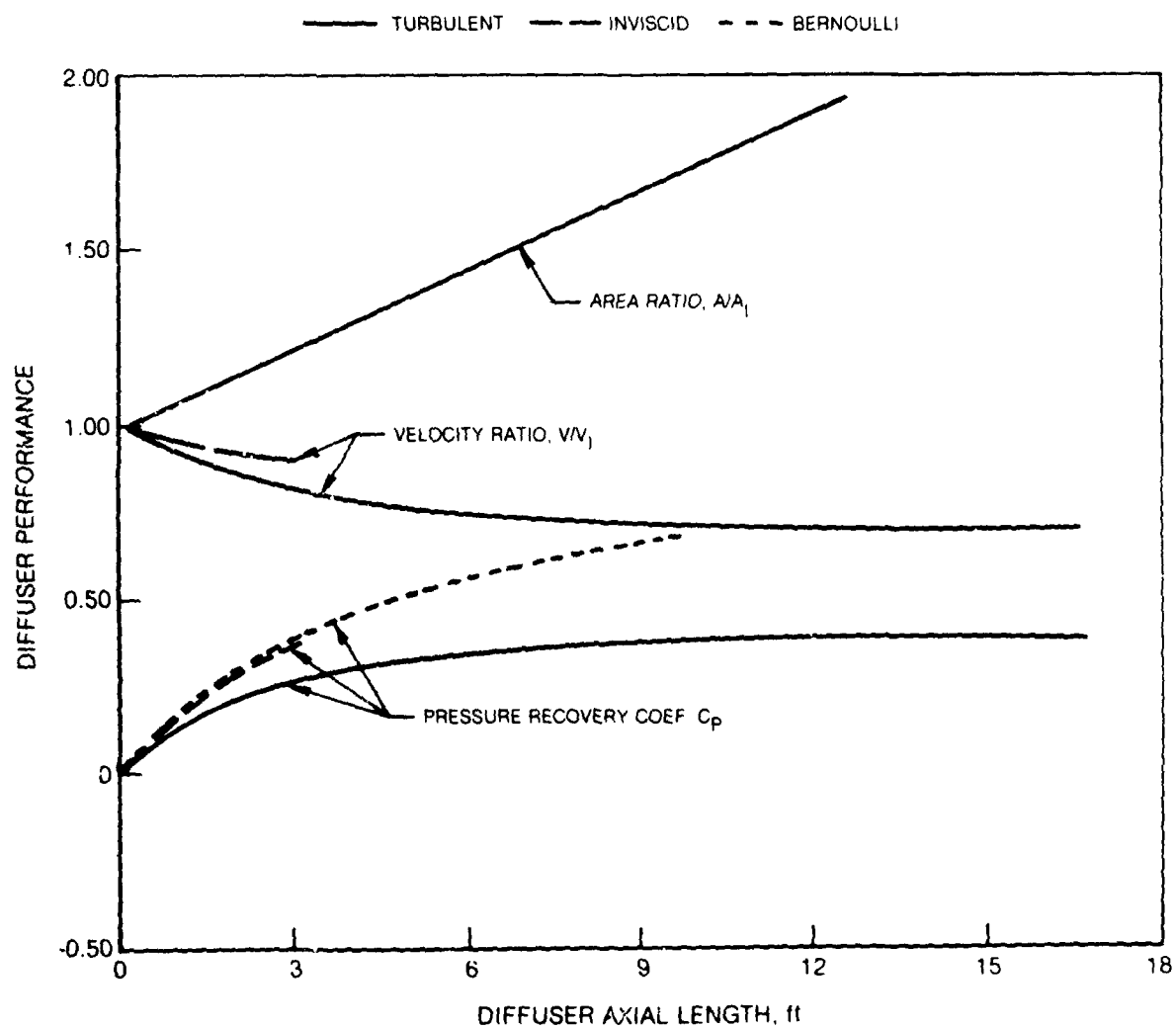


MASS-FLUX DISTRIBUTION CHARACTERISTICS FOR CASE NO. 22

SCALE

DIFFUSER:	0	2 ft
MASS	0	40 lb/ft ² -sec

COMPARISON OF PERFORMANCE CHARACTERISTICS FOR A TWO-DIMENSIONAL DIFFUSER



AD-A104 560

UNITED TECHNOLOGIES RESEARCH CENTER EAST HARTFORD CT

F/G 20/4

FLOW DISTRIBUTION CONTROL CHARACTERISTICS IN MARINE GAS TURBINE--ETC(U)

AUG 81 S C KUO, H SHU

N00014-80-C-0476

UNCLASSIFIED

UTRC/R81-955200-4

NL

2 of 2

AD-A
104 560

END

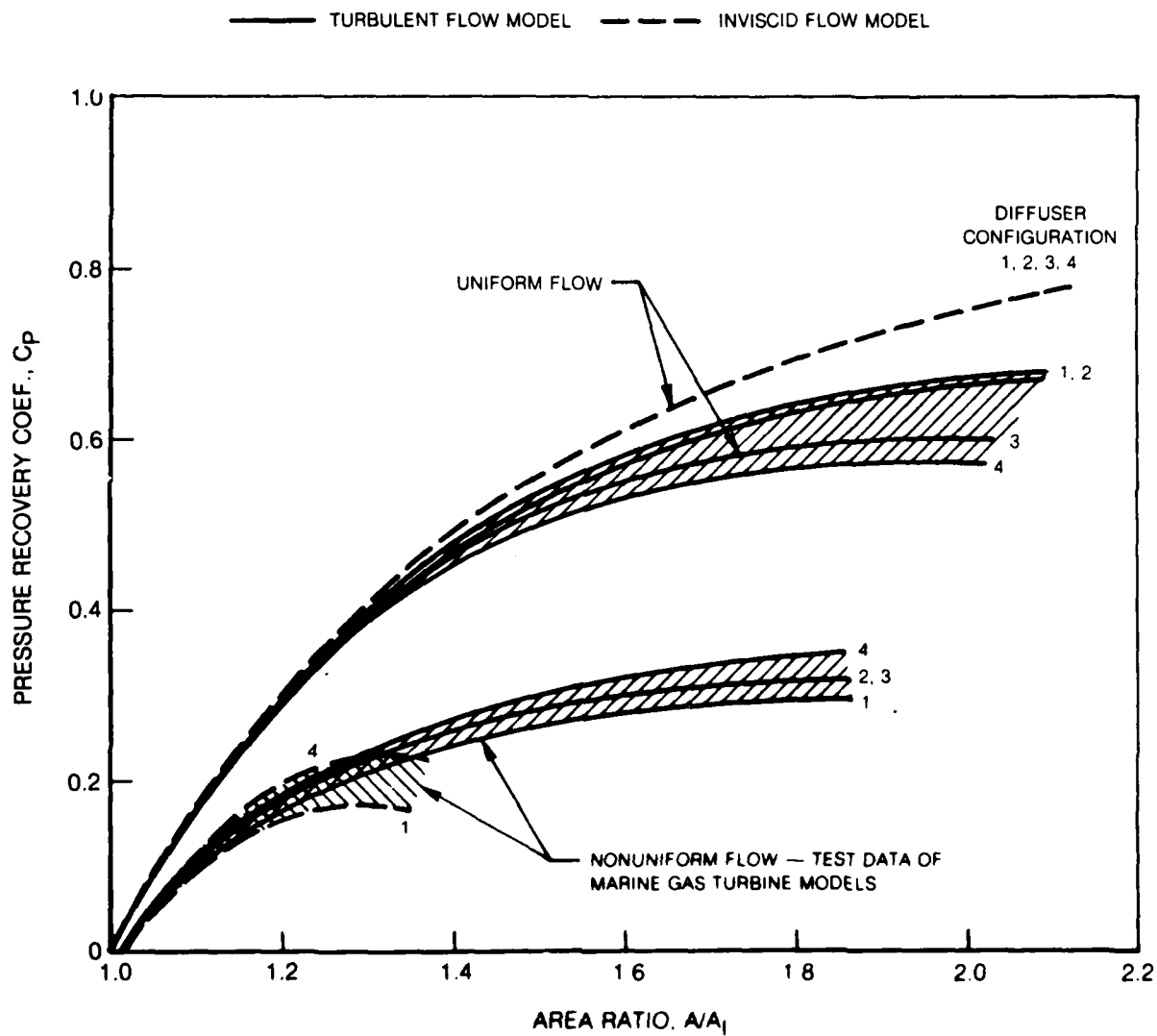
DATE

FORMED

10-81

DTIC

COMPARISON OF PERFORMANCES FOR TWO-DIMENSIONAL DIFFUSERS



SECTION V

DIFFUSER PERFORMANCE WITH FLOW-DISTRIBUTION CONTROL

Results of parametric analyses for diffuser performance presented in Section IV indicate that the nonuniform flow distribution at the diffuser inlet would remain nonuniform in the absence of flow-distribution control as the fluid travels through the diffuser. The nonuniform flow distribution would cause as much as a 50 percent reduction in diffuser efficiency (or the pressure recovery coefficient) as compared with the uniform-flow case. This would definitely offer the incentives for developing and implementing suitable flow distribution control devices for diffusers. In this section, effective flow-distribution control methods identified in the study are reviewed, and their effect on diffuser performance and flow-distribution characteristics are presented.

V.1 Selection of Flow Distribution Control Methods

Based on results of diffuser performance analyses presented in Section IV, configurations No. 2 and No. 5 of Fig. IV.1 were selected as candidate diffusers for flow-distribution control studies. Using the same nonuniform flow-distribution data, configuration No. 4 would perform better than No. 3, No. 2 and No. 1 in that order. However, the differences between the highest and the lowest efficiencies obtained for the four configurations were not more than 5 percent. This was considered insignificant in comparison to the advantages of simplicity and availability which configuration No. 2 could offer for the current DD963-class destroyer applications. In addition, the flow-distribution control method developed based on configuration No. 2 would have more direct applications for the Navy. Hence, it is believed that the selection of configuration No. 2 as one of the candidate diffusers is appropriate. Because configuration No. 5 is considered as a typical very-wide-angle diffuser which can offer the advantages of significant savings in size (length) and weight for marine waste-heat recovery application, it was selected as the second candidate diffuser for the flow-distribution control study.

Among those practical flow-distribution control methods shown in Table I.1, the method that could most effectively produce more uniform flow is the use of flow-guide vanes. To use flow-guide vanes, one must assume that: (1) the mass-flow rate in each flow "channel" be proportional to its own exit flow area, and (2) the input velocity profile will not be affected by the insertion of the flow-guide vane(s). The second assumption implies that the flow-guide vanes must be specially designed such that they can completely segregate the flow in each flow stream and not allow the streams to recombine at the exit of the diffuser.

It is known that when flow-distribution vanes are used, the diffuser is essentially divided into several sub-diffusers which would perform differently and provide different down-stream flow conditions. If one allows these flow streams to mix downstream, a completely new down-stream condition would be created which would alter the original computation results as well as the input velocity profile.

The candidate flow-distribution data selected for this study were DATA-2 of Table II.1. This means that cases No. 10 and 23 of Fig. IV.1 were selected for the flow-distribution control study. The mass-flux profile of these candidate data was plotted in Fig. V.1 to illustrate the selection process of appropriate flow-guide vanes.

Figure V.1 clearly shows that the mass flux is severely distorted and is more densely distributed in the left-hand region of the diffuser. In order to properly divide the mass flux into several regions for flow-guide vanes, the mass flux was integrated across the diffuser which are presented in non-dimensional form as shown in Fig. V.2.

Figure V.2 can be used easily to determine the accurate location of the flow-guide vanes at the diffuser inlet section. To do so, one simply divides the vertical coordinate into regions according to the mass-flow rates desired for each channel, and then one draws a straight line horizontally until it intersects with the integrated mass-flow line. The readings on the abscissa for the intersection points are the places where the vanes should be located. For instance, if one wishes to use a single vane and desires to divide the total mass flow equally into two streams, the flow-guide vane should be located at approximately 34 percent inlet width (or 1.7 ft) from the left wall.

Determining the location of the flow-guide vane at the diffuser exit is more flexible. One desirable choice is to equally divide the exit area of the diffusers such that the heating elements in the boiler can be designed as interchangeable modules. Between the two locations (the inlet and the exit), the flow-guide vane can have any shape. The most commonly used shape is a flat plate. A curved plate, however, might offer some advantage in preventing or delaying boundary-layer separation. But, for the purpose of studying basic flow-distribution phenomena, the flat-plate vane will suffice.

V.2 Diffuser Performance with Flow-Distribution Control

Three flow-distribution control methods were investigated: (1) flow injection; (2) flow-distribution vanes; and (3) a combination of methods (1) and (2). The injection flow could be the cooling flow from the casing of the gas turbine (Fig. II.1). The results of this study are presented below.

Figure V.3 shows the mass-flux distribution characteristics for the candidate diffuser with one point of flow injection on the right-side wall of the diffuser. The flow-injection slot was located approximately 14 ft from the diffuser inlet, which is the location where boundary-layer separation occurred. The flow rate of injection was approximately 17 lb/sec (or 10 percent of the main stream). It was found that the boundary-layer separation was completely suppressed, and that the diffuser performance improved slightly (which improvement will be discussed later in conjunction with Fig. V.8). However, flow distribution at the exit of the diffuser was not improved significantly.

To use flow-distribution vanes, it was assumed that the mass-flow rate and the flow area at the diffuser exit were both equally divided into two channels. The diffuser geometries and flow-field coordinates for this case are shown in Fig. V.4. The mass-flux profiles at three selected streamline stations are shown in Fig. V.5. This figure also shows the development of boundary-layer flow separation and reverse-flow on the left-side wall of the diffuser. The flow separation actually started approximately 4 ft from the diffuser inlet. The numerical calculation was continued and finally interrupted due to numerical instability at approximately 15 ft from the diffuser inlet. Again, the flow distribution at the diffuser exit for this case is still not quite sufficiently uniform.

The last attempt to control the flow distribution was to combine the above two methods, namely, flow injection and a flow-guide vane. Results of this study are selectively presented in Figs. V.6 and V.7 for the mass-flux distribution and pressure-recovery profiles, respectively. The flow-injection was made on the left-hand wall of the diffuser at approximately 7 ft from the diffuser inlet. The rate of injection was approximately 16 lb/sec (approximately 9 percent of the main stream). Figure V.6 clearly shows that the flow distribution at the diffuser exit for this case is much more uniform as compared with those shown in Figs IV.12, V.3, or V.5. The pressure-recovery profiles are shown in Fig. V.7 where the diffuser on the left side was performing better than the one on the right side. This is because the flow on the left-hand channel has a higher inlet velocity (or inlet kinetic energy) to be diffused. As long as the flows from the two channels do not mix together, the results of this study are physically sound.

It should be mentioned that the velocity and temperature profiles are not shown because the former has almost exactly the same shape as the mass-flux profile, and the latter is uniformly distributed over the entire flow field.

Comparisons of diffuser performance with and without flow-distribution control for this candidate diffuser (Configuration No. 2 of Figure IV.1) are shown in Fig. V.8. In this figure, the dotted curve represents the diffuser efficiency obtained from a uniform-flow assumption and has a maximum value of approximately 75 percent, while the bottom curve represents the efficiency of the same diffuser based on DATA-2 non-uniform flow at the inlet without flow distribution control. This curve has a peak value of approximately 36 percent. The results of diffuser performance analysis with three flow-distribution-control methods fall between the above two extremes as expected. It was found that with one point of flow injection and one flow-distribution guide vane, an improvement of more than 20 percentage points in diffuser efficiency can be expected as compared with the results from the case without flow-distribution control.

A similar study was also made of the very-wide-angle diffuser (configuration No. 5 of Fig. IV.1). Figures V.9 shows the mass-flux for this configuration using the same flow-distribution data shown in Fig. V.1 and one flow-distribution vane. Because the left channel has a diffusion angle of approximately 42° (which is still too large), therefore boundary-layer separation was expected and severely stalled flow is seen on the left-wall. In the right-hand channel, no boundary-layer separation occurred throughout the entire flow field. The pressure-recovery characteristics for this diffuser configuration are shown in Fig. V.10, where two negative-value regions are seen near the wall at the diffuser throat. This negative value means a pressure loss, which is attributed to the wall friction acting on the fluid when it flows through the constant-area duct in the front section of the diffuser. This pressure loss was quickly recovered as the fluid flows through each channel. Figure V.10 also show that the left channel is performing much better than the right channel because of the higher dynamic head at the diffuser inlet.

To eliminate flow separation, the flow-injection method was also employed. The improved mass-flux distribution with flow injection is shown in Fig. V.11. In this case, the injection flow rate was approximately 16 lb/sec and the injection slot was located on the left wall at a location 1.5 ft downstream of the diffuser inlet. The injection pressure was assumed equal to the local pressure which was identified as 14.84 psia.

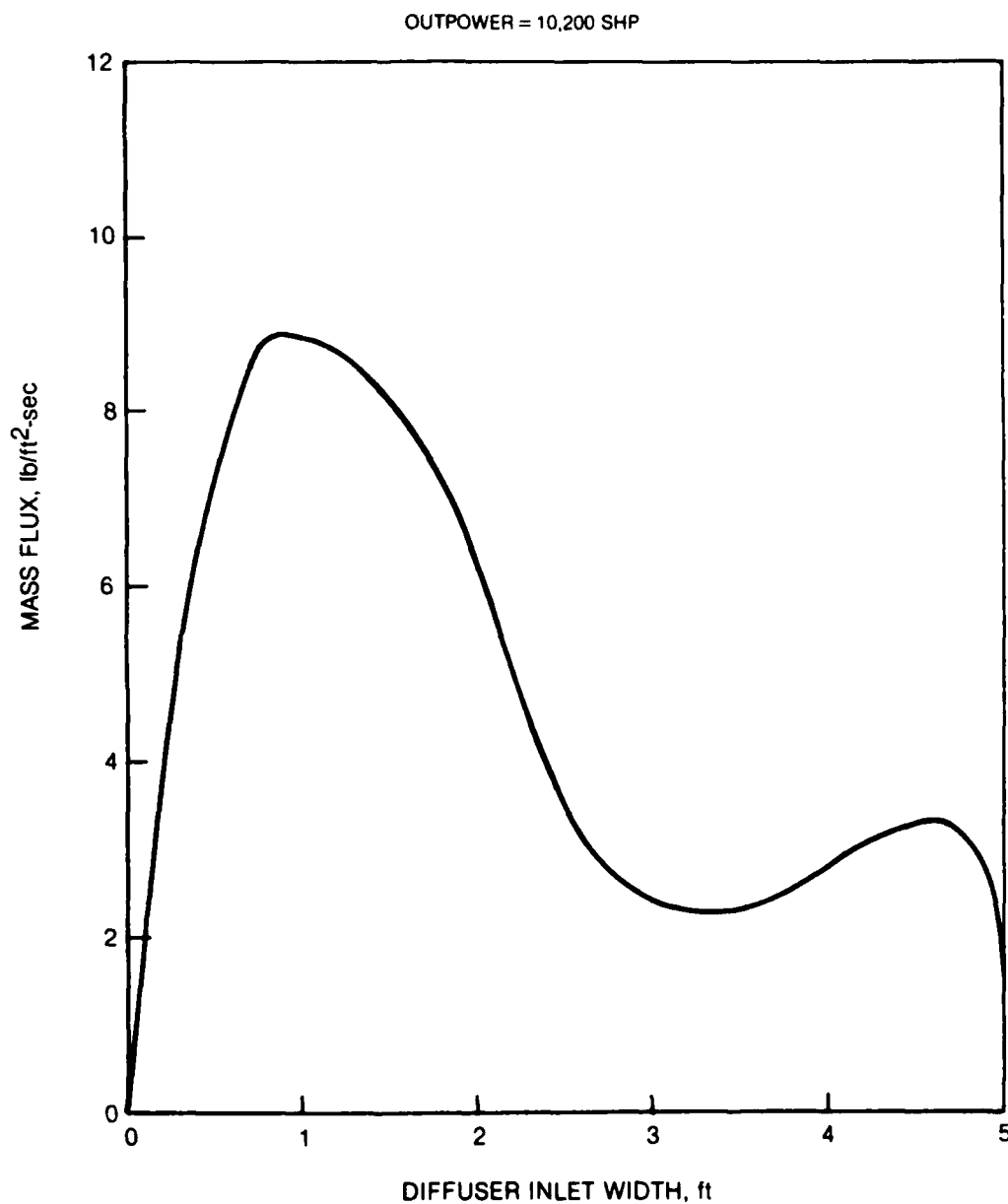
The comparison of diffuser efficiencies for this study is given in Fig. V.12. In this figure, the dotted curve represents the diffuser efficiency (or pressure-recovery coefficient) for the case without control. This curve ends shortly after the diffuser inlet because of the numerical instability caused by the severe flow separation that occurred in this region. The diffuser efficiency for this case was almost zero. In contrast, the solid line represents the results for the controlled case using one flow-distribution vane and one point of flow injection. The results show that the pressure loss for the controlled case is higher than that of the non-controlled case near the diffuser inlet due to friction losses on the flow-guide vane. However the overall diffuser efficiency was found to be approximately 22 percent with only a flow-distribution vane, and that would be improved by approximately 15 percentage points by using flow injection also to control boundary-layer separation.

V.3 Impact of Flow-Distribution Control on Waste-Heat Recovery System

Results of the above studies indicate that either one of the two flow-distribution-control methods considered (flow-guide vane and flow injection) can improve the flow distribution in the diffuser which, in turn, would yield a better diffuser efficiency. However the best results can be obtained by properly combining the two methods. The overall improvement of diffuser efficiency was approximately 20 percentage points for Configuration No. 2 and 36 percentage points for Configuration No. 5. This improvement of 20- to 36-percentage points in diffuser efficiency is equivalent to 0.8 to 1.4 inches of water in static pressure increase. This increased static pressure at the diffuser exit means that the waste-heat boiler can be designed with higher pressure loss and the waste-heat recovery system could be smaller and lighter. A more uniform flow distribution can not only improve diffuser efficiency, but also improve boiler efficiency. According to reference 4.11, as much as a 30 percent increase in efficiency of the overall heat-transfer unit could be expected for certain types of heat exchangers. The impact of this flow-distribution control on the marine gas turbine waste-heat boiler will be investigated in Part II of this study.

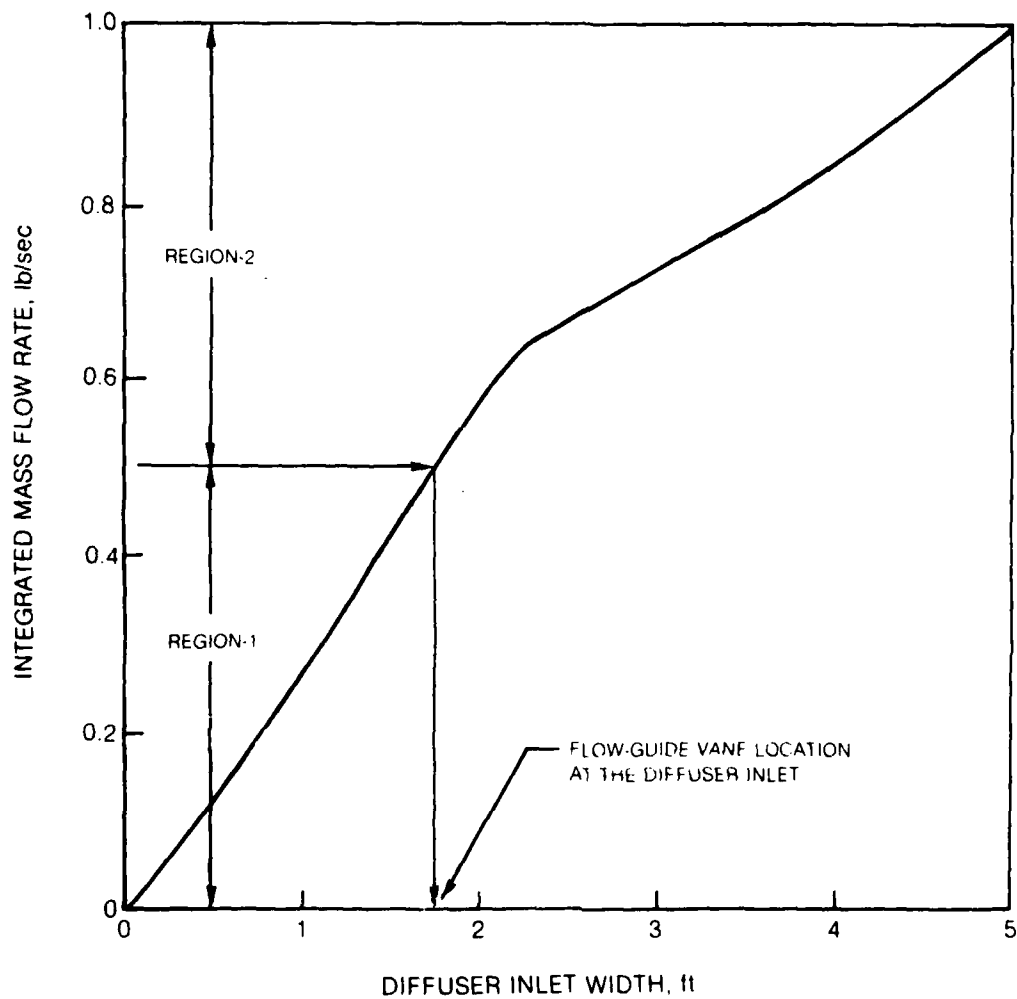
As mentioned earlier, the purpose of using the flow-distribution vane was to properly divide the mass flow into each channel so that the heat-transfer element of the waste-heat boiler can be modularized. In addition, the flow-distribution vane can also reduce the overall diffusion angle which would be beneficial to prevent boundary-layer separation in the diffuser. If boundary-layer separation can not be eliminated by the flow-guide vane, the flow-injection method should be used. This method would require an independent flow-injection stream, which could be available from the engine cooling flow as shown previously in Fig. II.1. However, a monitoring device would be needed to maintain this stream at a suitable flow rate and pressure level.

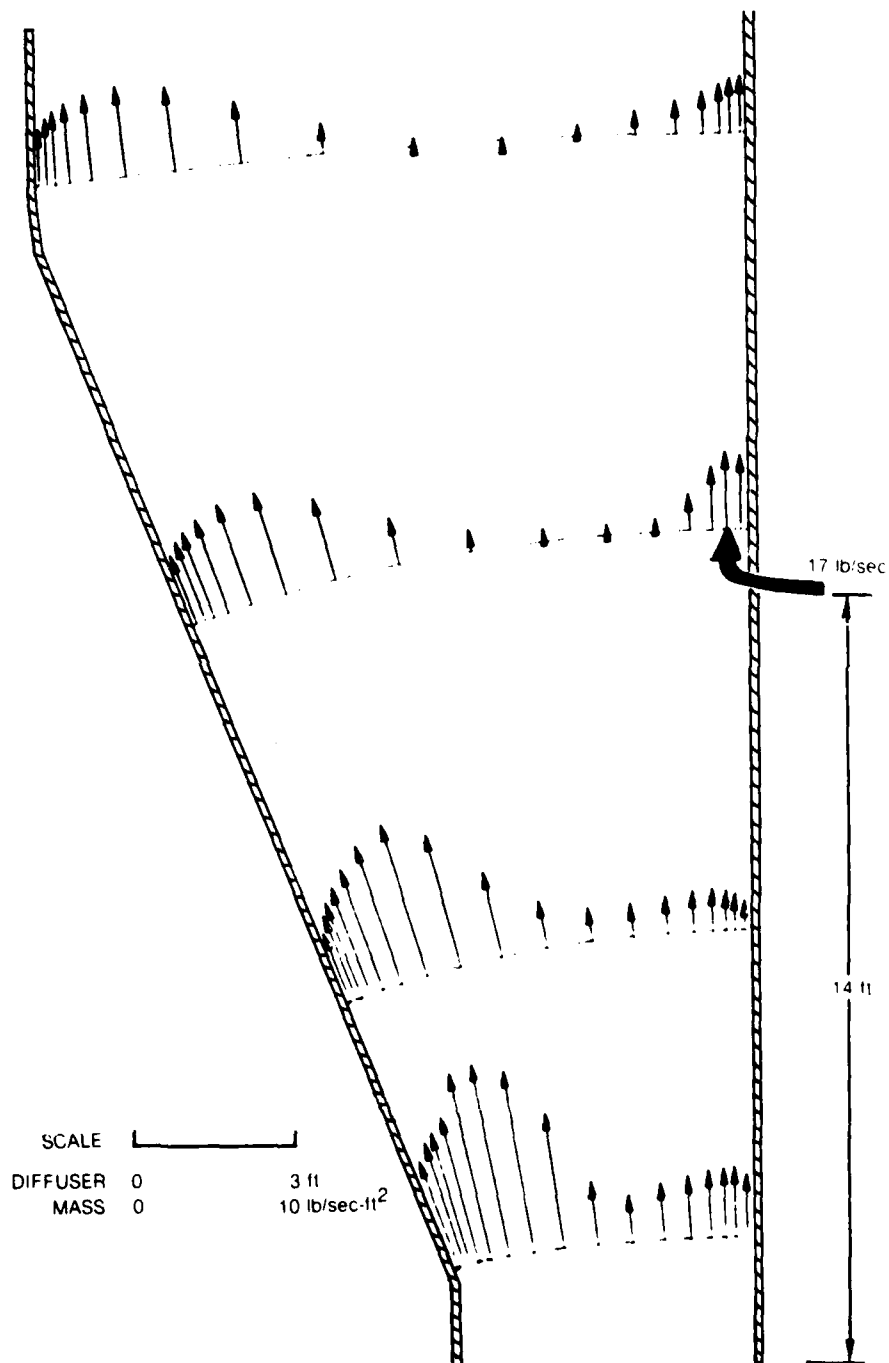
**EXHAUST-GAS MASS-FLUX PROFILES OF DD-963 CLASS DESTROYER
PROTOTYPE GAS TURBINE MODULE 2B**



INTEGRATED MASS FLOW RATE AND METHOD OF DETERMINING THE LOCATION OF FLOW DISTRIBUTION VANES

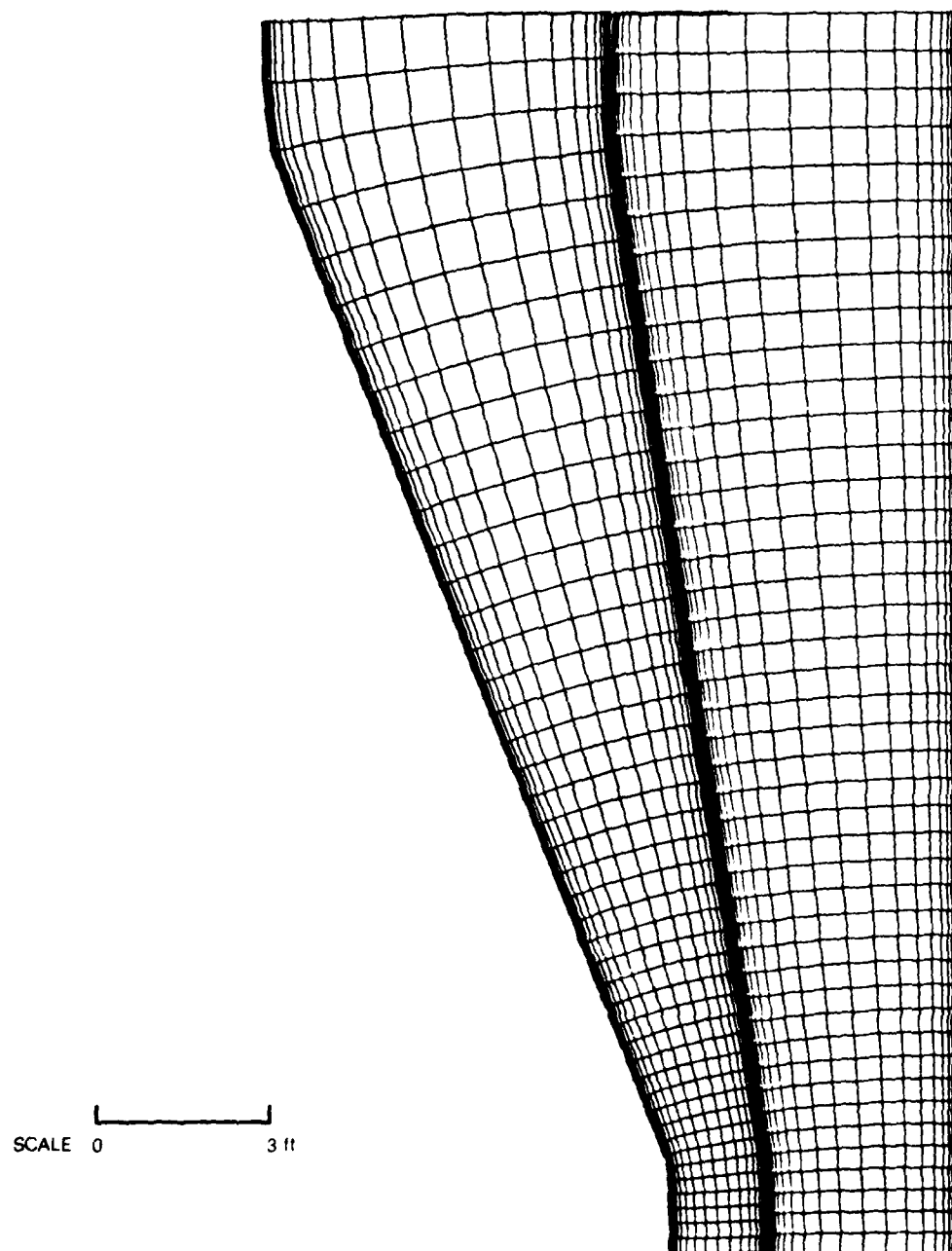
- DD963 CLASS DESTROYER PROTOTYPE GAS TURBINE MODEL 2B
- OUTPUT POWER = 10,200 SHP



MASS-FLUX PROFILES FOR CANDIDATE FLOW SYSTEM NO. 1 WITH ONE FLOW INJECTION

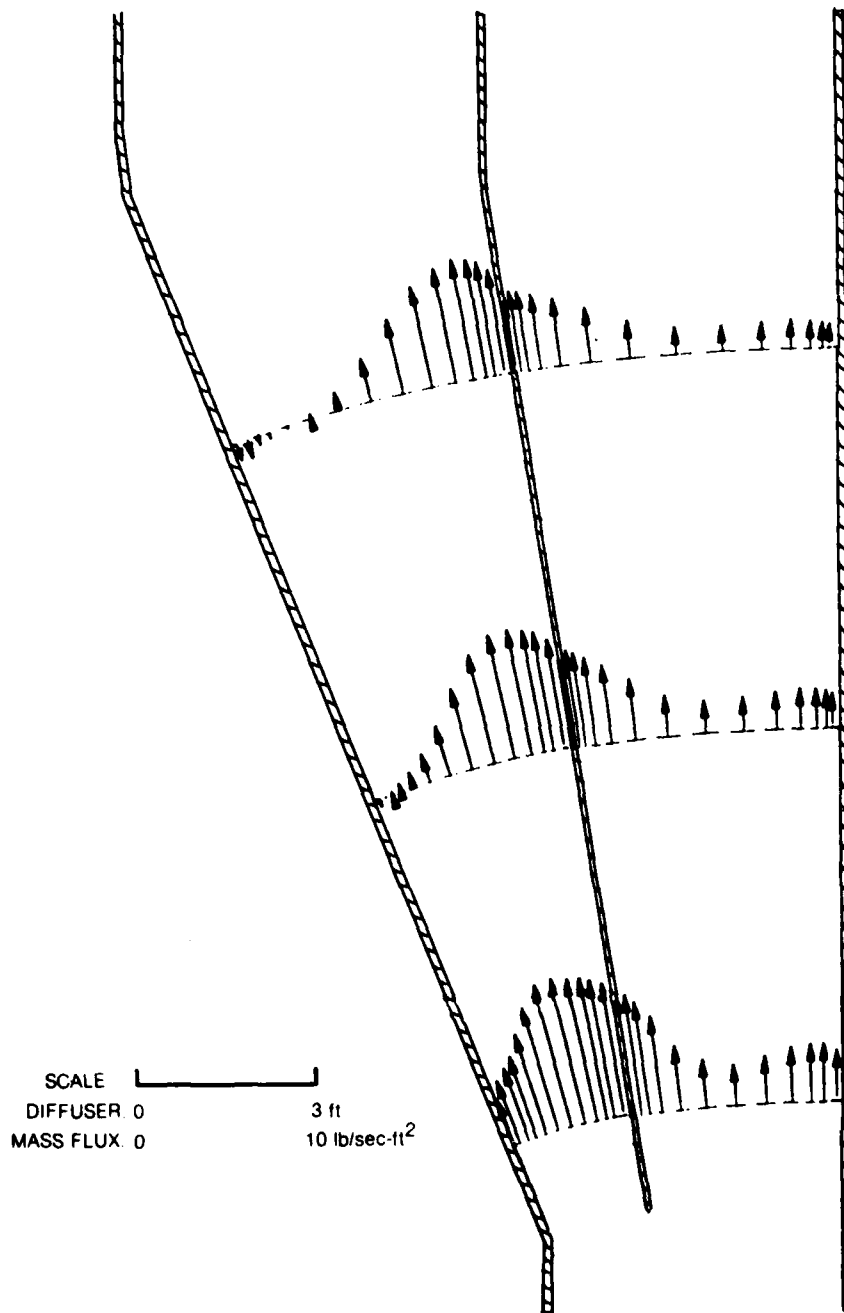
81-6-158-5

**FLOW-FIELD COORDINATES FOR CANDIDATE DIFFUSER NO.1
WITH ONE FLOW-DISTRIBUTION VANE**

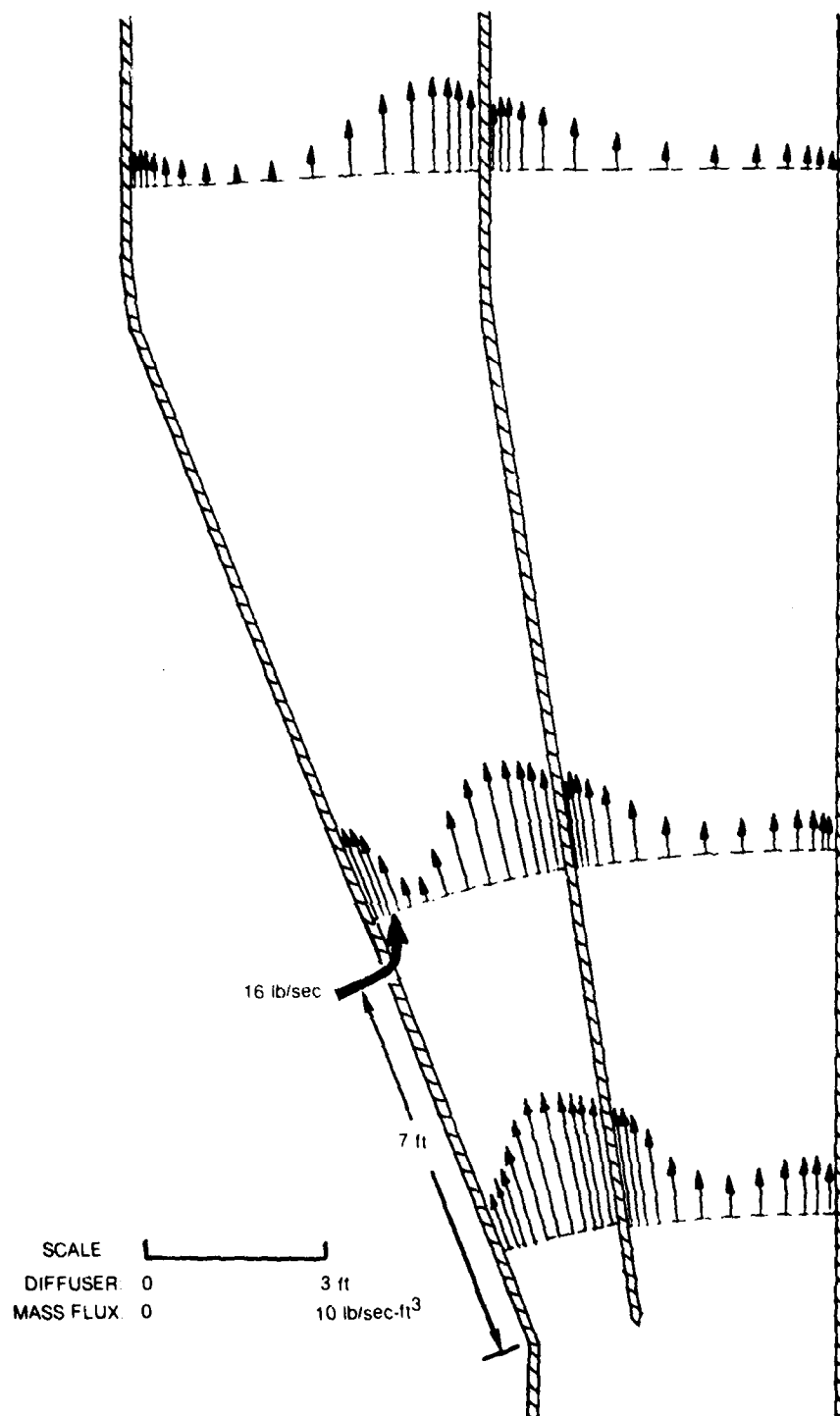


81-6-158-6

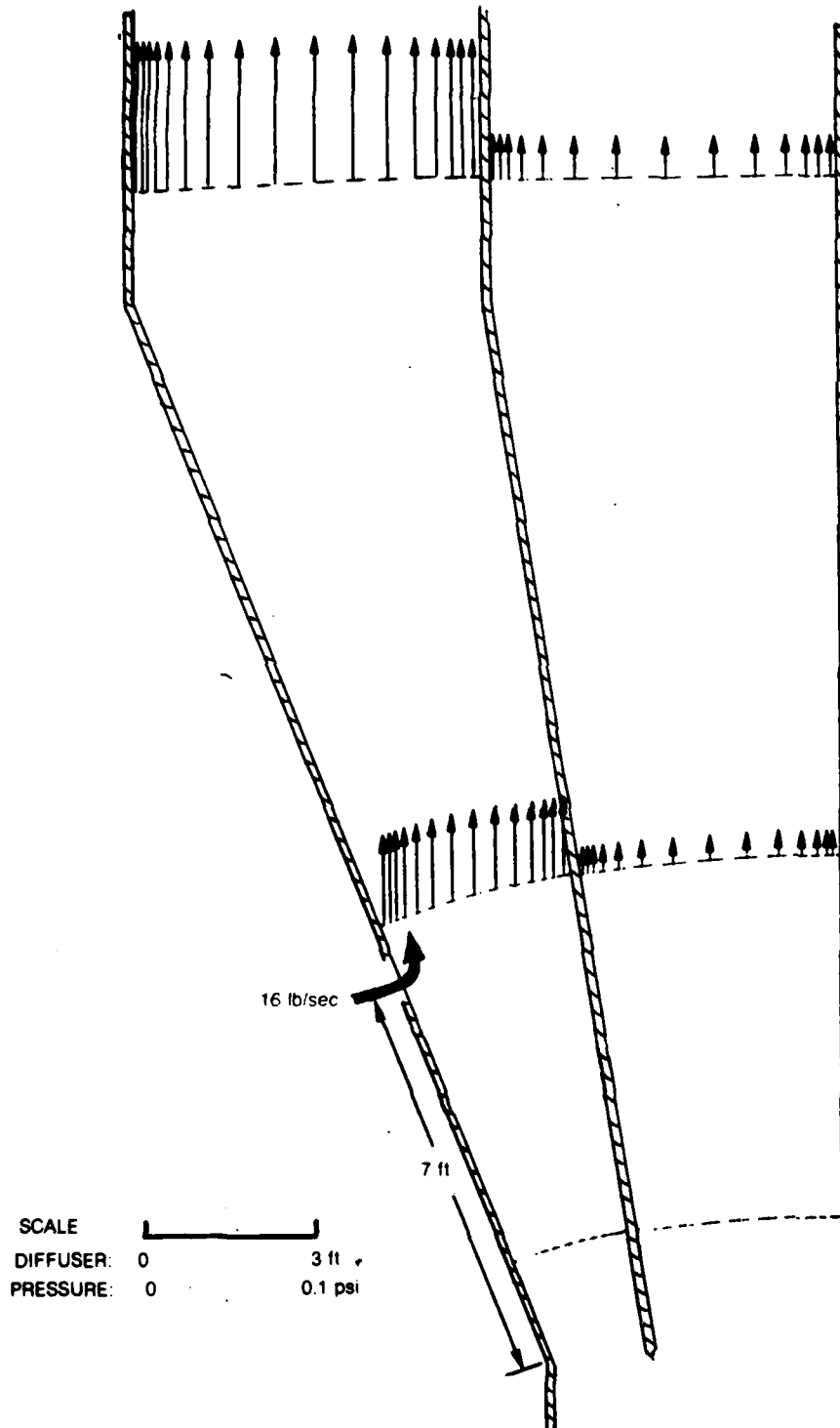
**MASS-FLUX PROFILES FOR CANDIDATE FLOW SYSTEM NO. 1
WITH ONE FLOW-DISTRIBUTION VANE**



**MASS-FLUX PROFILES FOR CANDIDATE FLOW SYSTEM NO. 1
WITH ONE FLOW-GUIDE VANE AND ONE FLOW INJECTION**

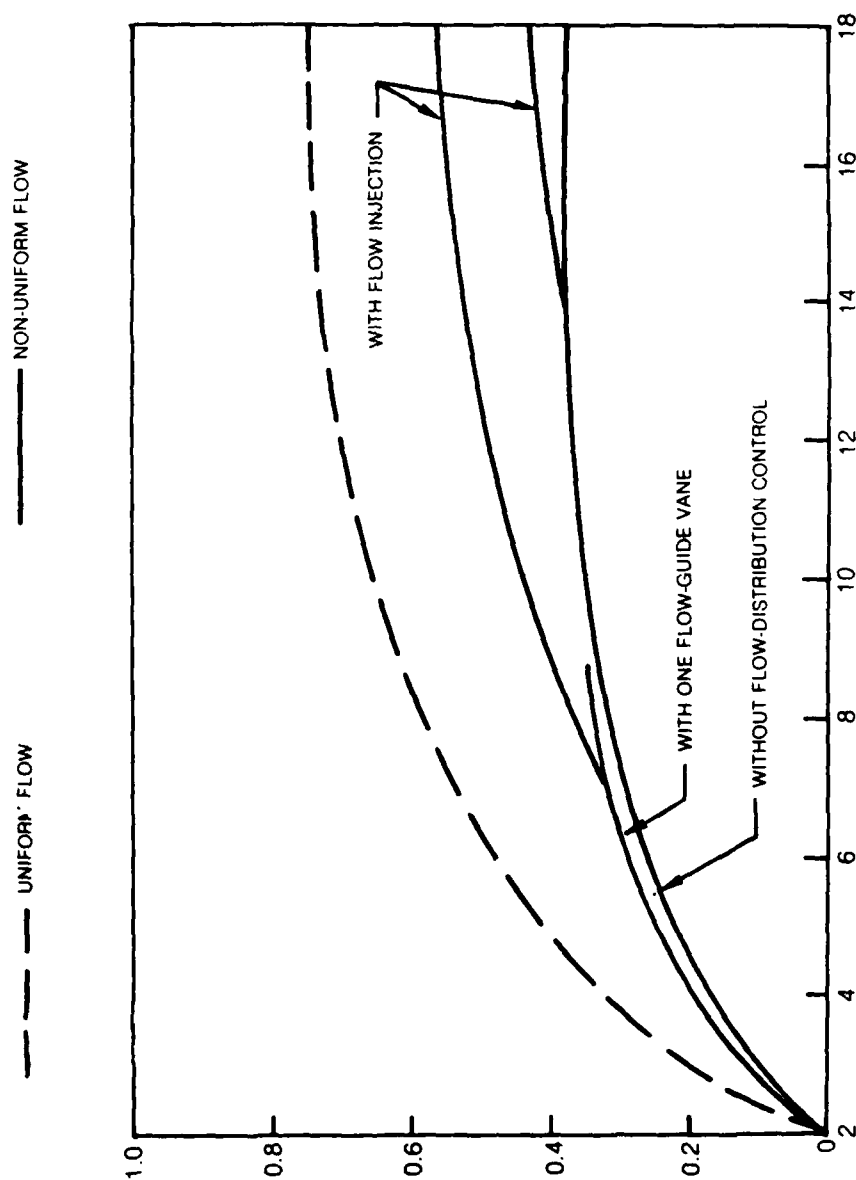


**PRESSURE-RECOVERY PROFILES FOR CANDIDATE SYSTEM NO. 1
WITH ONE FLOW-GUIDE VANE AND ONE FLOW INJECTION**

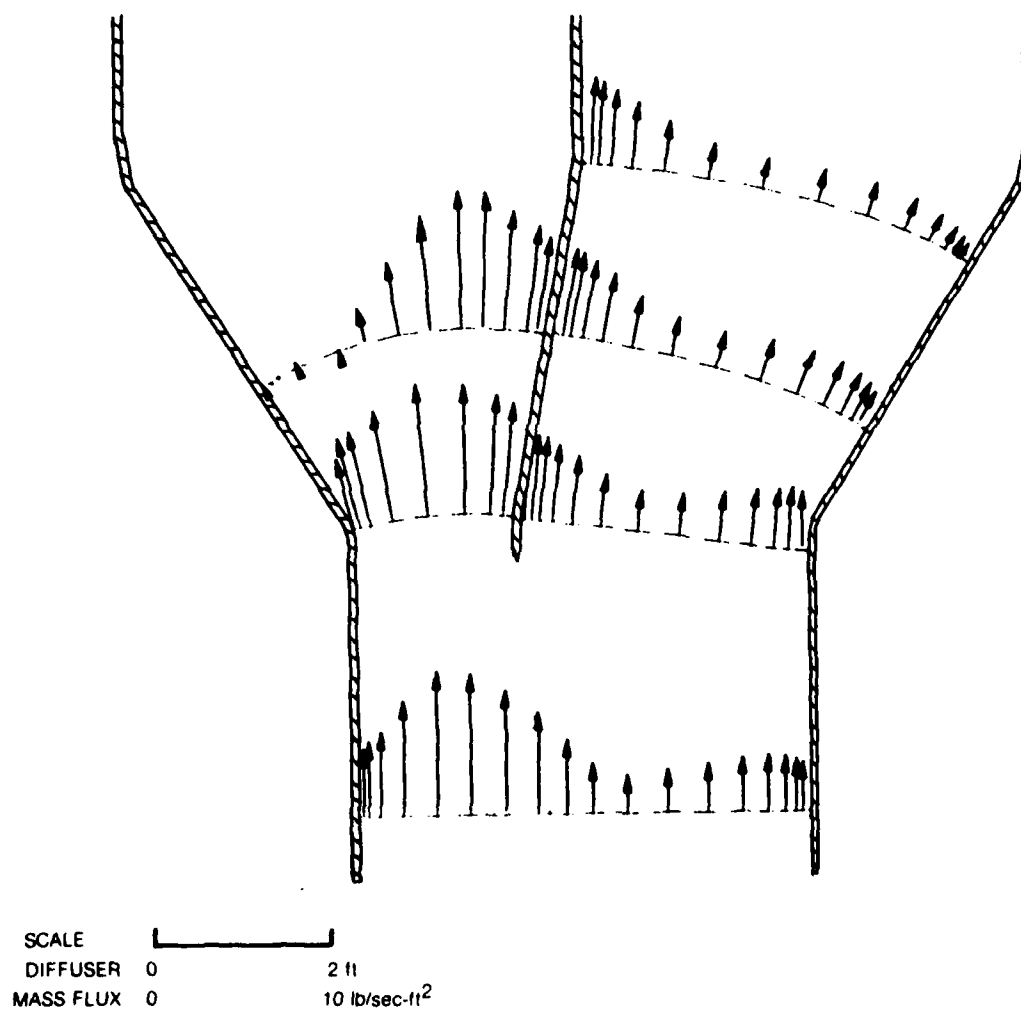


81-6-158-9

COMPARISON OF DIFFUSER PERFORMANCE FOR CONFIGURATION NO. 2
WITH AND WITHOUT FLOW-DISTRIBUTION CONTROL

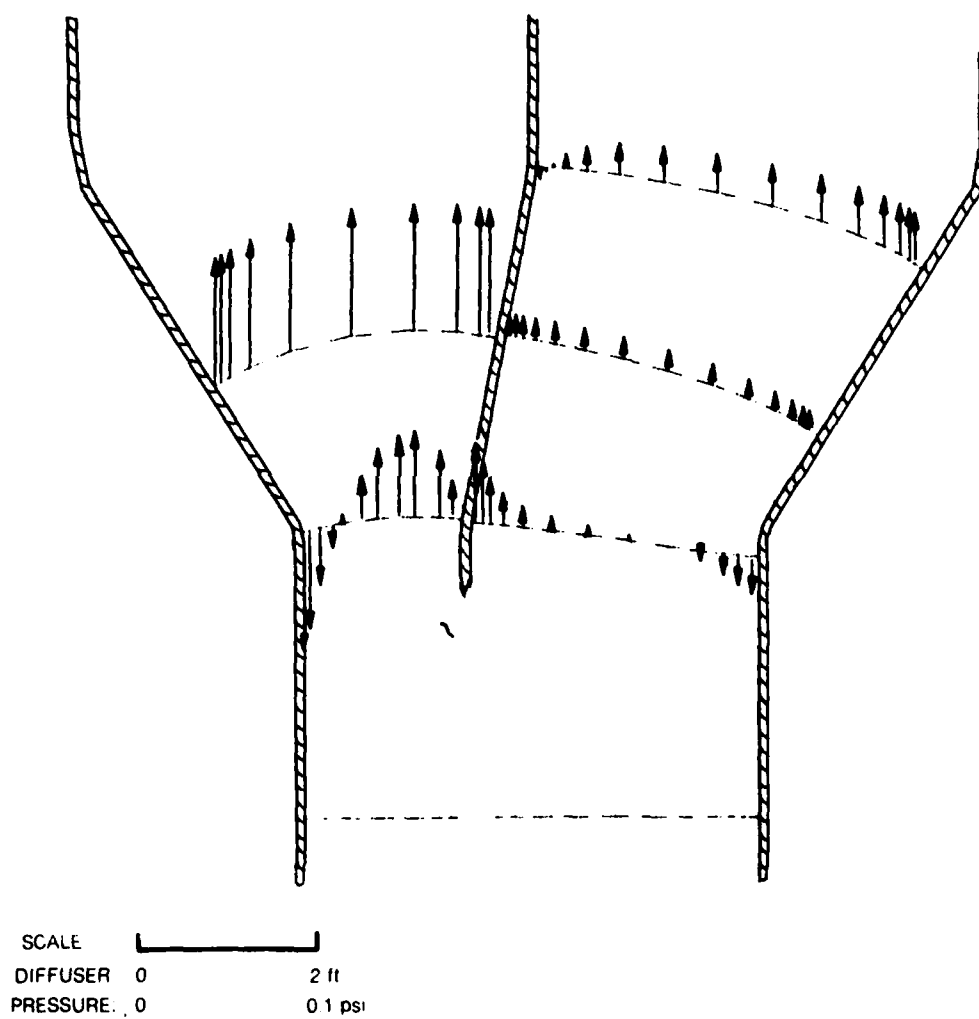


**MASS-FLUX PROFILES FOR CANDIDATE FLOW SYSTEM NO. 2
WITH ONE FLOW-GUIDE VANE**



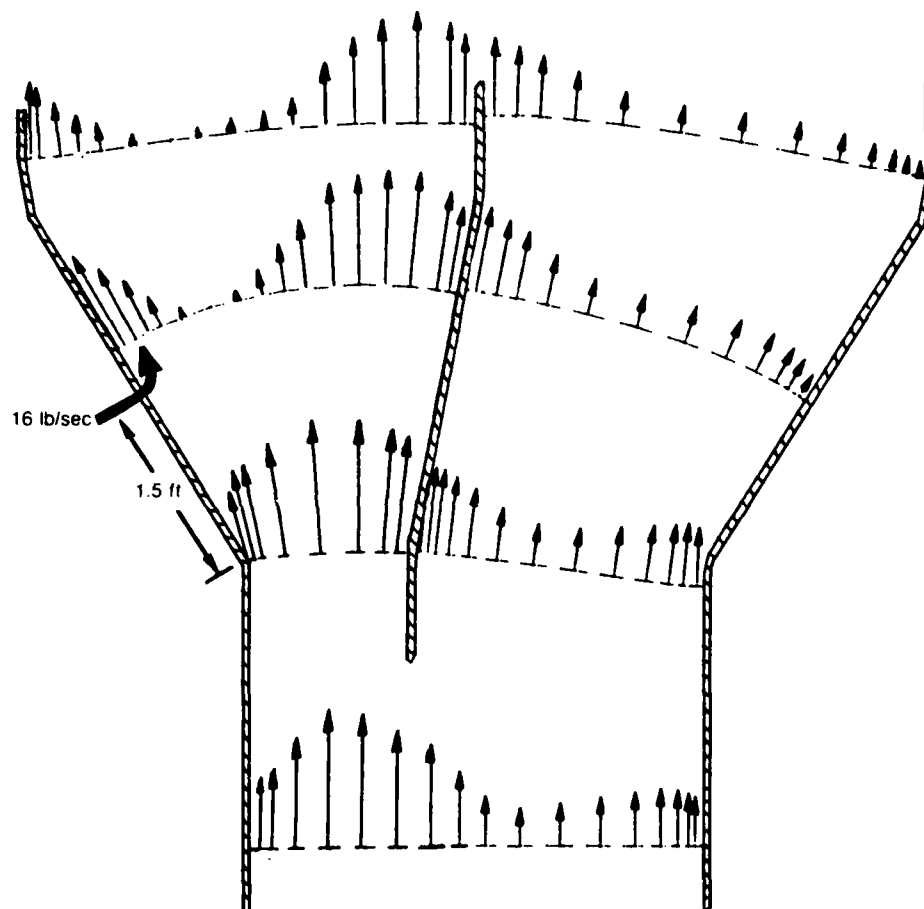
81-8-158-10


**PRESSURE-RECOVERY PROFILES FOR CANDIDATE FLOW SYSTEM
NO. 2 WITH ONE FLOW-GUIDE VANE**



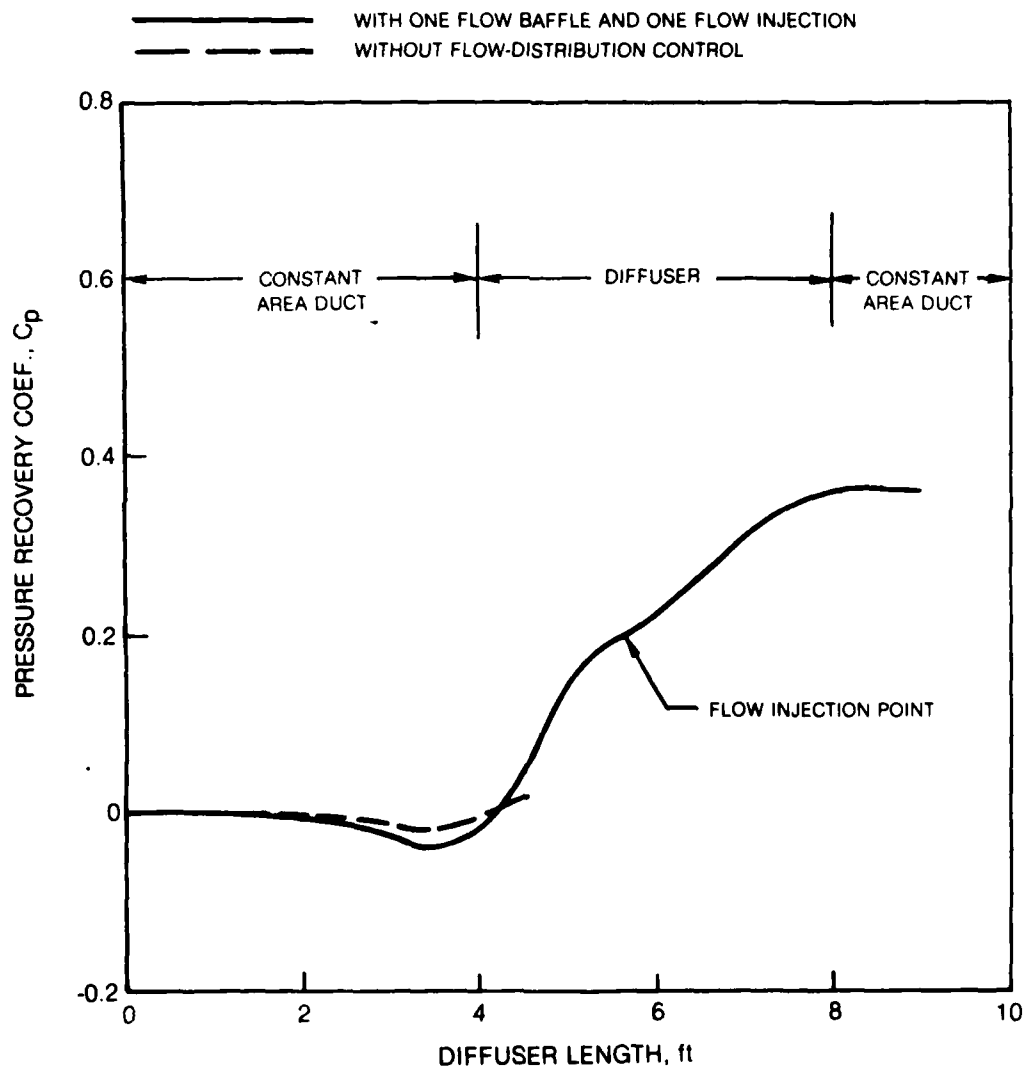
81-6-168-11

**MASS-FLUX PROFILES FOR CANDIDATES FLOW SYSTEM NO. 2
WITH ONE FLOW-GUIDE VANE AND ONE FLOW INJECTION**



SCALE 
DIFFUSER 0 2 ft
MASS FLUX 0 10 lb/sec-ft

**COMPARISON OF DIFFUSE PERFORMANCE FOR CONFIGURATION NO. 5
WITH AND WITHOUT FLOW-DISTRIBUTION CONTROL**



81-6-188-1

DISTRIBUTION LIST

Fluid Mechanics and Heat Transfer

One copy except
as noted

Mr. M. Keith Ellingsworth
Materials and Mechanics Programs
Office of Naval Research
800 N. Quincy Street
Arlington, VA 22203

5

Defense Documentation Center
Building 5, Cameron Station
Alexandria, VA 22314

12

Technical Information Division
Naval Research Laboratory
4555 Overlook Avenue SW
Washington, DC 20375

6

Dr. Al Wood
Director, Mechanics Program
Office of Naval Research
800 N. Quincy Street
Arlington, VA 22203

Professor Paul Marto
Department of Mechanical Engineering
US Naval Post Graduate School
Monterey, CA 93940

Professor Bruce Rankin
Naval Systems Engineering
US Naval Academy
Annapolism, MD 21402

Office of Naval Research Eastern/
Central Regional Office
Bldg. 114, Section D
666 Summer Street
Boston, MA 02210

Office of Naval Research Branch Office
536 South Clark Street
Chicago, IL 60605

R81-955200-4

Office of Naval Research
Western Regional Office
1030 East Green Street
Pasadena, CA 91106

Mr. Charles Miller, Code 05R13
Crystal Plaza #6
Naval Sea systems Command
Washington, DC 20362

Steam Generators Branch, Code 5222
National Center #4
Naval Sea Systems Command
Washington, DC 20362

Heat Exchanger Branch, Code 5223
National Center #3
Naval Sea Systems Command
Washington, DC 20362

Mr. Ed Ruggiero, NAVSEA 08
National Center #2
Washington, DC 20362

Dr. Earl Quandt Jr., Code 272
David Taylor Ship R&D Center
Annapolis, MD 21402

Mr. Wayne Adamson, Code 2722
David Taylor Ship R&D Center
Annapolis, MD 21402

Dr. Win Aung
Heat Transfer Program
National Science Foundation
Washington, DC 20550

Mr. Michael Perlsweig
Department of Energy
Mail Station E-178
Washington, DC 20545

Dr. W. H. Theilbahr
chief, energy Conservation Branch
Dept. of Energy, Idaho Operations Office
550 Second Street
Idaho Falls, Idaho 83401

R81-955200-4

Professor Ephriam M. Sparrow
Department of Mechanical Engineering
University of Minnesota
Minneapolis, MN 55455

Professor J.A.C. Humphrey
Department of Mechanical Engineering
University of California, Berkeley
Berkeley, CA 94720

Professor Brian Launder
Thermodynamics and Fluid Mechanics Division
University of Manchester
Institute of Science & Technology
PO88 Sackville Street
Manchester M601QD England

Professor Shi-Chune Yao
Department of Mechanical Engineering
Carnegie-Mellon University
Pittsburgh, PA 15213

Professor Charles B. Watkins
Chairman, Mechanical Engineering Department
Howard University
Washington, DC 20059

Professor Adrian Bejan
Department of Mechanical Engineering
University of Colorado
Boulder, CO 80309

Professor Donald M. McEligot
Department of Aerospace and Mechanical Engineering
Engineering Experiment Station
University of Arizona 85721

Professor Paul A. Libby
Department of Applied Mechanics and Engineering Sciences
University of California San Diego
Post Office Box 109
La Jolla, CA 92037

Professor C. Forbes Dewey Jr.
Fluid Mechanics Laboratory
Massachusetts Institute of Technology
Cambridge, MA 02139

Professor William G. Characklis
Dept. of Civil Engineering and Engineering Mechanics
Montana State University
Bozeman, Montana 59717

Professor Ralph Webb
Department of Mechanical Engineering
Pennsylvania State University
208 Mechanical Engineering Bldg.
University Park, PA 16802

Professor Warren Rohsenow
Mechanical Engineering Department
Massachusetts Institute of Technology
77 Massachusetts Avenue
Cambridge, MA 02139

Professor A. Louis London
Mechanical Engineering Department
Bldg. 500, Room 501B
Stanford University
Stanford, CA 94305

Professor James G. Knudsen
Associate Dean, School of Engineering
Oregon State University
219 Covell Hall
Corvallis, Oregon 97331

Professor Arthur E. Bergles
Mechanical Engineering Department
Iowa State University
Ames, Iowa 50011

Professor Kenneth J. Bell
School of Chemical Engineering
Oklahoma State University
Stillwater, Oklahoma 74074

Dr. James Lorenz
Component Technology division
Argonne National Laboratory
9700 South Cass Avenue
Argonne, IL 60439

R81-955200-4

Dr. David M. Eissenberg
Oak Ridge National Laboratory
P. O. Box Y, Bldg. 9204-1, MS-O
Oak Ridge, TN 37830

Dr. Jerry Taborek
Technical Director
Heat Transfer Research Institute
1000 South Fremont Avenue
Alhambra, CA 91802

Dr. Simion Kuo
Chief, Energy Systems
Energy Research Laboratory
United Technologies Research Center
East Hartford, CT 06108

Mr. Jack Yampolsky
General Atomic Company
P. O. Box 81608
San Diego, CA 92138

Mr. Ted Carnavos
Noranda Metal Industries, Inc.
Prospect Drive
Newtown, CT 06470

Dr. Ramesh K. Shah
Harrison Radiator Division
General Motors Corporation
Lockport, NY 14094

Dr. Ravi K. Sakhuja
manager, Advanced Programs
Thermo Electron Corporation
101 First Avenue
Waltham, MA 02154

Mr. Robert W. Perkins
Turbotec Products, Inc.
533 Downey Drive
New Britain, CT 06051

Dr. Keith E. Starner
York Division, Borg-Warner Corp.
P. O. Box 1592
York, PA 17405

R81-955200-4

Mr. Peter Wishart
C-E Power Systems
Combustion Engineering, Inc.
Windsor, CT 06095

Mr. Henry W. Braum
Manager, Condenser Engineering Department
Delaval
Front Street
Florence, NJ 08518

Dr. Thomas Rabas
Steam Turbine-Generator Technical Operations Division
Westinghouse Electric Corporation
Lester Branch
P. O. Box 9175 N2
Philadelphia, PA 19113

Mr. Walter Ritz
Code 033C
Naval Ships Systems Engineering Station
Philadelphia, PA 19112

Mr. Richard F. Wyvill
Code 5232
NC #4
Naval Sea Systems Command
Washington, DC 20362

Mr. Doug Marron, Code 5231
NC #4
Naval Sea Systems Command
Washington, DC 20362

Mr. T. M. Herder
Bldg. 46462
General Electric Co.
1100 Western Avenue
Lynn, MA 01910

Mr. Ed Strain
AiResearch of Arizona
Dept. 76, Mail Stop 301-2
P. O. Box 5217
Phoenix, AZ 85010
(Tel. 602-267-2797)

R81-955200-4

Mr. Norm McIntire
Solar Turbines International
2200 Pacific Highway
San Diego, CA 92101

Professor Daryl Metzger
Chairman, Mechanical and Energy
Systems Engineering
Arizona State University
Tempe, AZ 85281

D
FI
10